UNIVERSITY OF CALIFORNIA
RIVERSIDE

Genetics Characterization of Antiviral RNA Interference in *Caenorhabditis elegans*

A Dissertation submitted in partial satisfaction
of the requirements for the degree of

Doctor of Philosophy

in

Cell, Molecular, and Developmental Biology

by

Jing Zhong

August 2014

Dissertation Committee:
Dr. Shou-wei Ding, Chairperson
Dr. A.L.N Rao
Dr. Morris F. Maduro

The Dissertation of Jing Zhong is approved:

_____

_____

_____

Committee Chairperson

University of California, Riverside

Acknowledgements

First and foremost, I want to thank my major professor Dr. Shou-wei Ding for his extraordinary teaching and guidance. It has been an honor to become a PhD student of such a knowledgeable and successful scientist. I appreciate his contributions of funds from National Institute of Health, time, ideas and experimental assistance over the past seven years. Not only a mentor in academics, he has also been my tutor in life.

Moreover, I want to especially thank Dr. Morris Maduro, Ms. Gina Broitman-Maduro and other members in Morris lab like Dr. Melissa Antonio for their tremendous guidance, experimental materials and assistance offered in my research. I also want to thank Dr. A.L.N Rao who kindly served as my dissertation committee member and also my teacher. Except for Dr. Morris Maduro, Dr. Richard Cardullo, Dr. James Baldwin and emeritus professor Dr. Edward Platzer instructed me to be an effective educator and communicator. I also wish to thank the advisors at CMDB program: Dr. Jeff Bacchant, Dr. Patricia Springer, Dr. Peter Atkinson, Dr. Helen Henry and Ms. Kathy Redd.

I also appreciate all former or current lab members in Shou-wei Ding lab who have given me assistance or guidance towards the completion of this work like Ms. Wan-xiang Li, Dr. Rui Lu, Dr. Zhihuan Gao, Dr. Yanhong Han, Jinfeng Lu, Ms. Stephanie Coffman, Xiaoxu Fan and Ms. Yanhong Qiu.

My entire family, which includes my parents Hong Wang and Shuqing Guo, my grandparents Xingwen Zhong, Chengyun Guo and Gui'e Li, has given me tremendous help during my study and work in UC Riverside. I want to also thank my aunt Ms.

Shufang Guo, a virologist in China for fostering my interest in virology research. I regret that I was absent when my grandmother Changzhong Wang passed away, and I believe she would be proud seeing the completion of this work and what I achieved.

It has been my honor and pleasure to spend seven years working and living together with the brilliant colleagues- faculty and staff, postdocs and fellow students in University of California, Riverside community. I will honor this community throughout the rest of my career.

‘

ABSTRACT OF THE DISSERTATION

Genetics Characterization of Antiviral RNA Interference in *Caenorhabditis elegans*

by

Jing Zhong

Doctor of Philosophy, Graduate Program in Cell, Molecular and Developmental Biology
University of California, Riverside, August 2014
Dr. Shou-wei Ding, Chairperson

RNA interference (RNAi) acts as an antiviral defense mechanism in fungi, plants, nematodes, insects, and mammals. In antiviral RNAi, virus-specific double-stranded RNA is processed into small interfering RNAs (siRNAs) to guide specific viral RNA degradation by the RNAi machinery. Although antiviral RNAi is non cell-autonomous in plants, it is unknown if antiviral RNAi is also systemic in animals. In this dissertation, I characterized the nematode *Caenorhabditis elegans* mutants defective in systemic RNAi in their antiviral RNAi response induced by either the replication of a Flock house virus-derived replicon or the infection of Orsay virus. The results from these genetic studies provided evidence for the first time to support an antiviral function of systemic RNAi in animals. Comparison of the population of viral siRNAs by deep sequencing further revealed that *C. elegans* mutants with strong defects in systemic antiviral RNAi were all partially defective in the biogenesis of the viral secondary siRNAs. A possible role for the viral siRNAs in systemic antiviral RNAi is discussed.

Table of Contents

Chapter 4

Appendix

List of Figures

List of Tables

Chapter 1: Introduction

1.1 RNA interference

RNA interference (RNAi) refers to specific gene silencing by double-stranded RNA (dsRNA)-induced RNA degradation. RNAi was discovered in the model nematode *Caenorhabditis elegans* (Guo and Kemphues, 1995; Fire et al., 1998). It is mechanistically related to post-transcriptional gene silencing described earlier in transgenic plants (Napoli et al., 1990; Vanderkrol et al., 1990).

The initial step of RNAi is the processing of the dsRNA silencing trigger into small interfering RNAs (siRNAs). These siRNAs are 21 nucleotides (nt) in length, double-stranded and contain 5'-monophosphates (Hamilton and Baulcombe, 1999). The endonuclease responsible for the production of siRNAs is called Dicer, an RNase III family member which contains dual catalytic RNase domains, helicase domain and PAZ motifs. Dicer is ubiquitously present in almost every eukaryotic organism (Bernstein et al., 2001; Ketting et al., 2001; Knight and Bass, 2001; Hammond, 2005). Dicer also produces microRNAs (miRNA) from endogenous pre-miRNA molecules to regulate expression of numerous genes (Bernstein et al., 2001; Grishok et al., 2001). Both siRNAs and miRNAs are subsequently loaded into the effector of RNAi machinery: RNA-induced silencing complex (RISC) (Hammond et al., 2000). A key component of RISC is a protein called Argonaute which contains PAZ domain, MID domain and the catalytic PIWI domain which is structurally similar to RNase-H that usually carries out the slicing

activity of the mRNA complementary to the siRNA strands loaded in RISC. However, Argonaute proteins may not possess the slicer activity in all cases, indicating their functions vary though in the same family (Hutvagner and Simard, 2008).

Several key components of RNAi in the model system *C. elegans* have been identified by forward genetics screens. These include RNAi-Defective 1 (RDE-1) and RDE-4 that encodes an Argonaute protein and a dsRNA-binding protein respectively (Tabara et al., 1999; Parrish and Fire, 2001). RDE-1 and RDE-4 form a complex with the Dicer protein to process the dsRNA trigger into siRNAs (Ketting et al., 2001; Tabara et al., 2002). These primary siRNAs are loaded into RDE-1-containing RISC then recruit an RNA-dependent RNA polymerase (RdRp) onto the target mRNA sequences to synthesize secondary siRNAs (Miska and Ahringer, 2007; Sijen et al., 2007). These RdRps include RRF-1 which is expressed in somatic tissue, EGO-1 which is expressed in germline tissues and RRF-3 which is required for endogenous RNAi. Secondary siRNAs in *C. elegans* are not produced by Dicer; hence they carry tri-phosphate at 5' end. These secondary siRNAs are hence loaded into secondary Argonautes like CSR-1 or worm-specific Argonautes (WAGO) such as SAGO-1, SAGO-2- a clade of Argonautes found only in nematodes. While secondary Argonautes like CSR-1 are responsible for the slicer endonuclease activity guided by secondary siRNAs, most of the WAGOs lack residues in the PIWI domain which is thought to be necessary for the slicer activity and promote target mRNA decay or transcriptional gene silencing (TGS) (Aoki et al., 2007; Castel and Martienssen, 2013). Furthermore, wild type nematodes produce more abundant secondary

siRNAs than primary siRNAs during active RNAi, this finding further proves the importance of secondary siRNAs in *C. elegans* RNAi (Pak et al., 2012).

Endogenous siRNAs of *C. elegans* are predominantly 22nt long with a 5' guanine preference (Claycomb et al., 2009; Gu et al., 2009). These 22G siRNAs are produced by RdRp and thus have 5' terminal tri-phosphate modification, but they are different from exogenous secondary siRNAs since most of these 22G siRNAs do not appear to be secondary siRNA products. 22G siRNAs are classified into two categories according to the Argonautes they associate with: WAGO class 22G siRNAs and CSR-1 class 22G siRNAs. However, a small population of WAGO class 22G siRNAs are secondary products to a family of primary 26G siRNAs whose production requires Dicer, the exonuclease ERI-1 and the RdRp RRF-3 (Han et al., 2009; Gent et al., 2010). These 26G siRNAs are also further categorized into two classes distinguished by their association with either ERGO-1 or ALG-3/ALG-4 Argonautes (Conine et al., 2010; Vasale et al., 2010). ALG-3/ALG-4 class of 26G siRNAs are required for spermatogenesis whereas ERGO-1 class of 26G siRNAs are expressed in oocytes and embryos. Downstream 22G siRNAs produced from 26G siRNA targets are enriched in somatic tissues. Together these endo-siRNAs are required for the development and reproduction of *C. elegans.*

Animals including *C. elegans* also produce miRNA and piwi-interacting (piRNA). miRNAs are approximately 20-25 nucleotides and they regulate diverse processes such as cell fate specification, apoptosis, and metabolism. They are transcribed as approximate 1kb-long poly-adenylylated primary miRNAs from the genome. The pri-

miRNA is subsequently processed by the RNase III endonuclease- Drosha into a 60-70nt precursor miRNA (pre-miRNA) which can form a hairpin structure. Thus Dicer is able to recognize and process pre-miRNA to produce mature miRNA (Bartel, 2004). ALG-1 and ALG-2 are the Argonautes which associate with miRNAs to perform gene silencing (Grishok et al., 2001). piRNA functions to protect the inheritance of organisms over generations from harmful sequences like retroviruses or transposons (Ghildiyal and Zamore, 2009). Different from piRNAs in other organisms, *C. elegans* piRNAs are 21nt long with a 5' Uracil preference (Ruby et al., 2006; Batista et al., 2008; Das et al., 2008). Known as 21U RNAs, they are methylated and thus stabilized by HENN-1, a homolog of *Arabidopsis thaliana* HEN1 RNA-methyl-transferase in *C. elegans* (Kamminga et al., 2012). These 21U RNAs are mostly loaded into the *C. elegans* PIWI protein PRG-1 to trigger gene silencing specifically in germline tissues.

In the research targeting RNAi mechanisms, the nematode *C. elegans* has been utilized as an animal research model. *C. elegans* survives by feeding on microbes- most commonly bacteria like *E. coli. C. elegans* reproduces with a life cycle of about 3 days. Although in nature *C. elegans* population are almost solely comprised of hermaphrodites, the rare existence (0.05%) of males enables this system to undergo genetic crosses and analysis. Hermaphrodite individuals carry a pair of sex chromosome XX and haploid males merely carry one individual sexual chromosome X. Except for sexual chromosomes, *C. elegans* has a genome comprised of five pairs of autosomes: Chromosome I, II, III, IV and V. Totally *C. elegans* genome has 0.97 million base pairs, roughly the same size as the other organisms *Arabidopsis* and *Drosophila* genomes.

Among 18,452 *C. elegans* proteins, research results indicate that at least 83% (15,344 sequences) of *C. elegans* proteome have human homologs, with 7,954 records of C. elegans proteins matching known human gene transcripts (Lai et al., 2000).

1.2 RNAi-mediated antiviral immunity

RNAi directs specific antiviral immunity in fungi, plants, insects and nematodes. The first evidence of antiviral RNAi was from plants (Dougherty et al., 1994; Kumagai et al., 1995; Angell and Baulcombe, 1997) whereas the animal antiviral RNAi was first demonstrated in the *Drosophila* model (Li et al., 2002). In antiviral RNAi against RNA viruses, viral dsRNA replicative intermediates are processed by a Dicer protein into siRNAs, which are subsequently loaded into Argonaute proteins to guide specific degradation of the viral RNAs by RNAi. *Drosophila* antiviral RNAi requires the genes essential for the dsRNA-siRNA pathway of RNAi, including Dicer-2, Argonaute AGO-2 and the dsRNA-binding protein R2D2 (Aliyari et al., 2008). In the plant *Arabidopsis*, antiviral RNAi against Cucumber mosaic virus (CMV) is regulated by two Dicer proteins (DCL-2 and DCL-4) and two Argonaute proteins (AGO1 and AGO2) as well as two RdRps (RDR1 and RDR6). Therefore, plant antiviral RNAi depends on the production of secondary viral siRNAs amplified by host RdRps in contrast to *Drosophila.* Notably, recent studies also illustrated a natural antiviral function for RNAi in mammals (Li et al., 2013; Maillard et al., 2013), indicating that antiviral RNAi is a broadly conserved antiviral defense mechanism in diverse eukaryotic organisms (Mourrain et al., 2000;

Morel et al., 2002; Boutet et al., 2003; Diaz-Pendon et al., 2007; Qu et al., 2008; Qu, 2010; Wang et al., 2010).

The antiviral function of RNAi in *C. elegans* was first reported in 2005 using two independent systems (Lu et al., 2005; Schott et al., 2005; Lu et al., 2009). The first system used inducible transgene to launch the *in vivo* replication of a positive-strand RNA virus- Flock house virus (FHV) whereas the second system involves infection of cultured primary worm cells by a negative-strand RNA virus, Vesicular stomatitis virus (VSV) (Schott et al., 2005; Wilkins et al., 2005). The antiviral RNAi studies in *C. elegans* have attracted many researchers following the recent discovery of Orsay virus, which naturally infects *C. elegans* and is closely related to FHV (Felix et al., 2011). Antiviral RNAi in *C. elegans* requires genes such as DCR-1, RDE-1, RDE-4, and RRF-1 that are essential for RNAi induced by exogenous dsRNA (Lu et al., 2005; Lu et al., 2009). However, *C. elegans* antiviral RNAi also is dependent on Dicer-related helicase 1 (DRH -1) that is dispensable for exogenous RNAi (Figure 1.1). DRH-1 contains a DExD/H-box helicase domain and it has two homologs in *C. elegans*, DRH-2 and DRH-3. DRH-2 was previously described as a pseudogene while DRH-3 is required for germline RNAi and the biogenesis of endogenous siRNAs.

Recent studies have revealed distinct roles of DRH-1 and DRH-3 in antiviral RNAi (Ashe et al., 2013; Guo et al., 2013). Both *drh-1* and *drh-3* mutant strain animals are defective in antiviral RNAi and both of them support enhanced replication levels of FHV replicon and Orsay virus. However, *drh-1 C. elegans* strains exhibits defects in the

biogenesis of primary viral siRNAs, which are predominantly 23-nt with 5' mono-phosphate and are divided approximately equally into positive and negative strands. By contrast, *drh-3* worms have no defect in the biogenesis of primary viral siRNAs, but produce few secondary viral siRNAs, which are predominantly 22-nt in antisense to the viral genomic RNAs, with 5' tri-phosphate and a 5'-terminal G bias (Ashe et al., 2013; Guo et al., 2013). DRH-1 is considered as a homolog of RIG-I-like helicases (RLH) in mammals since they contain highly homologous RNA helicase and C-terminal domains. Recognition of viral dsRNA in the cytosol by the helicase and C-terminal domains of RLRs activates a signaling cascade that leads to production of type 1 interferon (IFNs) and protective immunity against diverse RNA viruses in mammals. Interestingly, both the helicase and C-terminal domains of human RIG-I can functionally replace the corresponding domains of DRH-1 to mediate antiviral RNAi in *C. elegans,* suggesting that DRH-1 has an essential activity in antiviral RNAi to detect viral dsRNA in a way analogous to virus dsRNA sensing by RIG-I in mammals (Guo et al., 2013). According to these evidence of antiviral RNAi like the importance of DRH-1 which was not required in classical RNAi, *C. elegans* is proven to host a specific antiviral RNAi mechanism different from both exogenous RNAi and endogenous RNAi (Figure 1.1).

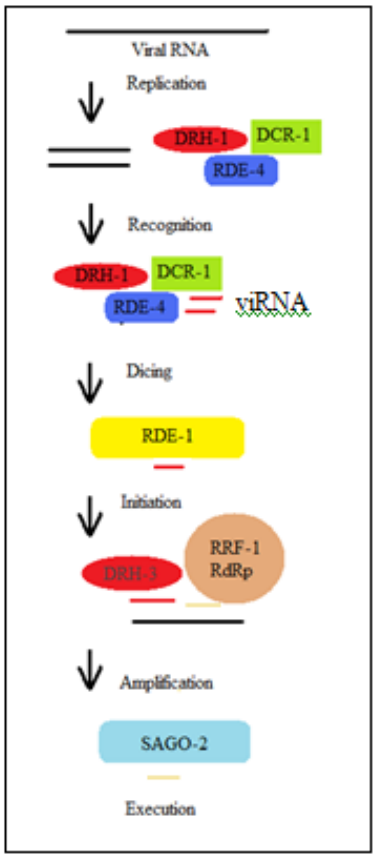

Figure 1.1 Model for antiviral RNAi in *C. elegans*

Model of antiviral RNA interference systems in C. elegans: DRH-1 is required for the biogenesis of primary viRNAs, and DRH-3 is required for the biogenesis of secondary viRNAs. After the amplification of antiviral RNAi signals, these secondary viRNAs are loaded into secondary argonaute SAGO-2 for functioning (modified from Alyson Ashe. et al., 2013).

As defense, viruses have evolved to encode viral suppressors of RNAi (VSRs) which are essential for their infection of plants and animals. These include VSRs targeting the protein and RNA components of RNAi (Wu et al., 2010). For example, one of the VSR activities of the Cucumber mosaic virus 2b protein is to bind AGO1 and inhibit *in vitro* slicing of the target RNA. The VSR protein B2 from Flock house virus (FHV) contains a novel dsRNA domain and inhibits processing of long dsRNA into siRNAs (Chao et al., 2005; Lingel et al., 2005; Lu et al., 2005). Unlike the protein-targeting VSRs, dsRNA/siRNA-sequestering VSRs can have broad-spectrum RNAi suppression activities in diverse host organisms (Li et al., 2002).

1.3 Systemic RNAi

RNAi is systemic in *C. elegans* as is found in plants (Voinnet, 2005). This systemic nature is demonstrated by the fact that *C. elegans* RNAi can be triggered by soaking in dsRNA solutions or by feeding dsRNA (known as feeding RNAi). RNA silencing signals can be transferred between different tissues, indicating that *C. elegans* has unique pathways to regulate the spreading of RNA silencing signals. Genes required for systemic RNAi have been identified by forward genetics screens in *C. elegans* and can be grouped into two categories based on the susceptibility of the germline gene *pop-1* and the somatic gene *unc-22* feeding RNAi results (Winston et al., 2002; Tijsterman et al., 2004; Winston et al., 2007; Hinas et al., 2012; Jose et al., 2012). The first group of genes include RSD-2- a large protein with no discernible motifs or close homolog in other organisms, RSD-3- homolog of a human protein- enthoprotin involved in mammalian

vesicle trafficking, and RSD-6 which contains a Tudor domain frequently found in RNA binding proteins. These genes are required for the transmission of RNA silencing signals from somatic tissues to germline (Tijsterman et al., 2004).

The second group of genes encode SID-1 (also named RSD-8) and RSD-4 which appear to regulate the cellular uptake of silencing signals (Spradling et al., 2000; Tijsterman et al., 2004; Han et al., 2008). SID-1 is a dsRNA channel with conserved human and mouse homologs and it enables passive (ATP-independent) uptake of dsRNA to regulate the spreading of RNAi signals in *C. elegans*. The spreading RNAi signals in worms appear to be dsRNA (Feinberg and Hunter, 2003; Shih and Hunter, 2011). The size of RNA molecules is not directly related to the transport efficiency of SID-1 dsRNA channel (Shih et al., 2009; Luo et al., 2012). However, SID-1 is not required for the export of silencing signals (Jose et al., 2009). SID-2 is a single-pass transmembrane protein which requires an acidic extracellular environment and is selective for dsRNAs at least 50bp long. The function of SID-2 in RNAi spreading is related to endocytosis and is downstream of the uptake process mediated by SID-1 (McEwan et al., 2012). Although SID-1 and SID-2 are both required for the uptake of RNA silencing signals from environment, SID-1 also regulates the dissemination of silencing signals among the intestinal cells while SID-2 is only required for the silencing signals uptake from gut lumen. SID-3 is a cytoplasmic tyrosine kinase required for the efficient import of dsRNA into cells. The mammalian homolog of SID-3 is the activated cdc-42–associated kinase (ACK) that acts in many signaling pathways including responses to environmental changes and is known to directly associate with endocytic vesicles. Silencing signals

through SID-3 may promote the endocytic uptake of dsRNA for the eventual import through the dsRNA channel protein SID-1 into the cytoplasm in *C. elegans* (Jose et al., 2012). SID-5 is an endosome-associated protein required for intestinal transport of RNA silencing signals independent of SID-1. Unlike SID-1and SID-3, SID-5 is not required for the import of silencing signals but is essential for the SID-1 independent silencing signal export. SID-5 may also regulate cell-autonomous RNAi in addition to its role in systemic silencing (Hinas et al., 2012). In *C. elegans,* long dsRNA is indicated to be the RNAi spreading signal largely due to the role of SID-1 as a dsRNA channel protein (Shih et al., 2009; Shih and Hunter, 2011). However, systemic silencing is mediated in plants by the long-distance spread of siRNAs processed from long dsRNA (Dunoyer et al., 2010; Molnar et al., 2010; Melnyk et al., 2011).

1.4 Genetic screening in *C. elegans*

An opportune approach to determine the biological functions of genes in organism is to generate mutants with altered phenotypes or physiological responses through forward genetics screen. Various methods of forward genetics mutagenesis including chemicals- like N-Ethyl-N-Nitrosourea (ENU), EMS, Methylazoxymethanol (MAM) or Dimethyl sulfide(DMS) (Brenner, 1974; de Angelis et al., 2000; Hoffmann et al., 2002), radiation mutagenesis methods using X-ray or ultraviolet radiation and recombination related random insertion methods- like T-DNA insertion in plants have been developed (Zhang et al., 2011) . In the current post-genomic era when most model organisms like *Arabidopsis thaliana*, *Drosophila melanogaster, C. elegans* and *Mus musculus* were

completely sequenced, the usage of reverse genetic approach to study the genes functions has been widely applied. With development of forward genetics techniques such as Targeting induced local lesions in genomes (TILLING), EMS mutagenesis can be used for both forward and reverse genetic studies as generation of diverse mutant alleles in the same gene also provides critical tools to better understand the functions of a known gene (McCallum et al., 2000; Kim et al., 2006).

As a widely used mutagen in forward genetics research, EMS is a strong alkylation agent: it can induce chemical modification of nucleotides in the DNA molecules of the treated organism gametes. Alkylation agents like EMS can trigger strong and biased alkylation of guanine (G) residues, ending in previously G/C (Cytosine) pair being permanently substituted by a T (Thymine)/A (Adenine) pair in the gametes and subsequent progenies. This transition can result in various nonsense or missense mutations in *C. elegans* (Bokel, 2008; Kutscher and Shaham, 2014). Moreover, these point mutations may also lead to missense mutations which can cause the alteration of amino acids, and in rare occasions it may cause a deletion or insertion which can result in a frameshift that may lead to a different protein translation. Sometimes, missense mutations in certain critical genome sites may also lead to a partial deactivation of the function of the entire protein or even larger impact on the protein function (Karkkainen et al., 2000; Tijsterman et al., 2004; Gammie et al., 2007).

Among the genes required for RNAi in C. elegans, a large number of these members were discovered using EMS mutagenesis or other forward genetics mutagenesis method:

Craig Mello group has identified genes involved in the core RNAi machinery like RDE-1, RDE-2, and RDE-4 according to their susceptibility to feeding and microinjection RNAi. Moreover, Shouhong Guang discovered the nuclear RNAi pathway components NRDE-2 and NRDE-3 through EMS mutagenesis (Guang et al., 2008; Guang et al., 2010). Furthermore, *C. elegans* systemic RNAi genes: SID-1, SID-2, SID-3 and SID-5 were found by Craig Hunter group using a transgenic strain that allows simultaneous monitoring of localized and systemic RNAi by expressing two green fluorescent protein (GFP) transgenes in different tissues after EMS mutagenesis (Winston et al., 2002; Winston et al., 2007; Hinas et al., 2012; Jose et al., 2012). In addition, with technics including EMS mutagenesis and feeding RNAi targeting different genes in somatic tissues and germline, Marcel Tijsterman found that RSD-2, RSD-3, RSD-4 and also RSD-6 were required in the transmission of silencing signals as well (Tijsterman et al., 2004).

Due to the accessibility of gene knockdown in *C. elegans*, RNAi based reverse genetics screen has also been conducted for identification of gene functions from five respective chromosomes of *C. elegans* genomes by feeding worms with bacteria that expresses double-stranded RNA. These researches enhanced the understanding of *C. elegans* genome tremendously, for example, the functional genomics analysis conducted by Andrew G Fraser on chromosome I assigned functions to 13.9% of the genes analyzed, thus increasing the number of sequenced genes with known phenotypes on chromosome I from 70 to 378 (Fraser et al., 2000). Pierre Gönczy also utilized high

throughput reverse genetics screen and found that 6% of the 2,300 open reading frames in *C. elegans* were important in the *C. elegans* cell division (Gonczy et al., 2000).

Reverse genetics screen also helped researchers to search for genes related to different diseases both in plants and in animals. For example, a pilot reverse genetics screen was conducted in *C. elegans* targeting antiviral immunity related genes by Rui Lu from our lab and identified genes including RSD-2 and RRF-1 as requirements for antiviral immunity (Lu et al., 2009).

1.5 Two viruses used in this research

In this research, Flock house virus (FHV) and Orsay virus were used to study the systemic RNAi genes roles in antiviral immunity. Flock house virus was originally isolated from the grass grub *Costelytra zealandica* (Coleoptera) in New Zealand and is a member of *Nodaviridae* virus family (Scotti et al., 1983). Composed of alpha nodaviruses and beta nodaviruses, *Nodaviridae* family is known to be capable of infecting a vast range of hosts from vertebrates like fishes to invertebrates like insects (Furusawa et al., 2006; Bai et al., 2011). FHV is a bipartite virus containing RNA1 which encodes the Protein A- a RNA dependent RNA polymerase and RNA2 which encodes the virus capsid protein (Johnson and Ball, 1997). A subgenomic RNA3 derived from RNA1contains two Open reading frames (ORFs) and encodes B2 protein as viral suppressors of RNAi (VSRs) (Lingel et al., 2005).

Being a model virus for replication and immunity research, FHV was clearly demonstrated in its replication process by various researches. FHV forms ~50-nm

replication spherules on the outer membrane of mitochondria of the infected cells (Miller et al., 2001; Kopek et al., 2007). The replication of FHV requires both cis-acting activation and trans-acting activation. For instance, two distinct replication elements are required to produce RNA1 and two cis elements- a proximal control element and a distal control element command the production of RNA3 (Lindenbach et al., 2002). Furthermore, the replication of RNA2 requires *in trans* activation of subgenomic RNA3 (Eckerle and Ball, 2002). In addition, replication of an RNA2 derivative is dependent on RNA1 templates capability of forming the long-distance interaction that controls RNA3 production (Lindenbach et al., 2002). The packaging of FHV virus particle and replication process are intimately coupled (Venter et al., 2009); and the transcription of FHV CP mRNA (RNA2) and its translation must be synchronized to confer packaging specificity (Annamalai et al., 2008). Not only is a model for replication research, as a non-enveloped RNA virus FHV also widely used as a model system for non-enveloped RNA virus entry and membrane penetration (Odegard et al., 2010).

Another virus used in this research is Orsay virus. Found together in 2011, Orsay virus, Le Blanc virus and Santeuil virus are capable of replicating respectively in different *C. elegans* and *C. briggsae* field isolates (Felix et al., 2011; Franz et al., 2012). All of them are bipartite RNA viruses with a relative homology to FHV virus. Like FHV and other nodaviruses, Orsay virus also encodes an RNA1 molecule which is the RdRp responsible for the replication of Orsay virus, and an RNA2 molecule which encodes the viral capsid protein. But different from FHV, Orsay virus does not encode any protein with viral suppressor activity (Guo and Lu, 2013). Therefore, Orsay virus could hardly

infect wild type canonical strain nematodes. Also differing from nodaviruses, the Orsay virus RNA2 segment encodes a putative novel delta protein with unknown function. And it uses a ribosomal frameshifting strategy to express a novel fusion protein from the viral capsid (alpha ORF) and delta ORFs (Jiang et al., 2014).

1.6 Scope of research

The aim of this dissertation is to determine if systemic RNAi plays an important role in antiviral RNAi in *C. elegans*. It is clear that systemic RNAi is indispensable for the antiviral defense and it is specifically targeted for suppression by VSRs in plants (Voinnet et al., 1998; Voinnet, 2005).

For example, most phytoviruses activate an RNA silencing defense, and systemic silencing is a component of this response (Voinnet, 2005). However, although loss of SID-1 did not enhance the infection of cultured *C. elegans* primary cells by VSV (Schott et al., 2005), knockdown of RSD-2 by feeding RNAi enhanced the accumulation of the GFP-expressing FHV replicon in *C. elegans* animals (Lu et al., 2009). In Chapter 1 of this dissertation, a potential antiviral role for RSD-2 and other genes implicated in systemic RNAi was examined using the FHV replicon and genetic loss-of-function *C. elegans* mutants. Chapter 2 further characterized the antiviral function of systemic RNAi genes during infection of *C. elegans* by Orsay virus. And Appendix section describes the efforts on EMS mutagenesis forward genetic screen as well snip-SNPs mapping.

As a member of alphanodavirus, FHV infects both fruit fly, the wax moth *Galleria mellonella* and *Nicotiana benthamiana* plants, and it can also replicate in yeast

and mammalian cells like BHK21 (Selling et al., 1990; Ball et al., 1994; Price et al., 1996; Mahajan-Miklos et al., 1999; Seo et al., 2012). As a result, FHV is widely used as a model virus to study virus replication and packaging as well as antiviral RNAi (Li et al., 2002; Wang et al., 2006; Annamalai et al., 2008; Seo et al., 2012). Orsay virus was isolated from a *C. elegans* strain defective in DRH-1 (Felix et al., 2011). Studies based on authentic infection by Orsay virus have confirmed the importance of RNAi pathway genes in antiviral immunity (Felix et al., 2011). Therefore, in this research these two viruses were selected for the research of antiviral immunity related genes in *C. elegans*.

1.7 References

Aliyari, R., Q. F. Wu, H. W. Li, X. H. Wang, F. Li, L. D. Green, C. S. Han, W. X. Li and S. W. Ding (2008). Mechanism of Induction and Suppression of Antiviral Immunity Directed by Virus-Derived Small RNAs in Drosophila. *Cell Host & Microbe* **4**(4): 387-97.

Angell, S. M. and D. C. Baulcombe (1997). Consistent gene silencing in transgenic plants expressing a replicating potato virus X RNA. *Embo Journal* **16**(12): 3675-84.

Annamalai, P., F. Rofail, D. A. Demason and A. L. Rao (2008). Replication-coupled packaging mechanism in positive-strand RNA viruses: synchronized coexpression of functional multigenome RNA components of an animal and a plant virus in Nicotiana benthamiana cells by agroinfiltration. *J Virol* **82**(3): 1484-95.

Annamalai, P., F. Rofail, D. A. DeMason and A. L. N. Rao (2008). Replication-coupled packaging mechanism in positive-strand RNA viruses: Synchronized coexpression of functional multigenome RNA components of an animal and a plant virus in Nicotiana benthamiana cells by agroinfiltration. *Journal of Virology* **82**(3): 1484-95.

Aoki, K., H. Moriguchi, T. Yoshioka, K. Okawa and H. Tabara (2007). In vitro analyses of the production and activity of secondary small interfering RNAs in C-elegans. *Embo Journal* **26**(24): 5007-19.

Ashe, A., T. Belicard, J. Le Pen, P. Sarkies, L. Frezal, N. J. Lehrbach, M. A. Felix and E. A. Miska (2013). A deletion polymorphism in the Caenorhabditis elegans RIG-I homolog disables viral RNA dicing and antiviral immunity. *Elife* **2**.

Bai, H., Y. Wang, X. Li, H. Mao, Y. Li, S. Han, Z. Shi and X. Chen (2011). Isolation and characterization of a novel alphanodavirus. *Virol J* **8**: 311.

Ball, L. A., B. Wohlrab and Y. Li (1994). Nodavirus Rna Replication - Mechanism and Harnessing to Vaccinia Virus Recombinants. *Archives of Virology*: 407-16.

Bartel, D. P. (2004). MicroRNAs: Genomics, biogenesis, mechanism, and function. *Cell* **116**(2): 281-97.

Batista, P. J., J. G. Ruby, J. M. Claycomb, R. Chiang, N. Fahlgren, K. D. Kasschau, D. A. Chaves, W. F. Gu, J. J. Vasale, S. H. Duan, D. Conte, S. J. Luo, G. P. Schroth, J. C. Carrington, D. P. Bartel and C. C. Mello (2008). PRG-1 and 21U-RNAs interact to form the piRNA complex required for fertility in C-elegans. *Molecular Cell* **31**(1): 67-78.

Bernstein, E., A. A. Caudy, S. M. Hammond and G. J. Hannon (2001). Role for a bidentate ribonuclease in the initiation step of RNA interference. *Nature* **409**(6818): 363-66.

Bokel, C. (2008). EMS screens : from mutagenesis to screening and mapping. *Methods Mol Biol* **420**: 119-38.

Boutet, S., F. Vazquez, J. Liu, C. Beclin, M. Fagard, A. Gratias, J. B. Morel, P. Crete, X. M. Chen and H. Vaucheret (2003). Arabidopsis HEN1: A genetic link between endogenous miRNA controlling development and siRNA controlling transgene silencing and virus resistance. *Current Biology* **13**(10): 843-48.

Brenner, S. (1974). Genetics of Caenorhabditis-Elegans. *Genetics* **77**(1): 71-94.

Castel, S. E. and R. A. Martienssen (2013). RNA interference in the nucleus: roles for small RNAs in transcription, epigenetics and beyond. *Nature Reviews Genetics* **14**(2): 100-12.

Chao, J. A., J. H. Lee, B. R. Chapados, E. W. Debler, A. Schneemann and J. R. Williamson (2005). Dual modes of RNA-silencing suppression by Flock House virus protein B2. *Nat Struct Mol Biol* **12**: 952-57.

Claycomb, J. M., P. J. Batista, K. M. Pang, W. F. Gu, J. J. Vasale, J. C. van Wolfswinkel, D. A. Chaves, M. Shirayama, S. Mitani, R. F. Ketting, D. Conte and C. C. Mello (2009). The Argonaute CSR-1 and Its 22G-RNA Cofactors Are Required for Holocentric Chromosome Segregation. *Cell* **139**(1): 123-34.

Conine, C. C., P. J. Batista, W. F. Gu, J. M. Claycomb, D. A. Chaves, M. Shirayama and C. C. Mello (2010). Argonautes ALG-3 and ALG-4 are required for spermatogenesis-specific 26G-RNAs and thermotolerant sperm in Caenorhabditis elegans. *Proceedings of the National Academy of Sciences of the United States of America* **107**(8): 3588-93.

Das, P. P., M. P. Bagijn, L. D. Goldstein, J. R. Woolford, N. J. Lehrbach, A. Sapetschnig, H. R. Buhecha, M. J. Gilchrist, K. L. Howe, R. Stark, N. Matthewss, E. Berezilkov, R. F. Ketting, S. Tavare and E. A. Miska (2008). Piwi and piRNAs act upstream of an endogenous siRNA pathway to suppress Tc3 transposon mobility in the Caenorhabditis elegans germline. *Molecular Cell* **31**(1): 79-90.

de Angelis, M. H., H. Flaswinkel, H. Fuchs, B. Rathkolb, D. Soewarto, S. Marschall, S. Heffner, W. Pargent, K. Wuensch, M. Jung, A. Reis, T. Richter, F. Alessandrini, T. Jakob, E. Fuchs, H. Kolb, E. Kremmer, K. Schaeble, B. Rollinski, A. Roscher, C. Peters, T. Meitinger, T. Strom, T. Steckler, F. Holsboer, T. Klopstock, F. Gekeler, C. Schindewolf, T. Jung, K. Avraham, H. Behrendt, J. Ring, A. Zimmer, K. Schughart, K.

Pfeffer, E. Wolf and R. Balling (2000). Genome-wide, large-scale production of mutant mice by ENU mutagenesis. *Nature Genetics* **25**(4): 444-47.

Diaz-Pendon, J. A., F. Li, W. X. Li and S. W. Ding (2007). Suppression of antiviral silencing by cucumber mosaic virus 2b protein in Arabidopsis is associated with drastically reduced accumulation of three classes of viral small interfering RNAs. *Plant Cell* **19**(6): 2053-63.

Dougherty, W. G., J. A. Lindbo, H. A. Smith, T. D. Parks, S. Swaney and W. M. Proebsting (1994). Rna-Mediated Virus-Resistance in Transgenic Plants - Exploitation of a Cellular Pathway Possibly Involved in Rna Degradation. *Molecular Plant-Microbe Interactions* **7**(5): 544-52.

Dunoyer, P., G. Schott, C. Himber, D. Meyer, A. Takeda, J. C. Carrington and O. Voinnet (2010). Small RNA duplexes function as mobile silencing signals between plant cells. *Science* **328**(5980): 912-6.

Eckerle, L. D. and L. A. Ball (2002). Replication of the RNA segments of a bipartite viral genome is coordinated by a transactivating subgenomic RNA. *Virology* **296**(1): 165-76.

Feinberg, E. H. and C. P. Hunter (2003). Transport of dsRNA into cells by the transmembrane protein SID-1. *Science* **301**(5639): 1545-47.

Felix, M. A., A. Ashe, J. Piffaretti, G. Wu, I. Nuez, T. Belicard, Y. F. Jiang, G. Y. Zhao, C. J. Franz, L. D. Goldstein, M. Sanroman, E. A. Miska and D. Wang (2011). Natural and Experimental Infection of Caenorhabditis Nematodes by Novel Viruses Related to Nodaviruses. *Plos Biology* **9**(1).

Fire, A., S. Q. Xu, M. K. Montgomery, S. A. Kostas, S. E. Driver and C. C. Mello (1998). Potent and specific genetic interference by double-stranded RNA in Caenorhabditis elegans. *Nature* **391**(6669): 806-11.

Franz, C. J., G. Zhao, M. A. Felix and D. Wang (2012). Complete genome sequence of Le Blanc virus, a third Caenorhabditis nematode-infecting virus. *J Virol* **86**(21): 11940.

Fraser, A. G., R. S. Kamath, P. Zipperlen, M. Martinez-Campos, M. Sohrmann and J. Ahringer (2000). Functional genomic analysis of C. elegans chromosome I by systematic RNA interference. *Nature* **408**(6810): 325-30.

Furusawa, R., Y. Okinaka and T. Nakai (2006). Betanodavirus infection in the freshwater model fish medaka (Oryzias latipes). *J Gen Virol* **87**(Pt 8): 2333-9.

Gammie, A. E., N. Erdeniz, J. Beaver, B. Devlin, A. Nanji and M. D. Rose (2007). Functional characterization of pathogenic human MSH2 missense mutations in Saccharomyces cerevisiae. *Genetics* **177**(2): 707-21.

Gent, J. I., A. T. Lamm, D. M. Pavelec, J. M. Maniar, P. Parameswaran, L. Tao, S. Kennedy and A. Z. Fire (2010). Distinct Phases of siRNA Synthesis in an Endogenous RNAi Pathway in C. elegans Soma. *Molecular Cell* **37**(5): 679-89.

Ghildiyal, M. and P. D. Zamore (2009). Small silencing RNAs: an expanding universe. *Nature Reviews Genetics* **10**(2): 94-108.

Gonczy, P., C. Echeverri, K. Oegema, A. Coulson, S. J. M. Jones, R. R. Copley, J. Duperon, J. Oegema, M. Brehm, E. Cassin, E. Hannak, M. Kirkham, S. Pichler, K. Flohrs, A. Goessen, S. Leidel, A. M. Alleaume, C. Martin, N. Ozlu, P. Bork and A. A. Hyman (2000). Functional genomic analysis of cell division in C-elegans using RNAi of genes on chromosome III. *Nature* **408**(6810): 331-36.

Grishok, A., A. E. Pasquinelli, D. Conte, N. Li, S. Parrish, I. Ha, D. L. Baillie, A. Fire, G. Ruvkun and C. C. Mello (2001). Genes and mechanisms related to RNA interference regulate expression of the small temporal RNAs that control C-elegans developmental timing. *Cell* **106**(1): 23-34.

Gu, W. F., M. Shirayama, D. Conte, J. Vasale, P. J. Batista, J. M. Claycomb, J. J. Moresco, E. M. Youngman, J. Keys, M. J. Stoltz, C. C. G. Chen, D. A. Chaves, S. H. Duan, K. D. Kasschau, N. Fahlgren, J. R. Yates, S. Mitani, J. C. Carrington and C. C. Mello (2009). Distinct Argonaute-Mediated 22G-RNA Pathways Direct Genome Surveillance in the C. elegans Germline. *Molecular Cell* **36**(2): 231-44.

Guang, S., A. F. Bochner, K. B. Burkhart, N. Burton, D. M. Pavelec and S. Kennedy (2010). Small regulatory RNAs inhibit RNA polymerase II during the elongation phase of transcription. *Nature* **465**(7301): 1097-101.

Guang, S., A. F. Bochner, D. M. Pavelec, K. B. Burkhart, S. Harding, J. Lachowiec and S. Kennedy (2008). An Argonaute transports siRNAs from the cytoplasm to the nucleus. *Science* **321**(5888): 537-41.

Guo, S. and K. J. Kemphues (1995). Par-1, a Gene Required for Establishing Polarity in C-Elegans Embryos, Encodes a Putative Ser/Thr Kinase That Is Asymmetrically Distributed. *Cell* **81**(4): 611-20.

Guo, X. and R. Lu (2013). Characterization of virus-encoded RNA interference suppressors in Caenorhabditis elegans. *J Virol* **87**(10): 5414-23.

Guo, X. Y., R. Zhang, J. Wang, S. W. Ding and R. Lu (2013). Homologous RIG-I-like helicase proteins direct RNAi-mediated antiviral immunity in C. elegans by distinct mechanisms. *Proceedings of the National Academy of Sciences of the United States of America* **110**(40): 16085-90.

Hamilton, A. J. and D. C. Baulcombe (1999). A species of small antisense RNA in posttranscriptional gene silencing in plants. *Science* **286**(5441): 950-52.

Hammond, S. M. (2005). Dicing and slicing - The core machinery of the RNA interference pathway. *Febs Letters* **579**(26): 5822-29.

Hammond, S. M., E. Bernstein, D. Beach and G. J. Hannon (2000). An RNA-directed nuclease mediates post-transcriptional gene silencing in Drosophila cells. *Nature* **404**(6775): 293-96.

Han, T., A. P. Manoharan, T. T. Harkins, P. Bouffard, C. Fitzpatrick, D. S. Chu, D. Thierry-Mieg, J. Thierry-Mieg and J. K. Kim (2009). 26G endo-siRNAs regulate spermatogenic and zygotic gene expression in Caenorhabditis elegans. *Proceedings of the National Academy of Sciences of the United States of America* **106**(44): 18674-79.

Han, W., P. Sundaram, H. Kenjale, J. Grantham and L. Timmons (2008). The Caenorhabditis elegans rsd-2 and rsd-6 genes are required for chromosome functions during exposure to unfavorable environments. *Genetics* **178**(4): 1875-93.

Hinas, A., A. J. Wright and C. P. Hunter (2012). SID-5 Is an Endosome-Associated Protein Required for Efficient Systemic RNAi in C. elegans. *Current Biology* **22**(20): 1938-43.

Hoffmann, G. R., D. J. Crowley and P. J. Theophiles (2002). Comparative potencies of induction of point mutations and genetic duplications by the methylating agents methylazoxymethanol and dimethyl sulfate in bacteria. *Mutagenesis* **17**(5): 439-44.

Hutvagner, G. and M. J. Simard (2008). Argonaute proteins: key players in RNA silencing. *Nature Reviews Molecular Cell Biology* **9**(1): 22-32.

Jiang, H. B., C. J. Franz, G. Wu, H. Renshaw, G. Y. Zhao, A. E. Firth and D. Wang (2014). Orsay virus utilizes ribosomal frameshifting to express a novel protein that is incorporated into virions. *Virology* **450**: 213-21.

Johnson, K. L. and L. A. Ball (1997). Replication of flock house virus RNAs from primary transcripts made in cells by RNA polymerase II. *J Virol* **71**(4): 3323-7.

Jose, A. M., Y. A. Kim, S. Leal-Ekman and C. P. Hunter (2012). Conserved tyrosine kinase promotes the import of silencing RNA into Caenorhabditis elegans cells.

Proceedings of the National Academy of Sciences of the United States of America **109**(36): 14520-25.

Jose, A. M., J. J. Smith and C. P. Hunter (2009). Export of RNA silencing from C-elegans tissues does not require the RNA channel SID-1. *Proceedings of the National Academy of Sciences of the United States of America* **106**(7): 2283-88.

Kamminga, L. M., J. C. van Wolfswinkel, M. J. Luteijn, L. J. T. Kaaij, M. P. Bagijn, A. Sapetschnig, E. A. Miska, E. Berezikov and R. F. Ketting (2012). Differential Impact of the HEN1 Homolog HENN-1 on 21U and 26G RNAs in the Germline of Caenorhabditis elegans. *Plos Genetics* **8**(7).

Karkkainen, M. J., R. E. Ferrell, E. C. Lawrence, M. A. Kimak, K. L. Levinson, M. A. McTigue, K. Alitalo and D. N. Finegold (2000). Missense mutations interfere with VEGFR-3 signalling in primary lymphoedema. *Nat Genet* **25**(2): 153-9.

Ketting, R. F., S. E. J. Fischer, E. Bernstein, T. Sijen, G. J. Hannon and R. H. A. Plasterk (2001). Dicer functions in RNA interference and in synthesis of small RNA involved in developmental timing in C-elegans. *Genes & Development* **15**(20): 2654-59.

Kim, Y., K. S. Schumaker and J. K. Zhu (2006). EMS mutagenesis of Arabidopsis. *Methods Mol Biol* **323**: 101-3.

Knight, S. W. and B. L. Bass (2001). A role for the RNase III enzyme DCR-1 in RNA interference and germ line development in Caenorhabditis elegans. *Science* **293**(5538): 2269-71.

Kopek, B. G., G. Perkins, D. J. Miller, M. H. Ellisman and P. Ahlquist (2007). Three-dimensional analysis of a viral RNA replication complex reveals a virus-induced mini-organelle. *PLoS Biol* **5**(9): e220.

Kumagai, M. H., J. Donson, G. Dellacioppa, D. Harvey, K. Hanley and L. K. Grill (1995). Cytoplasmic Inhibition of Carotenoid Biosynthesis with Virus-Derived Rna. *Proceedings of the National Academy of Sciences of the United States of America* **92**(5): 1679-83.

Kutscher, L. M. and S. Shaham (2014). Forward and reverse mutagenesis in C. elegans. *WormBook*: 1-26.

Lai, C. H., C. Y. Chou, L. Y. Ch'ang, C. S. Liu and W. C. Lin (2000). Identification of novel human genes evolutionarily conserved in Caenorhabditis elegans by comparative proteomics. *Genome Research* **10**(5): 703-13.

Li, H. W., W. X. Li and S. W. Ding (2002). Induction and suppression of RNA silencing by an animal virus. *Science* **296**(5571): 1319-21.

Li, Y., J. Lu, Y. Han, X. Fan and S. W. Ding (2013). RNA interference functions as an antiviral immunity mechanism in mammals. *Science* **342**(6155): 231-4.

Lindenbach, B. D., J. Y. Sgro and P. Ahlquist (2002). Long-distance base pairing in flock house virus RNA1 regulates subgenomic RNA3 synthesis and RNA2 replication. *J Virol* **76**(8): 3905-19.

Lindenbach, B. D., J. Y. Sgro and P. Ahlquist (2002). Long-distance base pairing in flock house virus RNA1 regulates subgenomic RNA3 synthesis and RNA2 replication. *Journal of Virology* **76**(8): 3905-19.

Lingel, A., B. Simon, E. Izaurralde and M. Sattler (2005). The structure of the flock house virus B2 protein, a viral suppressor of RNA interference, shows a novel mode of double-stranded RNA recognition. *Embo Reports* **6**(12): 1149-55.

Lu, R., M. Maduro, F. Li, H. W. Li, G. Broitman-Maduro, W. X. Li and S. W. Ding (2005). Animal virus replication and RNAi-mediated antiviral silencing in Caenorhabditis elegans. *Nature* **436**(7053): 1040-3.

Lu, R., E. Yigit, W. X. Li and S. W. Ding (2009). An RIG-I-Like RNA Helicase Mediates Antiviral RNAi Downstream of Viral siRNA Biogenesis in Caenorhabditis elegans. *Plos Pathogens* **5**(2).

Luo, Y., X. H. Wang, D. Yu and L. Kang (2012). The SID-1 double-stranded RNA transporter is not required for systemic RNAi in the migratory locust. *Rna Biology* **9**(5): 663-71.

Mahajan-Miklos, S., M. W. Tan, L. G. Rahme and F. M. Ausubel (1999). Molecular mechanisms of bacterial virulence elucidated using a Pseudomonas aeruginosa Caenorhabditis elegans pathogenesis model. *Cell* **96**(1): 47-56.

Maillard, P. V., C. Ciaudo, A. Marchais, Y. Li, F. Jay, S. W. Ding and O. Voinnet (2013). Antiviral RNA Interference in Mammalian Cells. *Science* **342**(6155): 235-38.

McCallum, C. M., L. Comai, E. A. Greene and S. Henikoff (2000). Targeting induced local lesions IN genomes (TILLING) for plant functional genomics. *Plant Physiol* **123**(2): 439-42.

McEwan, D. L., A. S. Weisman and C. P. Huntert (2012). Uptake of Extracellular Double-Stranded RNA by SID-2. *Molecular Cell* **47**(5): 746-54.

Melnyk, C. W., A. Molnar and D. C. Baulcombe (2011). Intercellular and systemic movement of RNA silencing signals. *Embo J* **30**(17): 3553-63.

Miller, D. J., M. D. Schwartz and P. Ahlquist (2001). Flock house virus RNA replicates on outer mitochondrial membranes in Drosophila cells. *J Virol* **75**(23): 11664-76.

Miska, E. A. and J. Ahringer (2007). RNA interference has second helpings. *Nature Biotechnology* **25**(3): 302-03.

Molnar, A., C. W. Melnyk, A. Bassett, T. J. Hardcastle, R. Dunn and D. C. Baulcombe (2010). Small silencing RNAs in plants are mobile and direct epigenetic modification in recipient cells. *Science* **328**(5980): 872-5.

Morel, J. B., C. Godon, P. Mourrain, C. Beclin, S. Boutet, F. Feuerbach, F. Proux and H. Vaucheret (2002). Fertile hypomorphic ARGONAUTE (ago1) mutants impaired in post-transcriptional gene silencing and virus resistance. *Plant Cell* **14**(3): 629-39.

Mourrain, P., C. Beclin, T. Elmayan, F. Feuerbach, C. Godon, J. B. Morel, D. Jouette, A. M. Lacombe, S. Nikic, N. Picault, K. Remoue, M. Sanial, T. A. Vo and H. Vaucheret (2000). Arabidopsis SGS2 and SGS3 genes are required for posttranscriptional gene silencing and natural virus resistance. *Cell* **101**(5): 533-42.

Napoli, C., C. Lemieux and R. Jorgensen (1990). Introduction of a Chimeric Chalcone Synthase Gene into Petunia Results in Reversible Co-Suppression of Homologous Genes in Trans. *Plant Cell* **2**(4): 279-89.

Odegard, A., M. Banerjee and J. E. Johnson (2010). Flock house virus: a model system for understanding non-enveloped virus entry and membrane penetration. *Curr Top Microbiol Immunol* **343**: 1-22.

Pak, J., J. M. Maniar, C. C. Mello and A. Fire (2012). Protection from Feed-Forward Amplification in an Amplified RNAi Mechanism. *Cell* **151**(4): 885-99.

Parrish, S. and A. Fire (2001). Distinct roles for RDE-1 and RDE-4 during RNA interference in Caenorhabditis elegans. *Rna-a Publication of the Rna Society* **7**(10): 1397-402.

Price, B. D., R. R. Rueckert and P. Ahlquist (1996). Complete replication of an animal virus and maintenance of expression vectors derived from it in Saccharomyces cerevisiae. *Proceedings of the National Academy of Sciences of the United States of America* **93**(18): 9465-70.

Qu, F. (2010). Antiviral Role of Plant-Encoded RNA-Dependent RNA Polymerases Revisited with Deep Sequencing of Small Interfering RNAs of Virus Origin. *Molecular Plant-Microbe Interactions* **23**(10): 1248-52.

Qu, F., X. H. Ye and T. J. Morris (2008). Arabidopsis DRB4, AG01, AG07, and RDR6 participate in a DCL4-initiated antiviral RNA silencing pathway negatively regulated by DCL1. *Proceedings of the National Academy of Sciences of the United States of America* **105**(38): 14732-37.

Ruby, J. G., C. Jan, C. Player, M. J. Axtell, W. Lee, C. Nusbaum, H. Ge and D. P. Bartel (2006). Large-scale sequencing reveals 21U-RNAs and additional microRNAs and endogenous siRNAs in C-elegans. *Cell* **127**(6): 1193-207.

Schott, D. H., D. K. Cureton, S. P. Whelan and C. P. Hunter (2005). An antiviral role for the RNA interference machinery in Caenorhabditis elegans. *Proc Natl Acad Sci U S A* **102**(51): 18420-4.

Scotti, P. D., S. Dearing and D. W. Mossop (1983). Flock House Virus - a Nodavirus Isolated from Costelytra-Zealandica (White) (Coleoptera, Scarabaeidae). *Archives of Virology* **75**(3): 181-89.

Selling, B. H., R. F. Allison and P. Kaesberg (1990). Genomic Rna of an Insect Virus Directs Synthesis of Infectious Virions in Plants. *Proceedings of the National Academy of Sciences of the United States of America* **87**(1): 434-38.

Seo, J. K., S. J. Kwon and A. L. N. Rao (2012). A Physical Interaction between Viral Replicase and Capsid Protein Is Required for Genome-Packaging Specificity in an RNA Virus. *Journal of Virology* **86**(11): 6210-21.

Shih, J. D., M. C. Fitzgerald, M. Sutherlin and C. P. Hunter (2009). The SID-1 double-stranded RNA transporter is not selective for dsRNA length. *Rna-a Publication of the Rna Society* **15**(3): 384-90.

Shih, J. D. and C. P. Hunter (2011). SID-1 is a dsRNA-selective dsRNA-gated channel. *Rna-a Publication of the Rna Society* **17**(6): 1057-65.

Sijen, T., F. A. Steiner, K. L. Thijssen and R. H. A. Plasterk (2007). Secondary siRNAs result from unprimed RNA synthesis and form a distinct class. *Science* **315**(5809): 244-47.

Spradling, K. D., T. J. Burke, J. Lohi and B. K. Pilcher (2000). Cloning and initial characterization of human epsin 3, a novel matrix-induced keratinocyte specific transcript. *Journal of Investigative Dermatology* **115**(2): 332-32.

Tabara, H., M. Sarkissian, W. G. Kelly, J. Fleenor, A. Grishok, L. Timmons, A. Fire and C. C. Mello (1999). The rde-1 gene, RNA interference, and transposon silencing in C-elegans. *Cell* **99**(2): 123-32.

Tabara, H., E. Yigit, H. Siomi and C. C. Mello (2002). The dsRNA binding protein RDE-4 interacts with RDE-1, DCR-1, and a DExX-box helicase to direct RNAi in C-elegans. *Cell* **109**(7): 861-71.

Tijsterman, M., R. C. May, F. Simmer, K. L. Okihara and R. H. A. Plasterk (2004). Genes required for systemic RNA interference in Caenorhabditis elegans. *Current Biology* **14**(2): 111-16.

Vanderkrol, A. R., L. A. Mur, P. Delange, J. N. M. Mol and A. R. Stuitje (1990). Inhibition of Flower Pigmentation by Antisense Chs Genes - Promoter and Minimal Sequence Requirements for the Antisense Effect. *Plant Molecular Biology* **14**(4): 457-66.

Vasale, J. J., W. F. Gu, C. Thivierge, P. J. Batista, J. M. Claycomb, E. M. Youngman, T. F. Duchaine, C. C. Mello and D. Conte (2010). Sequential rounds of RNA-dependent RNA transcription drive endogenous small-RNA biogenesis in the ERGO-1/Argonaute pathway. *Proceedings of the National Academy of Sciences of the United States of America* **107**(8): 3582-87.

Venter, P. A., D. Marshall and A. Schneemann (2009). Dual roles for an arginine-rich motif in specific genome recognition and localization of viral coat protein to RNA replication sites in flock house virus-infected cells. *J Virol* **83**(7): 2872-82.

Voinnet, O. (2005). Induction and suppression of RNA silencing: Insights from viral infections. *Nature Reviews Genetics* **6**(3): 206-U1.

Voinnet, O. (2005). Non-cell autonomous RNA silencing. *Febs Letters* **579**(26): 5858-71.

Voinnet, O., P. Vain, S. Angell and D. C. Baulcombe (1998). Systemic spread of sequence-specific transgene RNA degradation in plants is initiated by localized introduction of ectopic promoterless DNA. *Cell* **95**(2): 177-87.

Wang, X. B., Q. F. Wu, T. Ito, F. Cillo, W. X. Li, X. M. Chen, J. L. Yu and S. W. Ding (2010). RNAi-mediated viral immunity requires amplification of virus-derived siRNAs in Arabidopsis thaliana. *Proceedings of the National Academy of Sciences of the United States of America* **107**(1): 484-89.

Wang, X. H., R. Aliyari, W. X. Li, H. W. Li, K. Kim, R. Carthew, P. Atkinson and S. W. Ding (2006). RNA interference directs innate immunity against viruses in adult Drosophila. *Science* **312**(5772): 452-4.

Wilkins, C., R. Dishongh, S. C. Moore, M. A. Whitt, M. Chow and K. Machaca (2005). RNA interference is an antiviral defence mechanism in Caenorhabditis elegans. *Nature* **436**(7053): 1044-47.

Winston, W. M., C. Molodowitch and C. P. Hunter (2002). Systemic RNAi in C-elegans requires the putative transmembrane protein SID-1. *Science* **295**(5564): 2456-59.

Winston, W. M., M. Sutherlin, A. J. Wright, E. H. Feinberg and C. P. Hunter (2007). Caenorhabditis elegans SID-2 is required for environmental RNA interference. *Proceedings of the National Academy of Sciences of the United States of America* **104**(25): 10565-70.

Wu, Q. F., X. B. Wang and S. W. Ding (2010). Viral Suppressors of RNA-Based Viral Immunity: Host Targets. *Cell Host & Microbe* **8**(1): 12-15.

Zhang, C., T. A. Montgomery, H. W. Gabel, S. E. J. Fischer, C. M. Phillips, N. Fahlgren, C. M. Sullivan, J. C. Carrington and G. Ruvkun (2011). mut-16 and other mutator class genes modulate 22G and 26G siRNA pathways in Caenorhabditis elegans. *Proceedings of the National Academy of Sciences of the United States of America* **108**(4): 1201-08.

Chapter 2: Genetic characterization of systemic RNAi-defective mutant nematodes in the antiviral immunity induced by replication of an RNA viral replicon

Abstract

Previous reverse genetic screen identified RSD-2, a gene related to systemic and dosage-sensitive RNAi responses, was required in the *Caenorhabditis elegans* antiviral immunity. In this chapter, I verified the importance of RSD-2 using a null genetic mutant of *rsd-2* and the FHV replicon. Genetic mutants of other systemic RNAi genes including RSD-3, RSD-6, SID-1, and RSD-4 were also introduced to FHV transgenic system. The results indicated that RSD-3 and RSD-6 were required in the antiviral immunity whereas SID-1 and RSD-4 were not. As green fluorescence signals detection could be sometimes misleading, I utilized statistical analysis and western blot hybridization to confirm the result. The accumulation of FHV RNA1 and RNA3 were measured through northern blot hybridization.

2.1 Introduction

A previous study from our lab showed that knockdown of RSD-2 by feeding RNAi enhanced the accumulation of an FHV replicon in *Caenorhabditis elegans* animals (Lu et al., 2009). Since RSD-2 is a component of the systemic RNAi pathway in *C. elegans* that regulates the transmission of RNA silencing signals from somatic tissue to germline (Tijsterman et al., 2004; Han et al., 2008), the finding by Lu and colleagues suggested a possible role for systemic RNAi in antiviral immunity in animals. The finding by Schott and colleagues (Schott et al., 2005) does not argue against the hypothesis since antiviral defense by systemic RNAi is not expected to be functional in cultured cells.

The FHV replicon FR1gfp used by Lu and colleagues in our lab previously is a derivative of the infectious full-length cDNA clone of FHV RNA1. FHV RNA1 encodes the viral RdRp and the VSR B2 protein, the latter of which is translated from a subgenomic RNA, RNA3 (Figure 2.1) (Dearing et al., 1980; Scotti et al., 1983; Li et al., 2002; Li et al., 2004; Chao et al., 2005). Since most of the B2 coding sequence is replaced by eGFP coding sequence in FR1gfp (Figure 2.1), the FHV replicon is defective in RNAi suppression and shows an enhanced susceptibility to antiviral RNAi (Li et al., 2004). As a result, suppression of antiviral RNAi in the reporter nematodes carrying a chromosomally integrated FR1gfp transgene by either feeding RNAi knockdown of, or a loss-of-function genetic mutation in, the antiviral RNAi pathway will increase the expression of eGFP and the accumulation of FR1gfp RNAs 1 and 3 (Mello et al., 1991; Timmons and Fire, 1998; Lindenbach et al., 2002; Li et al., 2004). However, the study by Lu and colleagues did not verify the antiviral role of RSD-2 using a genetic loss-of-

function mutant of RSD-2 (Lu et al., 2009). Moreover, two recent studies show that RSD-2 and RSD-6 form a complex with RDE-10 and RDE-11 proteins that are required for the biogenesis of secondary siRNAs and the dosage sensitive RNAi responses (Yang et al., 2012; Zhang et al., 2012; Zhang and Ruvkun, 2012; Shirayama et al., 2014; Yang et al., 2014). Therefore, it remains unclear if systemic RNAi plays a specific role in antiviral RNAi in *C. elegans*.

In studies described in this Chapter, I characterized the antiviral role of RSD-2, RSD-3, RSD-4, RSD-6, and SID-1 genes using an improved *C. elegans* reporter strain constructed by Dr. Morris Maduro and Dr. Zhihuan Gao. The FR1gfp replicon in this new strain is also under the transcriptional control of the heat inducible promoter *hsp16-4* (Stringham et al., 1992). However, the ribozyme from Tobacco ringspot virus satellite RNA used in the previous reporter strain does not completely remove the non-viral sequence from the 3'-end of primary nuclear transcripts of FR1gfp (Figure 2.1). In addition, the previous usage of *rol-6* as the transgene marker decreases the efficiency in genetic crosses (Cox et al., 1980; Park and Horvitz, 1986; Feldstein and Bruening, 1993; Cai and Tinoco, 1996). To overcome these problems, the new reporter used mCherry as the marker for the FR1gfp transgene array and the ribozyme of Hepatitis delta virus that allows precise removal of the 3'-terminal non-viral sequence as described previously (Ferre-D'Amare et al., 1998; Doudna and Ferre-D'Amare, 1999; Johnson and Ball, 1999; Chai et al., 2012).

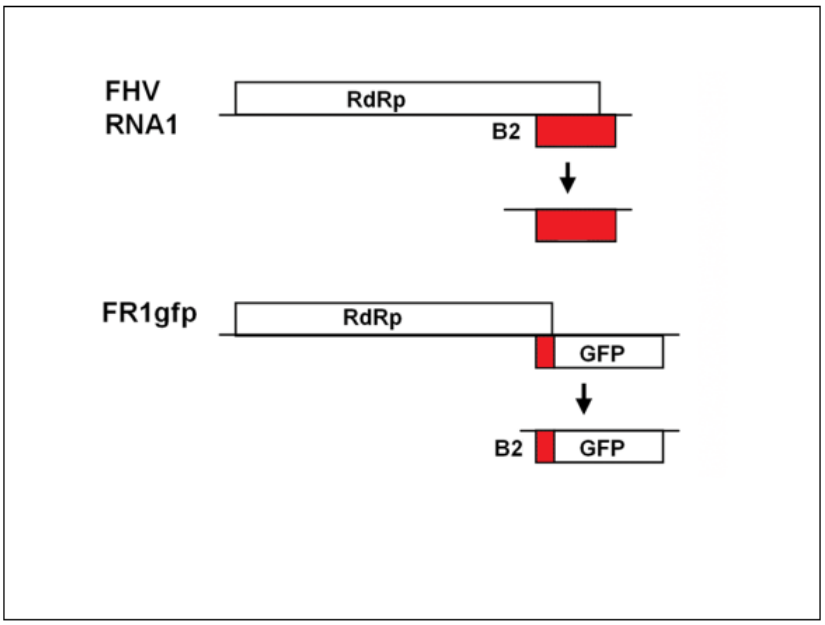

.

Figure 2.1 Genome structure and expression of wild type FHV and FR1gfp replicon

Genome structure and expression of wild type FHV RNA1 (FR1) and its B2-deficient mutant FR1gfp which expresses the enhanced GFP in place of B2 (modified from (Lu et al., 2009)).

2.2 Materials and methods

2.2.1 *C. elegans* strains

The Bristol N2 strain was used as the canonical wild type strain. Mutants of *C. elegans* used in the research described in this chapter include *rde-1(ne300), rde-4(ne337), drh-1(tm1329), rsd-2(nl3307), rsd-3(nl2013), rsd-6(nl3300), rsd-4(nl3304), sid-1(nl3321)* acquired from CGC *Caenorhabditis* Genetics Center at the University of Minnesota-Twin Cities, and the Flock house virus RNA1GFP transgenic worm strain was *irs91* constructed by Dr. Morris Maduro and Dr. Zhihuan Gao.

2.2.2 Maintenance of *C. elegans* strains

The animals were grown on Nematode growth media (NGM) plate (Containing 3 g NaCl, 17 g agar, and 2.5 g peptone in 975 ml H2O) seeded with OP50 E. coli strain as sole food source at room temperature 25°C. These plates were prepared using a peristaltic pump following sterilization protocols to dispense the NGM solution. The NGM filled plates were left at room temperature for 2 days before use to allow detection of possible contaminants especially to prevent mold growth and facilitate water evaporation. Plates were stored in an air-tight container at room temperature for up to two weeks. *E. coli* OP50 strain was inoculated in LB Broth and allowed to grow overnight at 37°C. The *E. coli* OP50 solution is then ready for use in seeding NGM plates. The contaminated plates were washed with sterilized M9 buffer. Liquid was collected in a sterilized 5mL conical centrifuge tube with cap. 0.5ml 5N NaOH solution was mixed with 1ml bleach. This bleach- sodium hydroxide solution was added to the centrifuge tube with the worms. The

animals and embryos in the tube were spin down in a table top centrifuge for 30 sec at 1300×g in order to pellet the released eggs.

2.2.3 Heat induction and subsequent fluorescence signals detection

FHV R1GFP transgenic animals were heat-treated for 3.5 hours in 34°C incubator, since more than 4 hour heat induction would harm the animals. Plates were sealed with parafilm tape to prevent dehydration effect of the NGM media which might hamper the animal growth. Since the temperature was critical to the efficiency of heat induction, the plates containing worm strains were kept rotation manually in the incubator to maintain their homogenized induction temperature. After heat induction, the worms were grown for another two days at 25°C room temperature. Then the visual green fluorescence signals and the percentage of worms which show green fluorescence were detected using fluorescence microscopy instruments. Worms were placed under close observation for the food supply and contamination as these stresses can weaken the worms' antiviral immunity. Contaminated plates were not used for fluorescence detection as more than usual amount of nematodes showed GFP expression in these plates after heat induction, possibility because the immunity system was saturated by anti-bacteria defense.

2.2.4 Feeding based assays for RNAi defects

The animals were allowed to feed for 2–3 days. Feeding L3/L4 worms was used if the assay was determined to be performed on the progeny. It was also possible to testify the progeny of RNAi treated L1s. *E. coli* designed for feeding experiments carried L4440 vectors which can express dsRNAs targeting UNC-22 and POP-1 sequences. *unc-22*

dsRNA feeding experiment has been applied to detect the efficiency of body tissue RNA interference and *pop-1* dsRNA feeding experiment was aiming at testifying the efficiency of germline RNA interference. The expression of dsRNA vectors was induced by IPTG at a 1mM concentration. POP-1 is required for development of *C. elegans* embryos while the UNC-22 encodes twitchin which was a giant intracellular protein with multiple fibronectin- and immunoglobulin-like domains and a single protein kinase domain and is required in muscle for regulation of the nematode actomyosin contraction-relaxation cycle and for maintenance of normal muscle morphology. While POP-1 is expressed mostly in germline, UNC-22 is expressed in the somatic tissues of *C. elegans.* The worms were fed with both *unc-22* and *pop-1* dsRNA in order to testify whether they were deficient in classical RNA interference.

2.2.5 Single worm DNA extraction

Simplified Worm Lysis Buffer was prepared by adding 2ul of 1×PCR buffer, 2ul of 10mg/ml proteinase K and 16ul of dd water were placed in top of 50ul PCR tube. Single health adult worms were picked from culture plate with worm pick, cleaned from bacteria to prevent bacteria DNA contamination and then placed into reaction tubes after eggs were laid. The animal was spin down to bottom of tubes by centrifugation for 15 seconds at 13,000 rpm or simply flicks down. The tube containing the animal for sequencing was snap frozen and thawed in liquid nitrogen twice each for 1min. 2ul of mineral oil was added to the top of the Worm Lysis Buffer in order to prevent vaporization. The tubes containing Worm Lysis Buffer were incubated at 65°C for 180 minutes and subsequently inactivated by heating to 95°C for 15 min.

2.2.6 Genetic crosses

Male animals of FHV replicon FR1gp transgenic strain were produced through 30 min of 37°C heat treatment or 4 hours treatment. The males obtained were crossed with N2 hermaphrodites at early L4 stages (shown by the grey crescents at their abdomens) to produce more male progenies for genetic crosses. These males were subsequently crossed with mutants in systemic RNAi (*rde-1(ne300), rde-4(ne337), drh-1(tm1329), rsd-2(nl3307), rsd-3(nl2013), rsd-6(nl3300), rsd-4(nl3304), sid-1(nl3321)*). 3 to 1 ratio of males to hermaphrodite animals were placed on 30mm plates with limited food supply to decrease the moving spaces of nematodes and thus increase the successful rate of crosses. After two days growth at 25°C room temperature, more than twenty males of the R1gfp worms could be acquired from the heat treated plates. These FR1gfp transgenic males were then crossed with *rsd-2, rsd-3, rsd-6,* and *sid-1, rsd-4* mutants in an approximately 3:1 ratio. As these mutations are all recessive, F2 progenies were verified by feeding experiment and also by the presences of mCherry protein expression in the full bodies using RFP channel of fluorescent microscopy. It is possible that very weak GFP signals-only if strong enough, could leak through the RFP channel. *rsd-2, rsd-6* and *sid-1* FR1GFP mutants were further confirmed by sequencing results , *rsd-3* was confirmed by 3% agarose gel electrophoresis analysis due to it is a deletion mutant, and *rsd-4,* as it was not mapped to any specific location, was confirmed based on responses to feeding RNAi of this genetic mutant.

2.2.7 RNA sample preparation

In the northern blot hybridization, synchronized population of worms were acquired for the heat induction. Each time about 100 hermaphrodite animals were transferred to one 60mm plate seeded with plenty of OP50 *E. coli* bacteria lawn. After one to two days growth under room temperature, the worms were expected to lay thousands of progenies in the form of embryo eggs. After another less than two days of growth till a vast majority of nematodes reached late L4 stages with the mark of white crescent visible in the place where the vulva was undergoing morphogenesis. After a large amount of late L4 staged nematodes became available, the animals were treated with a standard 3.5 hours heat induction at 34ºC in the incubator with routinely rotation to ensure the temperature consistency, then the plates were placed in 25ºC room temperature for 48 hours growth. GFP reporter expression was detected using fluorescent microscopy. If the food supply was nearly depleted, the *E. coli* food was added immediately in order to avoid the starvation which can cause a vulnerable defense system. The worms were washed off the plate after the verification of heat induction efficiency with M9 buffer, centrifuged at 4000 rpm, the supernatant was removed and the worm sediments alone were left. The worms were further washed three times with M9 buffer in order to get isolated from the contamination of *E. coli* RNA. The bulk of worms settled at room temperature for 20min in order to let the worms digest the bacteria inside intestine completely. After the worms were collected in a cryogenic tube, they were frozen and thawed twice in liquid nitrogen to break the nematodes tissue cells. 500 ml of Trizol reagent was added to each tube, and these tubes were placed at room temperature for

5min to homogenize the samples in Trizol reagent. The worm tissue and cells were torn with a tissue tearor stirring for up to 2min till a pink solution was obtained and no visible amount of worms was detected. As worms contained a large proportion of fat and collagen, the sample solutions after tissue tearing were centrifuged at 8000 rpm to remove the remnants of nematodes tissues. 100ul of chloroform was added to each tube of 500ul Trizol, the tubes were reverted for two to three times at room temperature before they were left settle at room temperature for 5min. After settlements these tubes were centrifuged at 13000 rpm for 15min to separate the water phase which contained the RNA molecules from organic phase. After 15min centrifugation, the transparent water upper phase was collected, and 200ul of isopropanol was added to each tube for precipitation of worms RNA. The precipitation time varies by the amount of worms collected, two to three hours of precipitation was preferred. After an adequate precipitation was performed, the samples were centrifuged at 13000 rpm for 15 min. In the washing process, 500ul of 70% ethanol diluted in DEPC treated water was added to the RNA sediments, the tubes were centrifuged at 7000 rpm for 5min and the ethanol remnants was removed. The tubes were air-dried in the fume hood for 10min to clean the RNA sediments for dissolution. The RNA pellets were dissolved completed in DEPC treated water. Normally 100ul of DEPC treated water was added to each tube harvested from one 60mm plate, though a smaller amount of viral RNA requires less. RNA dissolution was facilitated by 10min incubation at 65°C, and then the tubes were aspirated frequently to get the RNA molecules dissolved. After no observable sediment was present, the tubes were placed in 4 centigrade overnight to make sure that the RNA

was fully dissolved and that the solution was well homogenized in order to get a more accurate RNA concentration measurement result. The concentration of RNA was measured using the thermo scientific nanodrop. The resulted RNA samples were frozen stocked at -80°C freezer for future use.

2.2.8 Northern blot hybridization

DNA sample was collected from the FHVR1GFP transgenic animals using the previous method in chapter II with the help of proteinase K degradation for three hours 65°C digestion. The samples were treated at 95°C for proteinase K deactivation. The DNA probes I used to detect the accumulation of viral RNA are amplified using the following set of primers- (Forward: TCACGCAATGTTTGAGGTCT Reverse: TCTGCTTG TCGGCCATGA) from the FHV R1GFP sequence. The concentrations of the recycled DNA products – probes were measured using nanodrop 2000 Spectrophotometer. The probes were labeled using Thermo Scientific DecaLabel DNA Labeling Kit following standard protocols. 1% agarose gel was utilized to separate the masses of RNA molecules. The RNA loading samples were prepared by adding 7.8uL RNA sampling buffer to the samples normalized ranging from 1ug to 5ug. DEPC treated water was added to finalize the volume of loading samples to 12ul. 2ul 6X RNA loading dye was added to each sample. As RNase is always a disturbing existence for a good northern blot, we cleaned the environment with RNase away frequently. The RNA gel electrophoresis was performed at a voltage between at 150volts for one to two hours. After the electrophoresis, the gel was placed on a gel transferring sets connected with vacuum pump. A GE Hybond N+- a positively charged nylon membrane capable of high

sensitivity was applied to the transferring set. The transferring process lasted for 3.5 hours. The RNA molecules on the membrane were fixed with the help of UV crosslinker. The fixed membrane was subsequently rinsed by 5x SSC buffer. rRNA bands can be detected using as loading controls as their concentration usually does not vary much among mutants. 0.04% Methylene blue in 0.5M NaAc was used to stain the rRNA bands. The membrane was placed at 65°C oven for one-hour pre-hybridization using prehybridization buffer. After one-hour prehybridization the RNA molecules on the membrane hybridized with 15ul of GFP probes labeled by gamma-dCTP overnight or at least over eight hours in hybridization buffer at 50rpm. After hybridization, the membranes were washed using 1% to 0.1% SDS rinsing buffer at 65°C for one hour. The membrane was placed in cassette to conduct X-ray film exposure or phosphoimage exposure.

2.2.9 Western blot hybridization

For the preparation of protein from a 50 worms sample volume, a mark was made on the Eppendorf tube at 25uL. 200μL of M9 was pipette into the tube. 50 worms were randomly picked regardless of the GFP expression level from the central region of the plate using a worm pick and then they were placed into the tubes containing M9 solutions. The worms were washed for 3 times with M9 buffer. The M9 buffer was pipette off and the worms were let settle in 25μL of M9 for minutes. The worms were then snap frozen and thawed in liquid nitrogen for twice. 25μL of 2X sample buffer was added to the solution. The solution was sonicated for 2 min in waterbath sonicator from

UCR core facility, and the solution was placed immediately at 95°C for 5 min to inhibit the functioning of proteases. 10μL of the final protein extract solution was loaded into the SDS-PAGE gel for western blot experiments. Filter paper sandwich was applied to the protein transferring set from the gel to PVDF (Polyvinylidene fluoride) membrane. PVDF membrane was rinsed in 100% ethanol and then gel transfers buffer each for 30 seconds before usage. The transferring process of PAGE gel takes 45 min at 15 volts constant voltage. The membrane was rinsed in 1X TBST twice for 15 min each to remove the transferring buffer. After rinsing process the membrane was cut into two pieces at around 40k Dolton by the prestain protein ladder to avoid crosslinking. The membrane was blocked using 5% nonfat milk for one hour at room temperature or at 4°C overnight in the hybridization reaction box. Subsequently the membrane was rinsed twice using 1X TBST to clean the primary antibody remnants. Membrane hybridizations were performed separately in TBST solutions containing 1:1000 diluted HRP (horseradish peroxidase)-linked antibodies for GFP protein and actin. The Lateral actin antibody for loading control was purchased from abcam.

2.3 Results

To verify the role of RSD-2 in antiviral immunity, genetic crosses were conducted to obtain a *C. elegans* strain carrying the FHV R1gfp transgene array in a genetic background homozygous for *rsd-2(pk3307)*, a null *rsd-2* allele reported previously (Tijsterman et al., 2004). Two days after heat treatment at 34°C for 3.5 hours to induce transcription and replication of the FR1gfp replicon, the *rsd-2(pk3307)* mutant worms

exhibited strong green fluorescence expression unlike in the wild type N2 worms (Figure 2.2, the middle panel). This result showed that worm antiviral RNAi was indeed defective in the absence of RSD-2, and it is consistent with the previous finding using the feeding RNAi approach (Lu et al., 2009).

To determine if *C. elegans* antiviral RNAi also depended on other genes essential for systemic RNAi, *rsd-3, rsd-4, rsd-6* and *sid-1* mutant worms were obtained from CGC. The responses of these mutants to feeding RNAi targeting *unc-22* (a somatically expressed gene) and *pop-1* (a germline expressed gene) were first experimentally verified. As expected (Table 2.1), N2 nematodes were susceptible to feeding RNAi of both genes, producing a large number of dead embryos (due to *pop-1* RNAi) or twitching and paralyzed worms (due to *unc-22* RNAi), whereas *rde-1* mutant worms were resistant to both. However, *rsd-2, rsd-3* and *rsd-6* mutants were defective in their responses to *pop-1* feeding RNAi and partially defective in responses to *unc-22* feeding RNAi since approximately half of the mutants showed twitching or paralyzed phenotypes after feeding dsRNA to target the mRNA coding sequence for UNC-22. By comparison, *rsd-4* and *sid-1* mutants exhibited more severe defects as both *pop-1* and *unc-22* feeding RNAi responses were compromised. These results confirmed the genotypes of the mutants obtained from CGC and other labs, and they also corresponded to what was previously reported- *rsd-2, rsd-3* and *rsd-6* were required in the somatic transmission of RNA silencing signals while rsd-4 and sid-1 were indispensable for the uptake of RNA silencing signals from the environment.

	pop-1 RNAi	*unc-22* RNAi (percentage twitching/paralyzed) (n=100)
N2	++++	34%(t)/55%(p)
rde-1	-	2%(t)/0(p)
rsd-2	+	21%(t)/27%(p)
rsd-3	+	38%(t)/7%(p)
rsd-6	+	36%(t)/19%(p)
rsd-4	-	16%(t)/0(p)
sid-1	-	7%(t)/1%(p)

Table 2.1 Assays of systemic RNAi related mutants feeding RNAi defects

Plates carrying L4440 vector which can express dsRNAs of *pop-1* and *unc-22* were used to feed the mutants of *rsd-2*, *rsd-3*, *rsd-6*, *rsd-4* and *sid-1*, wild type-Bristol N2 worms served as negative control and *rde-1* served as positive control of deficiency in RNA interference machinery. In the left panel of *pop-1* feeding RNAi results, "–" stood for no visible dead embryos on the plate after feeding while "++++" represented almost no larvae hatched. "+" represented a small number of dead embryos. In the right panel, (t) represented the percentage of worms which showed twitching phenotype, and (p) represented the percentage of worms unable to move. Dead embryos and twitching/paralyzed are the phenotypes caused by *unc-22* feeding RNAi.

Each of the mutant alleles was then introduced into FR1gfp worms by genetic crosses and their genotypes were verified by approaches described in section 2.2.6. After heat induction at 34°C for 3.5 hours and two days growth at 25°C, the FR1gfp worms in N2 and mutant genetic backgrounds were examined for green fluorescence signals using microscopy. Similar to *rsd-2* mutant, *rsd-3* and *rsd-6* mutant worms displayed strong expression of eGFP both in the head and the pharyngeal tissues and some of these worms were green fluorescent across the whole worm body (Figure 2.2). I noted that the eGFP signals were frequently absent in intestinal cells. However, such an enhanced expression of eGFP was not observed in both *rsd-4* and *sid-1* mutant worms (Figure 2.2), similar to the wild type *N2* worms. Although most worms among the *rsd-3, sid-1* and N2 population did not show green fluorescence signaling, I picked the individuals which showed a weak green fluorescence signals to illustrate the signal patterns in these mutants. Very few (less than 1%) of these strains presented a strong green fluorescence signal among the nematodes bodies, and many of them appeared to be unhealthy or stressful. Moreover, change in the heat induction time for the FR1gfp promoter might also trigger a strengthened/weakened green fluorescence signaling in the worm population. Therefore it is important to keep consistent heat-induction temperature and induction time to maintain the consistency of experiments.

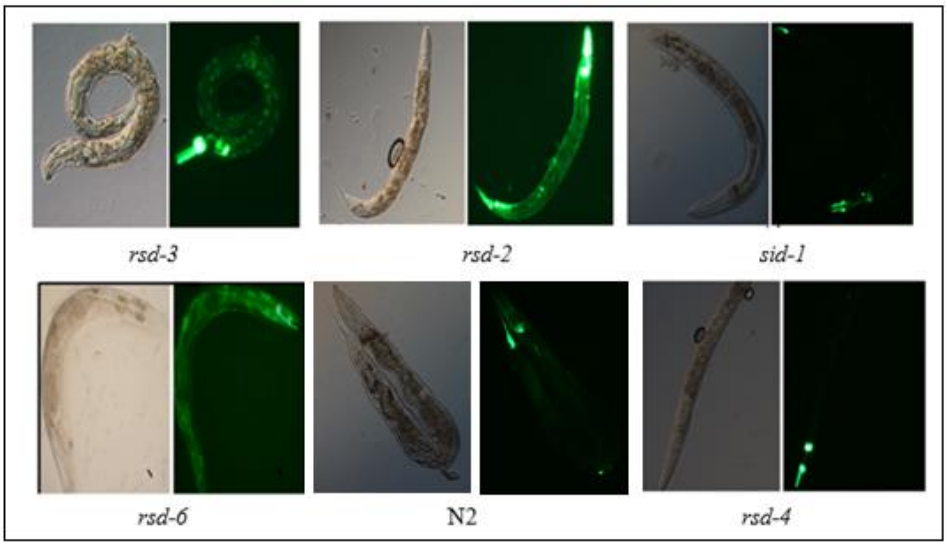

Figure 2.2 Genetic rescue of FHV replicon accumulation

Genetic rescue of FHV replicon accumulation in *rsd-2*, *rsd-3*, and *rsd-6* mutant worms visualized by GFP expression, but not in *rsd-4* and *sid-1* worms. Worms were photographed 48 hours for green fluorescence (right in each panel) or under white light (left in each panel) after induction of the replicon replication by heat treatment. N2/FR1gfp worms also occasionally displayed weak green fluorescence in the pharynx, and so did *rsd-4* and *sid-1* worms.

Although whole body green fluorescence was frequently observed in *rde-1, rde-4* and *drh-1* mutant worms defective in antiviral RNAi, weak eGFP expression was detectable in the head region and pharynx tissues of a small proportion of N2 worms and strong eGFP expression was not always visible in every *rde-1, drh-1* or *rde-4* mutant animal. In very rare occasions, even stronger green fluorescence signals might be observable in N2 worms, thus render the individual green fluorescence expressions less consistent. To overcome these problems, I measured for each worm genotype the percentages of worms that expressed green fluorescence regardless of the tissue expression pattern, and the percentages of worms that showed GFP expression throughout the nematode body after FR1 replication from 3 independent experiments, each of which included 100 adult worms. The results from this analysis presented in Figure 2.3 further supported an antiviral role for *rsd-2, rsd-3* and *rsd-6*, but not for *rsd-4* and *sid-1*. Similar to *rde-1* mutant worms, expression of eGFP was detected in 50% to 75% of *rsd-2, rsd-3* and *rsd*-6 mutant worms respectively (Figure 2.3A), 10% to 30% of which exhibited full body green fluorescence (Figure 2.3B). In contrast, both *sid-1* and *rsd-4* mutants showed no significant difference in both of the measurements to wild type N2 animals. Three repeat experiments were conducted for each of the strain, and Standard Error of the Mean (SEM) calculations were utilized to prove the consistencies between different repeats.

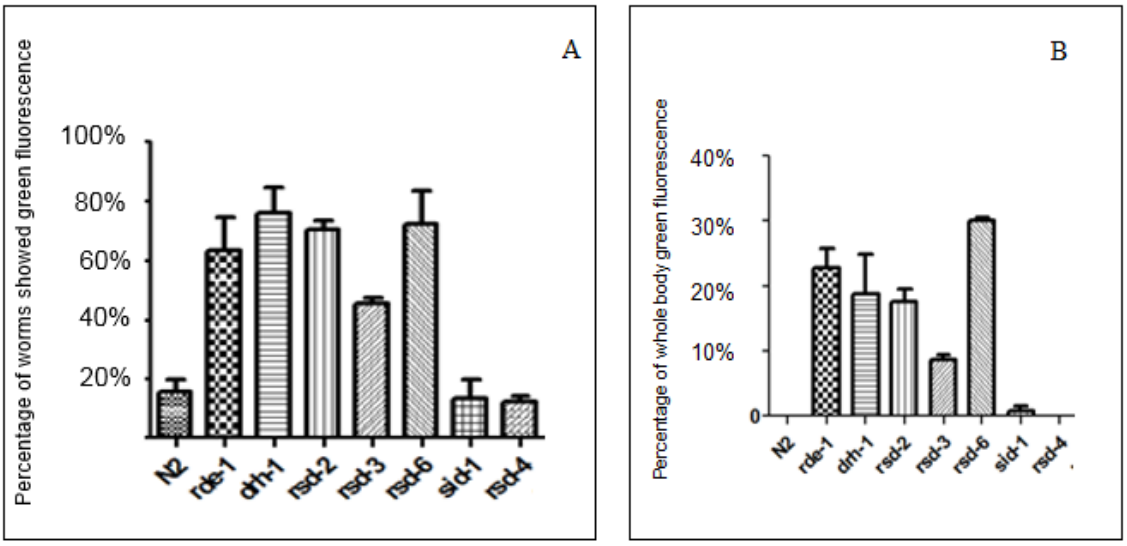

Figure 2.3 Statistics detection of green fluorescence in *FR1gfp* reporter worms

The systemic RNAi mutants in FHV RNA1FR1gfp transgenic strain were heat induced at 34°C for 3.5 hours. Green fluorescence signals were detected using fluorescence microscope after 48 hours growth in room temperature. For each mutant, 100 individuals were counted per experiment and error bars represented the Standard Error Median (SEM) values of three respective biological repeats. Left Panel A represented the percentage of worms which showed green fluorescence; Panel B illustrated percentage of worms which showed whole body green fluorescence expression.

Northern blot hybridization was subsequently used to detect the accumulation levels of the genomic RNA (RNA1) and its subgenomic RNA (RNA3) from the FHV replicon using a DNA probe targeting eGFP sequence- which was used as a reporter protein to replace B2 coding sequence of RNA3 in FR1gfp replicon. The result from northern blot hybridization was consistent to the visual detection of the eGFP expressions in different *C. elegans* strains. The accumulation levels of both RNA1 and RNA3 of FR1gfp in *rsd-2, rsd-3, and rsd-6* mutants were comparable to those in *rde-1* and *drh-1* mutant worms and were much higher than those in *N2* worms. However, presence of *sid-1* or *rsd-4* allele did not enhance the accumulation of FR1gfp RNAs compared to that in wild type N2 worms. The expression of eGFP from the subgenomic RNA produced after FR1gfp replication in *rsd-2, rsd-3* and *rsd-6* mutants was analyzed by Western blotting using anti-GFP antibodies in order to verify the previous observation based on visually detectable green fluorescence signals. The results, presented in Figure 2.4, confirmed that the high level expression once again demonstrated that the viral RNA accumulation level can be indicated by the visual detection of green fluorescence signals and the comparison results remain consistent.

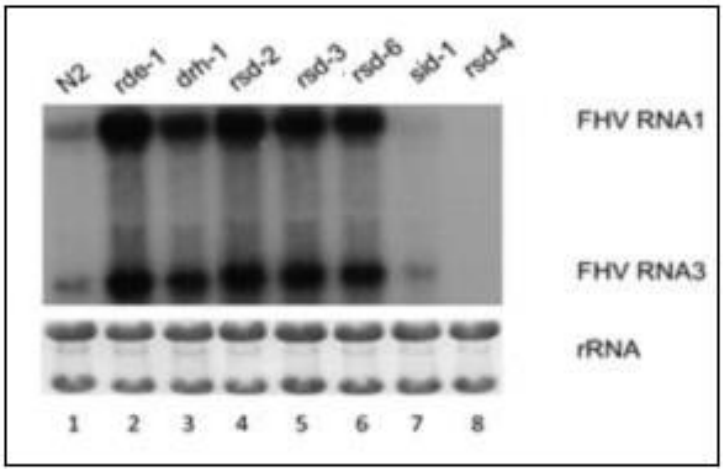

Figure 2.4 Northern blot detection of FHV FR1gfp RNA1 and RNA3 accumulation

Accumulation levels of FHV RNA1 and RNA3 were detected using GFP probes labeled with radioactive 32P. Worms were treated with 34°C heat induction and two days post induction growth in room temperature 25°C. N2 strain served as negative control whereas *rde-1, drh-1* served as positive controls. Ribosomal RNA staining was used as loading control.

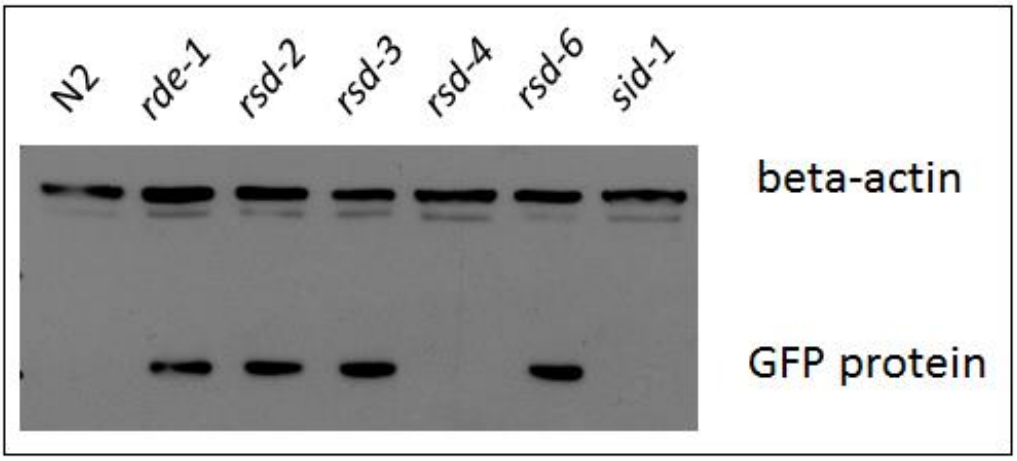

Figure 2.5 Western blot hybridization of FHV FR1gfp expression levels

The protein samples were prepared from 50 animals respectively for the protein of each worm strain. Anti-actin antibodies from abcam were used to detect beta-actin as loading controls. The worms were harvested two days post 37°C heat induction after visual GFP expression detection using fluorescent microscope. *rde-1* represented the positive control and N2 represented the negative control.

The translational levels of FHV R1GFP (Figure 2.5) were shown to be consistent to the results of GFP expression visual signals detection and statics, as well as the result of RNA1 and RNA3 RNA accumulations. *rsd-2, rsd-3* and *rsd-6* mutants showed strong expression of GFP protein whose levels were comparable to *rde-1* mutant, whereas *rsd-4* and *sid-1* mutants, like N2, did not present observable GFP protein expression. This experiment result further verified our previous result based upon visual detection of the GFP fluorescent signals. Moreover, it indicated that RSD-2, RSD-3, RSD-6 were unlikely to affect the translation levels of FHV R1GFP replicon as the western blot hybridization results and northern blot hybridization results correspond well with each other comparably.

In summary, antiviral functions of *rsd-2, rsd-3* and *rsd-6* existed, but SID-1 and RSD-4 appeared to not have antiviral functions. Previous research identified RSD-2, RSD-3 and RSD-6 involved in the systemic RNA interference by regulating the transmission of spreading RNA interference signals from germline to somatic tissues while SID-1 and RSD-4 were involved in the uptake of RNA silencing signals. From the results listed above based on the FHV RNA1 transgenic nematode system, *C. elegans* systemic RNA interference machinery components RSD-2- a gene uniquely exists in *C. elegans*, RSD-3- a homolog of Enthoprotin which was implicated in mammalian vesicle trafficking and RSD-6- which contained an RNA binding motif Tudor domain, were the most crucial genes in worms' antiviral immunity, while the roles of SID-1 and RSD-4 appeared to be less important comparably.

2.4 Discussion

In this chapter, I used visual fluorescence signals detection, Western and Northern blotting analyses to compare the replication and accumulation of the FHV replicon between the wild type and mutant worms, especially a panel of mutants defective in systemic RNAi. The results demonstrated that the FHV replicon replicated to high levels in *rsd-2*, *rsd-3* and *rsd-6* mutant worms as found in worm mutants such as *rde-1* or *drh-1* known to be defective in antiviral RNAi. The observed antiviral activities of independent genes implicated in the systemic RNAi pathway therefore suggested a specific antiviral function for systemic RNAi in *C. elegans.* Moreover, my findings indicated that antiviral RNAi may require RNAi spreading between tissues since RSD-2, RSD-3 and RSD-6 appeared to control the transmission of RNAi signals from somatic tissues to germline (Tijsterman et al., 2004). RSD-2 is a huge gene that does not have a homolog in other organisms and RSD-6 contains a Tudor RNA binding domain. Although the mammalian RSD-3 homolog Enthoprotin is a membrane associated protein related to vesicles trafficking, systemic RNAi is known to not require vesicle trafficking in *C. elegans* (Winston et al., 2002; Winston et al., 2007; Jose et al., 2009; Lu et al., 2009; Hinas et al., 2012; Jose et al., 2012), hence the systemic RNAi spreading mechanism through RSD-2, RSD-3 and RSD-6 is complicated to research.

Interestingly, no enhancement in the accumulation of the viral replicon was observed in *sid-1* and *rsd-4* mutant worms compared to worms in wild type N2 genetic background. Previous studies have shown that SID-1 and RSD-4 are essential for the uptake of systemic RNAi signals, in particular, long dsRNA from gut lumen (Winston et

al., 2002; Tijsterman et al., 2004; Winston et al., 2007; Hinas et al., 2012; Jose et al., 2012). Although many animals including mammals have SID-1 homolog (FLJ20174), they do not have systemic RNAi responses and the delivery of dsRNAs becomes difficult in RNAi therapy (Duxbury et al., 2005; Li et al., 2006). One remaining possibility is that in the FR1gfp worms, antiviral RNAi triggered by the viral replicon under the control of heat shock promoter occurs in most cells so that systemic RNAi becomes less important, these questions were tested in the following chapter using authentic virus infection system- Orsay virus which was discovered in 2011.

2.5 References

Cai, Z. P. and I. Tinoco (1996). Solution structure of loop a from the hairpin ribozyme from tobacco ringspot virus satellite. *Biochemistry* **35**(19): 6026-36.

Chai, Y. P., W. Li, G. X. Feng, Y. H. Yang, X. M. Wang and G. S. Ou (2012). Live imaging of cellular dynamics during Caenorhabditis elegans postembryonic development. *Nature Protocols* **7**(12): 2090-102.

Chao, J. A., J. H. Lee, B. R. Chapados, E. W. Debler, A. Schneemann and J. R. Williamson (2005). Dual modes of RNA-silencing suppression by flock house virus protein B2. *Nature Structural & Molecular Biology* **12**(11): 952-57.

Cox, G. N., J. S. Laufer, M. Kusch and R. S. Edgar (1980). Genetic and Phenotypic Characterization of Roller Mutants of Caenorhabditis-Elegans. *Genetics* **95**(2): 317-39.

Dearing, S. C., P. D. Scotti, P. J. Wigley and S. D. Dhana (1980). A Small Rna Virus Isolated from the Grass Grub, Costelytra-Zealandica (Coleoptera, Scarabaeidae). *New Zealand Journal of Zoology* **7**(2): 267-69.

Doudna, J. A. and A. R. Ferre-D'Amare (1999). Crystal structure of a hepatitis delta virus ribozyme. *Faseb Journal* **13**(7): A1319-A19.

Duxbury, M. S., S. W. Ashley and E. E. Whang (2005). RNA interference: A mammalian SID-1 homologue enhances siRNA uptake and gene silencing efficacy in human cells. *Biochemical and Biophysical Research Communications* **331**(2): 459-63.

Feldstein, P. A. and G. Bruening (1993). Catalytically Active Geometry in the Reversible Circularization of Minimonomer Rnas Derived from the Complementary Strand of Tobacco Ringspot Virus Satellite Rna. *Nucleic Acids Research* **21**(8): 1991-98.

Ferre-D'Amare, A. R., K. H. Zhou and J. A. Doudna (1998). Crystal structure of a hepatitis delta virus ribozyme. *Nature* **395**(6702): 567-74.

Han, W., P. Sundaram, H. Kenjale, J. Grantham and L. Timmons (2008). The Caenorhabditis elegans rsd-2 and rsd-6 genes are required for chromosome functions during exposure to unfavorable environments. *Genetics* **178**(4): 1875-93.

Hinas, A., A. J. Wright and C. P. Hunter (2012). SID-5 Is an Endosome-Associated Protein Required for Efficient Systemic RNAi in C. elegans. *Current Biology* **22**(20): 1938-43.

Johnson, K. L. and L. A. Ball (1999). Induction and maintenance of autonomous flock house virus RNA1 replication. *J Virol* **73**(10): 7933-42.

Jose, A. M., Y. A. Kim, S. Leal-Ekman and C. P. Hunter (2012). Conserved tyrosine kinase promotes the import of silencing RNA into Caenorhabditis elegans cells. *Proceedings of the National Academy of Sciences of the United States of America* **109**(36): 14520-25.

Jose, A. M., J. J. Smith and C. P. Hunter (2009). Export of RNA silencing from C-elegans tissues does not require the RNA channel SID-1. *Proceedings of the National Academy of Sciences of the United States of America* **106**(7): 2283-88.

Li, C. X., A. Parker, E. Menocal, S. L. Xiang, L. Borodyansky and J. H. Fruehauf (2006). Delivery of RNA interference. *Cell Cycle* **5**(18): 2103-09.

Li, H. W., W. X. Li and S. W. Ding (2002). Induction and suppression of RNA silencing by an animal virus. *Science* **296**(5571): 1319-21.

Li, W. X., H. W. Li, R. Lu, F. Li, M. Dus, P. Atkinson, E. W. A. Brydon, K. L. Johnson, A. Garcia-Sastre, L. A. Ball, P. Palese and S. W. Ding (2004). Interferon antagonist proteins of influenza and vaccinia viruses are suppressors of RNA silencing. *Proceedings of the National Academy of Sciences of the United States of America* **101**(5): 1350-55.

Lindenbach, B. D., J. Y. Sgro and P. Ahlquist (2002). Long-distance base pairing in flock house virus RNA1 regulates subgenomic RNA3 synthesis and RNA2 replication. *Journal of Virology* **76**(8): 3905-19.

Lu, R., E. Yigit, W. X. Li and S. W. Ding (2009). An RIG-I-Like RNA Helicase Mediates Antiviral RNAi Downstream of Viral siRNA Biogenesis in Caenorhabditis elegans. *Plos Pathogens* **5**(2).

Mello, C. C., J. M. Kramer, D. Stinchcomb and V. Ambros (1991). Efficient Gene-Transfer in C-Elegans - Extrachromosomal Maintenance and Integration of Transforming Sequences. *Embo Journal* **10**(12): 3959-70.

Park, E. C. and H. R. Horvitz (1986). Mutations with Dominant Effects on the Behavior and Morphology of the Nematode Caenorhabditis-Elegans. *Genetics* **113**(4): 821-52.

Schott, D. H., D. K. Cureton, S. P. Whelan and C. P. Hunter (2005). An antiviral role for the RNA interference machinery in Caenorhabditis elegans. *Proc Natl Acad Sci U S A* **102**(51): 18420-4.

Scotti, P. D., S. Dearing and D. W. Mossop (1983). Flock House Virus - a Nodavirus Isolated from Costelytra-Zealandica (White) (Coleoptera, Scarabaeidae). *Archives of Virology* **75**(3): 181-89.

Shirayama, M., W. Stanney, W. F. Gu, M. Seth and C. C. Mello (2014). The Vasa Homolog RDE-12 Engages Target mRNA and Multiple Argonaute Proteins to Promote RNAi in C. elegans. *Current Biology* **24**(8): 845-51.

Stringham, E. G., D. K. Dixon, D. Jones and E. P. M. Candido (1992). Temporal and Spatial Expression Patterns of the Small Heat-Shock (Hsp-16) Genes in Transgenic Caenorhabditis-Elegans. *Molecular Biology of the Cell* **3**(2): 221-33.

Tijsterman, M., R. C. May, F. Simmer, K. L. Okihara and R. H. A. Plasterk (2004). Genes required for systemic RNA interference in Caenorhabditis elegans. *Current Biology* **14**(2): 111-16.

Timmons, L. and A. Fire (1998). Specific interference by ingested dsRNA. *Nature* **395**(6705): 854-54.

Winston, W. M., C. Molodowitch and C. P. Hunter (2002). Systemic RNAi in C-elegans requires the putative transmembrane protein SID-1. *Science* **295**(5564): 2456-59.

Winston, W. M., M. Sutherlin, A. J. Wright, E. H. Feinberg and C. P. Hunter (2007). Caenorhabditis elegans SID-2 is required for environmental RNA interference. *Proceedings of the National Academy of Sciences of the United States of America* **104**(25): 10565-70.

Yang, H., J. Vallandingham, P. Shiu, H. Li, C. P. Hunter and H. Y. Mak (2014). The DEAD Box Helicase RDE-12 Promotes Amplification of RNAi in Cytoplasmic Foci in C. elegans. *Current Biology* **24**(8): 832-38.

Yang, H., Y. Zhang, J. Vallandingham, H. Li, L. Florens and H. Y. Mak (2012). The RDE-10/RDE-11 complex triggers RNAi-induced mRNA degradation by association with target mRNA in C. elegans (vol 26, pg 846, 2012). *Genes & Development* **26**(10): 1122-22.

Zhang, C., T. A. Montgomery, S. E. J. Fischer, S. M. D. A. Garcia, C. G. Riedel, N. Fahlgren, C. M. Sullivan, J. C. Carrington and G. Ruvkun (2012). The Caenorhabditis elegans RDE-10/RDE-11 Complex Regulates RNAi by Promoting Secondary siRNA Amplification. *Current Biology* **22**(10): 881-90.

Zhang, C. and G. Ruvkun (2012). New insights into siRNA amplification and RNAi. *Rna Biology* **9**(8): 1045-49.

Chapter 3: Genetic characterization of systemic RNAi-defective mutant nematodes in the antiviral immunity induced by Orsay viral infection

Abstract

In the previous chapter, I found that the genes responsible for controlling the transmission of systemic RNAi signals from somatic tissues to germline, including RSD-2, RSD-3 and RSD-6, played essential roles in antiviral RNAi induced by the replication of the FHV transgenic replicon. Here I showed that the same set of genes also controlled antiviral RNAi against the infection of *C. elegans* by Orsay virus. The antiviral function of RSD-2 and RSD-6 does not require the formation of the complex among RSD-2, RSD-6, RDE-10 and RDE-11 involved in the dsRNA dosage response. Moreover, comparison of the populations of viral siRNAs by deep sequencing revealed that *rsd-2, rsd-3* and *rsd-6* mutant worms were all partially defective in the biogenesis of the viral secondary siRNAs. Abolishing the function of the genes responsible for controlling the uptake or export of the RNAi spreading signals in systemic RNAi, including SID-1, RSD-4, SID-3 and SID-5, was insufficient to eliminate antiviral RNAi in *C. elegans*. However, usage of double mutant worms further revealed that the SID-1 pathway of systemic RNAi appeared to enhance antiviral RNAi against virus infection under conditions when Orsay virus efficiently replicated in *C. elegans*. These findings together with the results presented in the previous Chapter, provided evidence for the first time to support an antiviral function of systemic RNAi in animals.

3.1 Introduction

In order to determine whether genes involved in systemic RNA interference (RNAi) participated in the *C. elegans* antiviral RNAi process, I used both the Flock house virus (FHV) replicon (FR1gfp) and the Orsay virus, a natural pathogen of *C. elegans* (Lu et al., 2005; Lu et al., 2009; Felix et al., 2011). Orsay virus has close sequence similarity to members of the *Nodaviridae* family, but it does not encode the B2 protein or other viral silencing suppressors (Felix et al., 2011; Guo and Lu, 2013). As a result, Orsay virus is defective in the suppression of antiviral RNAi and accumulates to high levels only in RNAi-defective mutant worms (Felix et al., 2011; Guo and Lu, 2013). Notably, the genes found previously by our lab to be crucial for antiviral RNAi against the FHV replicon, including RDE-1, RDE-4, DRH-1, and DCR-1, are all required for the innate immune control of the natural Orsay virus infection. For example, the field isolate JU1580 from which Orsay virus was identified carries a deletion in *drh-1* gene shown previously by our lab to be critical for antiviral RNAi against the FHV replicon (Lu et al., 2009; Felix et al., 2011; Ashe et al., 2013).

Recent characterization of RDE-10 and RDE-11 genes involved in the exogenous and endogenous RNAi has revealed a new function for RSD-2 and RSD-6 (Yang et al., 2012; Zhang et al., 2012). RDE-10 encodes a protein without any conserved domain whereas RDE-11 encodes a protein with a RING-type zinc finger nucleic acid binding domain. Mutations in RDE-10 and RDE-11 genes cause dosage-sensitive RNAi response deficiencies, i.e. these mutants are resistant to low dosage but sensitive to high dosage of

dsRNA. In addition, RDE-10 and RDE-11 mutants are also defective in transgene silencing, possibly by acting in parallel to the Argonaute protein NRDE-3 from the nuclear RNAi pathway (Guang et al., 2008). Interestingly, RDE-10 and RDE-11 are found in a novel complex that also contains RSD-2 and RSD-6 and participates in the biogenesis of the WAGO class 22G secondary siRNAs downstream of ERGO-1 class 26G siRNAs. Moreover, RSD-2 and RSD-6 mutants exhibit dosage sensitive RNAi phenotypes and are defective in the biogenesis of endogenous 22G secondary siRNAs associated with WAGO class of Argonautes (Yang et al., 2012; Zhang et al., 2012).

In this chapter, I characterized the roles of RSD-2, RSD-3, RSD-4, RSD-6, and SID-1 genes as well as RDE-10 and RDE-11 genes in antiviral RNAi induced by Orsay virus infection. The potential contribution of SID-1 to antiviral RNAi was further examined in *sid-1* double mutants combined with *rsd-2*, *rsd-3* or *rrf-1* alleles.

3.2 Materials and methods

3.2.1 *C. elegans* strains

C. elegans strains used in this chapter included N2, *rsd-2(nl3307), rsd-3(nl2013), rsd-6(nl3300), rsd-4(nl3304), sid-1(nl3321), sid-3(vc787), sid-5- C04F12.1(tm1637) , rde-1(ne300), rde-4(ne337)* requested from CGC, *C. elegans* strains *rde-10(hj20)* and *rde-11(hj37)* were kindly provided by Dr. Ma Ho Yi's lab. These mutants were confirmed by PCR and/or feeding RNAi targeting *unc-22 or pop-1* as strains like *rsd-4* has not been successfully mapped to a specific position yet.

3.2.2 Orsay virus infection and brood size counting

Ten of L4 stage synchronized JU1580 animals with successful Orsay virus infection (verified by Real-Time qRT-PCR) were pick out and placed on one 90mm plate. The worms were left for two to four days growth at 20°C till a large amount of L4 stage to adult worm population were present on the plate. These animals were washed off the plate using 1M PH 7.8 Tris-HCl buffer and briefly spin at 5000 rpm, the supernatant was collected while the worms pellet was removed. The supernatant was centrifuged at 13000 rpm again for purification, and the secondary supernatant was kept subsequently. The supernatant was infiltrated using 0.22um filter, then stored at -20°C for further Orsay virus infection. 20ul of the supernatant containing Orsay virus particles was added to each of the 60mm plate which contained 10 to 20 young adult worms and was seeded with OP50 *E. coli* bacteria lawn. The animals were grown at 20°C for four to six days till majority of the population reached late L-4 stage or adults. The parental animals were transferred every day to a new plate until the end of progeny reproduction in order to enable a clear count of F1 progenies of the worms and excluding the possible effect from F2 progenies. The plates were incubated at 20°C for 2 days and kept at 4°C until scoring.

3.2.3 Orsay virus RNA1 negative strand riboprobe preparation

Orsay virus For Orsay virus RNA1 detection I used GW194+T7promoter primers set: 5′TAATACGACTCACTATAGGGACCTCACAACTGCCATCTACA and GW195 primer: 5′ GACGCTTCCAAGATTGGTATTGGT) followed PCR thermal cycling protocol as: Denaturing: 95°C - 5min, Denaturing: 95°C 30 sec, Annealing: 60°C 30 sec,

Extension at 72°C 45 sec , Repeat for 30 cycles, following by Elongation at 72°C for 5min. The DNA product was purified and collected after agarose gel extraction. UTP [α-32P] was applied to label and produce the riboprobes using Life technologies Megascript T7 transcription Kit following modified protocols on manuals. The only revision is that the UTP volume was reduced to 0.2ul whereas the [α-32P] UTP tracer volume was added to 4ul. Riboprobes were stored at -20°C for up to two weeks due to half-life limit of 32P. Quantification analysis was completed using Imagequant TL software located in UCR Core facility from the images obtained from Typhoon scanner, this work was completed with the assistances from two other members of our lab- Yunqi Yu, Dr. Mengji Cao.

3.2.4 Fluorescent in-situ hybridization

The probes used for Fluorescent In-Situ Hybridization (FISH) were prepared and kindly provided by Dr. Morris Maduro and Ms. Gina Maduro. Orsay virus infected late L4 or early adult worms were washed off of plate using M9 buffer. These worms were washed using M9 buffer for three times until all the bacteria has been removed. Collected animals were resuspend in 1ml fresh made Fixation Solution (40ml DEPC- H2O, 5ml 10x PBS, 5ml Formaldehyde) and incubated at room temperature for 45 min. Worms were subsequently spin down and Fixation Solution was removed as a result. Treated animals were washed twice with 1XPBS in DEPC-H2O.

Animals were then resuspended in 1ml 70% EtOH in DEPC- H2O and incubated for 1 hour to overnight at 4°C. Then these worms were washed twice with Wash Buffer. Animals were then resuspended in 100µl Hybridization Buffer and 1µL Orsay virus

probe (aliquots of 500µl Hybridization Buffer and 5µL orsay probe stored in the -20°C in the Maduro Lab). FISH Hybridization was conducted at 30°C overnight. Then worms were spin down and hybridization buffer was removed. These worms were washed twice with 2X SSC, they were then resuspended in 100-500µL 2X SSC. At this point worms can be stored at room temperature for long term use. Worms were mounted on slides, 40µL of worm to a slide, coverslip was placed over worms and excess SSC was wiped out using tissue paper. Once the worms were mounted on the slides, they would be suitable for fluorescence signal detection for about a day, though the signals would decrease in intensity shortly.

3.2.5 Orsay virus hybridization sample preparation and northern blot hybridization

Since a larger amount of worms were required for the RNA samples used for northern blotting hybridization targeting virus negative strand, and for the sake of a more efficient infection through horizontal transmission, four to six of 30mm plates were used to increase the chance of animal contacts. Five to ten adult worms were placed on each plate, 20ul of our previously collected centrifugation supernatant containing Orsay virus particles was disseminated onto each of the plates. The worms were left grow at 20 °C for four to six days till the majority of worms were in later L4 or adult stages suitable for RNA extraction. The same RNA extraction protocols as described in the FHVR1eGFP worms RNA extraction were applied. Three biological repeats were conducted by using 12 plates totally for each sample at different time. The efficiency of Orsay virus was verified by RT-PCR results from negative wild type worms and infected *rde-1* mutant

worms with limited thermo cycles (20 cycles) since no visible pathogenic symptoms can be applied to detect the efficiency of Orsay virus infection. The RT-PCR was also completed using mytaq One-Step RT-PCR kit, the reaction solution was: 2x MyTaq One-Step Mix 10ul, Forward and Reverse Primers 1ul totally, 20uM concentration; 0.5ul of Retro Transcriptase and 1ul of RNase inhibitor.

For the northern blot hybridization using Orsay virus negative strand riboprobe, I used methods optimized and modified from Felix et al., 2011. Blots were hybridized at 68 °C for 16 hours after 4 hours-prehybridization, the membrane was washed following these steps: 2X SSC/0.1%SDS 5 min X1 at 25°C, 1XSSC/0.1%SDS 10minX1 at 25°C,0.1XSSC/0.1%SDS 5minX1 at 25°C, 0.1X SSC/0.1% SDS 15minX2 at 42°C and 0.1XSSC/0.1%SDS 15minX1 at 68°C, washing steps appeared to be quite stringent, as unnecessary wash would weaken the hybridization signal intensities tremendously.

3.2.6 Quantitative RT-PCR

The RNA from worms that was used for qRT-PCR was prepared using a different method since the amount of worms used in this experiment was much lower. 20 worms were placed into 20µl of M9 in an RNase-free tube. Worms were spin briefly at 14,000 rpm. 250µL of Trizol solution was then added in the fume hood. The solution was subsequently aspirated for 30 seconds and then let settled at 4ºC until the worms dissolve for about 20 min, then 50µL of chloroform was added and the solution was aspirated again for 30 seconds. The solution was let sit at 25 ºC room temperature for 3 min and centrifuged at 12,000 rpm for 15 min at 4ºC. The clear top layer (~125µL) was

transferred into a new RNase-free Eppendorf tube. 125µL of 2-propanol was added and the tubes were inverted to mix; subsequently the extract was left settle again at room temperature for five minutes before the phase separation by spinning down at 12,000 rpm for 10 minutes at 4ºC. Then the supernatant was carefully decanted; a few micro liters were left at the bottom so as not to make the pellet disturbed. Pellet was washed with 70% ethanol in DEPC H2O and spin down at 12,000rpm for 5 minutes at 4ºC, then it was air dried and dissolved in 10µL of DEPC H2O. The reaction working solution included: 5x iScript reaction mix 4 µl, iScript reverse transcriptase 1 µl, Nuclease-free water 14 µl, RNA template 1 µl. After cDNA molecules were obtained using the cDNA Synthesis Kit, I took advantage of iScript Reverse Transcription Supermix for qRT PCR to conduct Quantitative RT-PCR experiment. And I used the following thermo cycle condition to complete the quantitative RT-PCR in *C. elegans*: 95°C Denaturing for 5mins; 95°C Denaturing for 30secs; 60°C Annealing 30secs; 72°C Extension 30secs with picture taken at this point, repeated for 40 cycles, followed by 5 min 72°C Elongation. These experiments were performed on the Bio-Rad CFX-96 and CFX-new real time PCR systems. Ct values were used to calculate the amount of Orsay viral RNA loads.

3.2.7 Small RNA sequencing

We used small RNA sequencing protocols from the research by Felix et al., 2011, and the methods provided by Craig Mello's group for small RNA sequencing. However, instead of TAP (tobacco acid pyrophosphatase), RPP (RNA 5' polyphosphatase) was utilized in this experiment for hydrolysis of the phosphoric acid anhydride bonds in the triphosphate

bridge. Four 90 mm OP50 *E. coli* seeded plates with 15–20 adults (N2, *rde-1, rsd-2, rsd-3, rsd-6, sid-1, rde-10, rsd-2;sid-1, rsd-3;sid-1*) were grown for 4 days at 20°C. Subsequently the mixed stage animals from all plates were collected, pooled, and frozen at −80°C. Total RNA was extracted using the standard Trizol method as previously described. A cDNA library that did not depend on 5′-monophosphate ligation was constructed by RNA 5'polyphosphatase treatment using recommended adapters. Small RNA libraries were sequenced using the Illumina/ HiSeq 2500 platform (from UC Riverside Core facility). Fastq data files were processed using Perl custom in-house viral silencing suppressors scripts. Sequences in the expected size range (18–30 nucleotides) were aligned to the *C. elegans* genome (WS190) downloaded from the UCSC Genome Browser website [31] and complete Orsay virus genome (Genbank ID: HM030970.2 and HM030971.2) was retrieved from Genbank. In this experiment I received tremendous assistance from other members in our lab. I completed the Orsay virus infection, RNA extraction and infection efficiency detection experiments using qRT-PCR; ligation-independent cloning using RPP, deep sequencing sample preparation and sample submission steps were completed by a postdoc researcher in our lab Dr. Yanhong Han, and data analysis/graph drawing using in-house Perl scripts was mostly done by fellow students in our lab Jinfeng Lu (Figure 3.4A, Figure 3.4C, Figure 3.5A, Figure 3.5B), and Stephanie Coffman(Figure 3.4B) with my attendance. mFold secondary structure prediction in Figure 3.5C was conducted by me using mFold server website at the University of Albany, New York.

3.2.8 Additional statistical analysis

Data were expressed as mean ± s.e.m (standard error of the mean). Statistics graphs were drawn using GraphPad Prism (version 5.03, GraphPad Software Inc., La Jolla, CA).

3.3 Results

3.3.1 Characterization of Orsay virus infection in single gene mutants defective in systemic RNAi

The identification of Orsay virus from *C. elegans* field isolates made it possible to determine if antiviral RNAi induced by natural viral infection also requires genes that regulate systemic RNAi. To this end, worm mutants defective in systemic RNAi and the controls N2 (Mock), N2 and *rde-1* worms were infected by Orsay virus as previously described (Felix et al., 2011). The accumulation levels of Orsay virus in the infected worms 2 days after inoculation were detected by Northern blot hybridization using a riboprobe complementary to negative-strand of the Orsay viral genomic RNA1: As replication products but not inoculated viral loads, negative strands of Orsay virus would be more convincing as the indicator of Orsay virus replication in *C. elegans* comparing to probes detecting dsRNA and sense strand RNA1 of Orsay virus that would also exist in viral loads from inoculation.

Figure 3.1 Orsay virus RNA1 accumulation in single mutants of systemic RNAi genes

rRNA served as loading controls. Worms were infected by Orsay virus and harvested after four days of growth. N2 wild type strain which was not susceptible to Orsay virus infection served as negative control/mock and *rde-1* served as positive control. (A) Northern blot hybridization detection of Orsay virus RNA1 accumulation using RNA1 negative strand targeting riboprobe in *rsd-2, rsd-3, rsd-6, sid-1* and *rsd-4* mutant strains. The values below referred to the relative hybridization signal intensities of genomic RNA 1 measured for each sample with the accumulation level in *rsd-2* mutant set as 1. (B) Northern blot detection of Orsay virus RNA1 accumulation in *sid-1, sid-3* and *sid-5* mutants using RNA1 negative strand targeting riboprobe. The values below referred to the relative hybridization signal intensities of genomic RNA 1 measured for each sample with the accumulation level in *rde-1* mutant set as 1. (C) Northern blot hybridization detection of Orsay virus RNA1 accumulation in *rde-10, rde-11* mutants using riboprobes targeting negative strand of RNA1. The values below referred to the relative hybridization signal intensities of genomic RNA 1 measured for each sample with the accumulation level in *rsd-2* mutant set as 1.

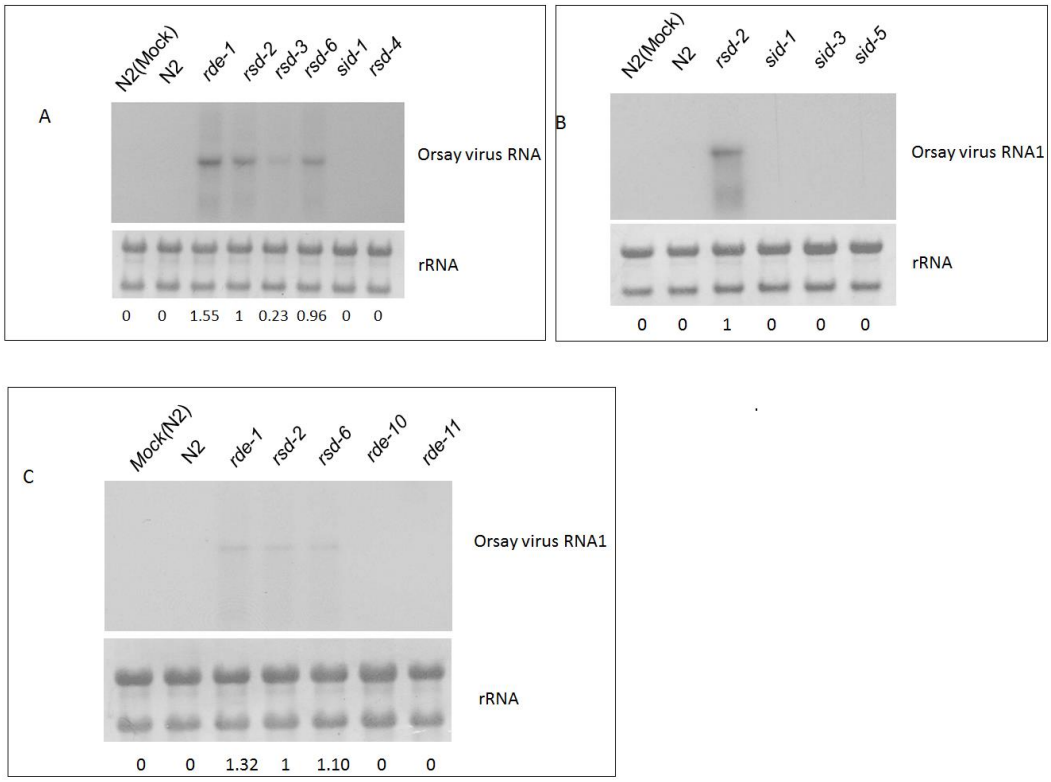
A
N2(Mock)
N2
rde-1
rsd-2
rsd-3
rsd-6
sid-1
rsd-4
Orsay virus RNA
rRNA
0 0 1.55 1 0.23 0.96 0 0
B
N2(Mock)
N2
rsd-2
sid-1
sid-3
sid-5
Orsay virus RNA1
rRNA
0 0 1 0 0 0
C
Mock(N2)
N2
rde-1
rsd-2
rsd-6
rde-10
rde-11
Orsay virus RNA1
rRNA
0 0 1.32 1 1.10 0 0

The results (Figure 3.1A) firstly confirmed that Orsay virus was indeed defective in the infection of N2 wild type worms but accumulated to high levels in *rde-1* mutant worms that are defective in antiviral RNAi as reported previously by others (Felix et al., 2011). I found that Orsay virus also accumulated to high levels in *rsd-2*, *rsd-3* and *rsd-6* mutant worms, but not in *rsd-4* or *sid-1*, mutants (Figure 3.1A). By comparison, the accumulation of the Orsay viral genomic RNA1 in *rsd-3* worms was lower compared to *rsd-2* and *rsd-6* mutant worms. These findings demonstrated that RSD-2, RSD-3 and RSD-6 genes were required for the *C. elegans* antiviral immunity against Orsay virus infection while RSD-2 and RSD-6 appeared to be more important comparing to RSD-3 gene. In contrast, a loss-of-function mutation in neither *rsd-4* nor *sid-1* mutant abolished the worm resistance to Orsay virus infection. These results were quite consistent with the findings based on the FHV replicon described in the previous Chapter and supported an antiviral role for the genes required for the spreading of RNAi signals from somatic tissues to germline.

Since *sid-1* and *rsd-4* mutants did not show significant enhancement in Orsay virus accumulation, I conducted experiments to determine if other worm genes from the SID-1/RSD-4 pathway of systemic RNAi were functional in antiviral immunity: For examples, SID-3 may act in the upstream of SID-1 to promote endocytic uptake of dsRNA whereas SID-5 is required for the export of *C. elegans* RNAi spreading signals independent of SID-1 (Jose et al., 2012). As shown in Figure 3.1B, it was found that neither *sid-3* nor *sid-5* mutant worms supported higher accumulation of Orsay virus than the N2 and *sid-1* worms did, in contrast to *rsd-2* mutant worms that consistently showed a

stable and robust Orsay virus replication. These findings demonstrated that removing any single gene from the SID-1 related pathway of systemic RNAi did not have a detectable negative effect on the antiviral immunity against Orsay virus infection.

To determine if the complex of RSD-2/RSD-6/RDE-10/RDE-11 implicated in dosage sensitive RNAi (Yang et al., 2012; Zhang et al., 2012) was involved in antiviral RNAi, I compared Orsay virus infection between N2 wild type worms and mutant strains defective in *rde-10* or *rde-11* using *rsd-2, rsd-6* and *rde-1* mutant worms as controls. Reproducible results obtained from these experiments showed that neither *rde-10* nor *rde-11* mutants supported higher Orsay viral accumulation compared to wild type N2 worms after Orsay virus infection (Figure 3.1C). This result illustrated that antiviral RNAi does not require the complex controlling the dosage-sensitive RNAi response. Based on these results together, I concluded that RSD-2, RSD-3 and RSD-6 genes participated in antiviral RNAi by promoting systemic RNAi in a mechanism independently of the assembly of RSD-2/RSD-6/RDE-10/RDE-11 complex and very possibly also the RNAi dosage response mechanisms. This conclusion is also supported by the observation that RSD-3 is required for both systemic RNAi and antiviral RNAi, but this protein is not found in the RSD-2/RSD-6/RDE-10/RDE-11 complex (Yang et al., 2012; Zhang et al., 2012).

I subsequently measured the brood sizes of mock and infected *rsd-2* and *rsd-3* animals to determine if Orsay virus infection affected host development or reproduction. Although Orsay virus infection did not alter the progeny number in *rsd-2* mutant

nematodes, the progeny production process was significantly slowed down during parents' adulthoods (Figure 3.2A). By contrast, Orsay virus infection had no detectable effect on the reproduction of *rsd-3* mutant worms (Figure 3.2B), similar to that reported previously for *drh-1* mutant worms (Felix et al., 2011). This study did not include *rsd-6* mutant since *rsd-6* worms already showed a reduction in progeny number before Orsay virus infection (Yang et al., 2012; Zhang et al., 2012). It is possible that the more efficient infection of Orasy virus in *rsd-2* mutant worms was responsible for a greater impact on the nematodes reproduction compared to *rsd-3* worms.

Fluorescent In-Situ Hybridization experiment (FISH), which detects complementary RNA sequences by fluorescent labeled DNA sequence, was conducted to localize the Orsay virus infection sites inside the whole animal bodies of *rsd-2, rsd-3,* and *rsd-6* worms (Figure 3.2C). As recently reported (Franz et al., 2014), Orsay virus infection was readily visible in *rde-1* mutant worms, but not in N2 worms, by the FISH detection of the viral genomic RNA1. Orsay virus FISH signals were also clearly detected in *rsd-2, rsd-3,* and *rsd-6* worms after infection (Figure 3.2C). The presence of Orsay virus FISH signals (Figure 3.2C) was limited to the intestinal cells in all of these mutant worms, but the signal spreading areas and pattern varied among different mutants and different individuals. This result was consistent to that reported previously by M.A Felix group using electron microscopy, which detected putative existence of viral particles in an intracellular multi-membrane compartment and in the intestinal lumen close to microvilli (Felix et al., 2011). Since the regions Orsay virus can infect were limited, the impacted tissue was also limited to *C. elegans* intestine, which may explain

why there were no strong and observable pathogenesis syndromes caused by Orsay virus in *C. elegans* body tissues.

Since fluorescence signals from individual animals were variable, the percentage of worms positive for the FISH signals was scored for each genotype of worms using fluorescent microscopy. The results revealed that Orsay virus infected 28%, 26%, and 18% of *rsd*-2, *rsd*-3 and *rsd*-6 mutant worms, respectively (Figure 3.2D), which were significantly higher than that (4%) observed after Orsay infection in the wild type N2 worms, though the FISH signals in *rsd-3* appeared to be much weaker.

I conducted qRT-PCR to measure the transcription levels of RSD-2 mRNA in *rde-4* mutant worms before and after Orsay virus infection, using *ama-1* mRNA encoding the large subunit of RNA polymerase II for quantity normalization. The *rde-4* mutant worms were chosen because the role of RSD-2 in antiviral RNAi was independent of RDE-4 (Guo et al., 2013). The RNA samples were collected after four days of Orsay virus infection. The results revealed an enhanced expression of RSD-2 gene by more than two folds in *rsd-4* mutant worms after Orsay virus infection (Figure 3.2E), suggesting that RSD-2 was induced by Orsay virus infection.

Figure 3.2 Orsay virus replication in *rsd-2, rsd-3* and *rsd-6* nematode bodies

(A) Orsay virus infection did not significantly alter the brood size of progeny production in *rsd-2* but it was able to slow down the reproduction of *rsd-2*. Error bars represented Standard Error of Mean (SEM) of three biological repeat experiments. Progeny numbers were counted from 10 parents per strain. **(**B) Orsay virus infection did not significantly alter the brood size of progeny production or the production rate of *rsd-3*. Error bars represented SEM of three biological repeats. **(**C) RNA FISH targeting Orsay virus RNA1. Images were detected using fluorescent microscopy in YFP channel. Yellow signals represented the Orsay virus RNA location, while red signals were the leaked signals from RFP channel of transgenic nematode strain mCherry marker. Probes were designed targeting Orsay virus RNA1. FISH probe hybridization was conducted four days post infection. **(**D) Percentage of nematodes showed fluorescent signals after FISH hybridization. 100 healthy animals of each strain were randomly selected and counted for the presence of FISH signals targeting Orsay virus RNA1. Error bars represented SEM of three respective experiments. FISH probe hybridization was conducted four days post virus infection. **(**E) qRT-PCR analysis indicated that expression of RSD-2 gene in *rde-4* worms was enhanced after Orsay virus infection**.** qRT-PCR levels were normalized to the expression of AMA-1- the large subunit of RNA polymerase II. The expression level of RSD-2 in mock animals without infection was set at 1. Error bars represented standard Error of Mean (SEM) of three biological repeat experiments. RNA was collected from worms after four days of Orsay virus infection.

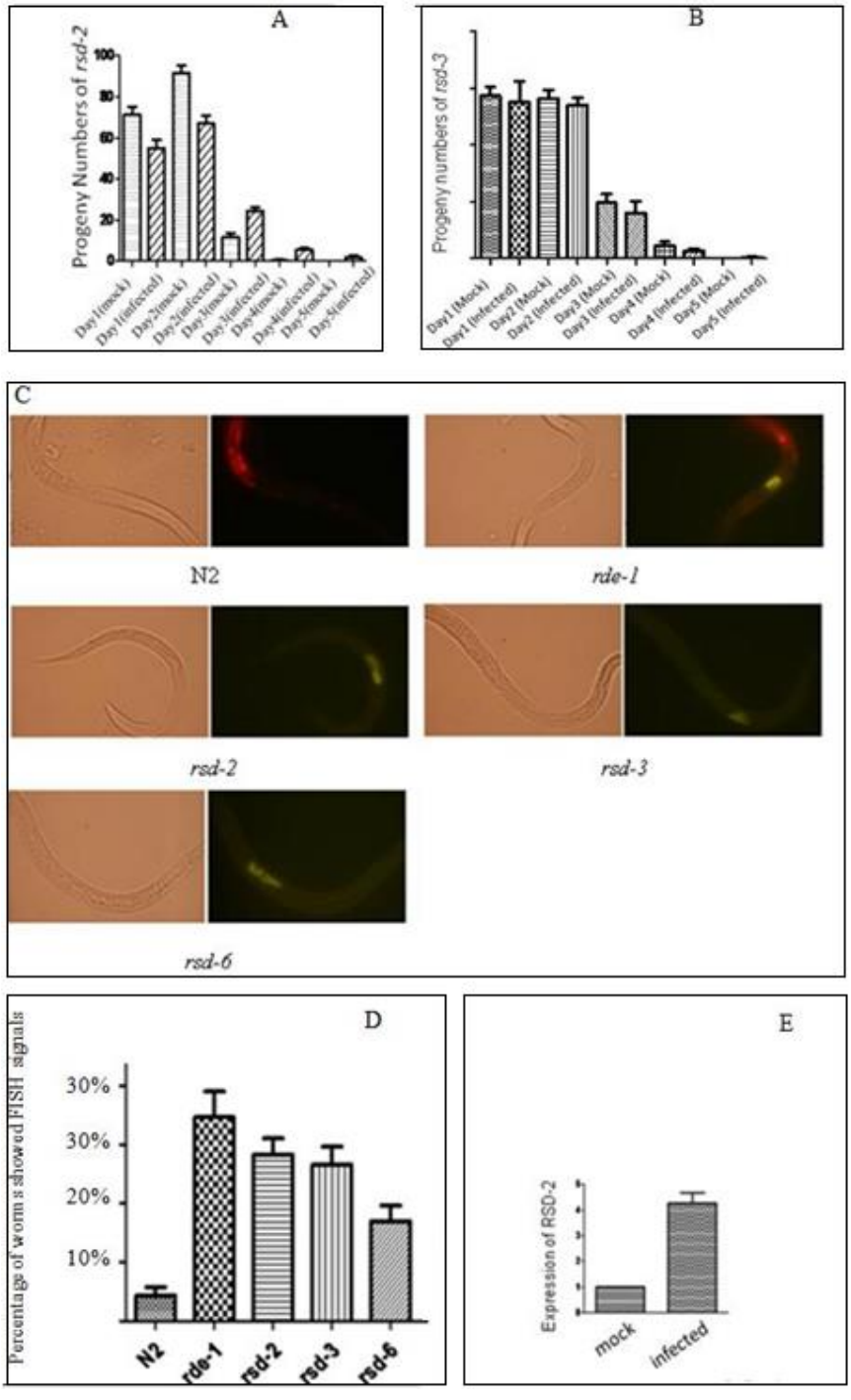
A
Progeny Numbers of rsd-2
B
Progeny numbers of rsd-3
C
N2
rde-1
rsd-2
rsd-3
rsd-6
D
Percentage of worms showed FISH signals
30%
30%
20%
10%
N2
rde-1
rsd-2
rsd-3
rsd-6
E
Expression of RSD-2
mock
infected

3.3.2 Characterization of Orsay virus infection in double mutants

Studies in plants indicate that viruses are targeted by RNAi in the infected cells (intracellular RNAi) and in the naïve cells (intercellular RNAi) where the incoming virus RNA is specifically degraded by RNAi initiated by the mobile silencing signal (Voinnet, 2005). The antiviral activity of intercellular RNAi is therefore detectable only when a virus is able to overcome intracellular RNAi and spread to neighboring cells and to distant tissues. Since the FHV replicon and Orsay virus used above are defective in RNAi suppression, *rsd-2;sid-1*, *rsd-3;sid-1* and *rrf-1;sid-1* double worm mutants were constructed. If SID-1contributed to antiviral RNAi, the presence of the *sid-1* allele was predicted to have an additive or synergistic effect on the accumulation of Orsay virus compared to that observed in *rsd-2*, *rsd-3* and *rrf-1* single mutants.

Both Northern blotting and qRT-PCR analysis revealed that Orsay virus accumulated in *rsd-2;sid-1* double mutant worms to levels significantly higher than those in *rsd-2* single mutant worms (Figure 3.3A/B). Orsay virus infection in the double mutant worms was also more efficient than in *rde-1* mutant worms and comparable to that in *rde-4* mutant worms. Orsay virus also accumulated to higher levels in *rsd-3;sid-1* double mutant worms than in *rsd-3* single mutant worm strains (Figure 3.3C), and similar result was found in *rrf-1;sid-1* double mutant worms comparing to in *rrf-1* single mutant worms (Figure 3.3D). RRF-1 encodes an RNA-dependent RNA polymerase (RdRp) required for somatic amplification of exogenous siRNA. These findings indicated that the SID-1 pathway of systemic RNAi also restricted Orsay virus infection.

Figure 3.3 Orsay virus infection in double gene mutants

(A) Northern blot hybridization detected Orsay virus genomic RNA1 negative strand in *rsd-2;sid-1* using negative strand RNA1 targeting riboprobes labeled with 32P. Worms were infected with Orsay virus and harvested after four days of growth. N2 strain served as negative control and *rde-1, rsd-2* served as positive controls. The values below referred to the relative hybridization signal intensities of Orsay virus genomic RNA1 measured for each sample with the accumulation level in *rsd-2* mutant set as 1. (B) qRT-PCR analysis of Orsay RNA1 viral load indicated that Orsay viral load in *rsd-2;sid-1* was more than two folds higher compared to *rsd-2* single mutant. qRT-PCR levels were normalized to the expression level of AMA-1. The viral RNA1 load in N2 wild type was set at 1. Error bars represented SEM of three biological replicates. RNA was collected from worms after four days post Orsay virus infection. (C) qRT-PCR analysis of Orsay RNA1 viral load indicated that Orsay viral load in *rsd-3;sid-1* was more than one fold higher compared to *rsd-3* single mutant. qRT-PCR levels were normalized to the expression of AMA-1. The viral RNA1 load in N2 wild type worms was set at 1. Error bars represented SEM of three biological replicates. RNA was collected from worms after four days of Orsay virus infection. (D) Northern blot hybridization detected Orsay virus genomic RNA1 negative strand of *rrf-1;sid-1* using riboprobes targeting Orsay virus RNA1. N2 strain served as negative control and *rsd-2, rrf-1* served as positive controls. The values below referred to the relative hybridization signal intensities of Orsay virus genomic RNA1 measured for each sample with the accumulation level in *rrf-1* mutant set as 1.

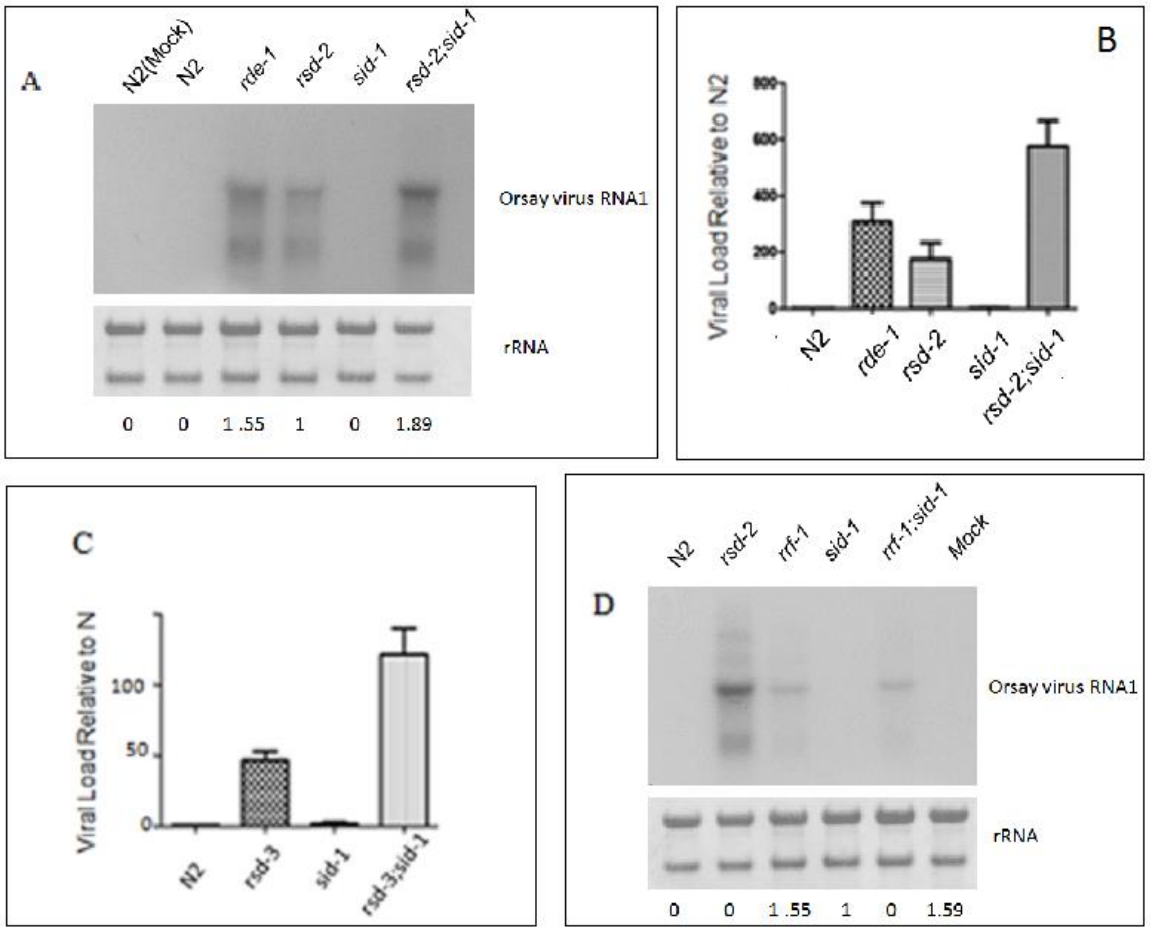
A
N2(Mock)
N2
rde-1
rsd-2
sid-1
rsd-2;sid-1
Orsay virus RNA1
rRNA
0 0 1.55 1 0 1.89
B
Viral Load Relative to N2
800
600
400
200
0
N2
rde-1
rsd-2
sid-1
rsd-2;sid-1
C
Viral Load Relative to N
100
50
0
N2
rsd-3
sid-1
rsd-3;sid-1
D
N2
rsd-2
rrf-1
sid-1
rrf-1;sid-1
Mock
Orsay virus RNA1
rRNA
0 0 1.55 1 0 1.59

3.3.3 Characterization of viral siRNA profiles in single and double mutants

To investigate the mechanism of systemic RNAi in antiviral immunity, I compared the populations of viral siRNAs between N2 and mutant worms after Orsay virus infection. The protocol to clone small RNAs by a ligation independent approach was used, which can analyze the total population of viral siRNAs including both primary and secondary siRNAs. Since the method more traditionally used- ligation dependent cloning would only be capable of capturing siRNA molecules with a 5'- monophosphate due to the activities of ligase was not able to process triphosphate modifications. As shown previously (Ashe et al., 2013; Guo and Lu, 2013), viral siRNAs produced in wild type N2 worms were predominantly antisense to the viral genomic RNAs (>95%, Figure 3.4C) and 22 nucleotides in length with a strong G bias at the 5'-termini (22G RNA: >50%, Figure 3.4A). The strong bias for negative-strand viral siRNAs (19%) and the preference for 22G RNAs in particular (2%) disappeared in *rde-1* mutant worms, known to be defective in the biogenesis of viral secondary siRNAs (Wu et al., 2010; Ashe et al., 2013; Guo and Lu, 2013).

I found that only 23%, 21% and 33% of the viral siRNA populations were 22G siRNAs in *rsd-2, rsd-3* and *rsd-6* mutants, respectively (Figure 3.4B). The total negative strand viral siRNAs were also less abundant in these mutants compared to N2 worms. Similar decreases in the abundance of total negative strands and 22G siRNAs were also detected in *rsd-2;sid-1*and *rsd-3;sid-1* double mutants. By contrast, the population profile of viral siRNAs in *sid-1* mutant worms was similar to that of N2 strain. Notably, *rde-10*

mutant worms also exhibited no defect in the biogenesis of the viral secondary siRNAs (Figure 3.4C), even though they were known to be defective in the biogenesis of the endogenous secondary siRNAs (Yang et al., 2012; Zhang et al., 2012). These results above indicated that RSD-2, RSD-3 and RSD-6, but not RDE-10 or SID-1, were required for the biogenesis of the viral secondary siRNAs for Orsay virus infection.

Mapping of the positive- and negative-strand viral siRNAs to the complete bipartite RNA genome of Orsay virus (Jiang et al., 2014) revealed that the production of viral siRNAs to target the genomic RNA2 was dramatically increased in *rde-1* mutant worms (Figure 3.5A/B). The relative abundance of RNA2-specific siRNAs was also much higher in *rsd-2*, *rsd-3*, *rsd-6* mutants compared to *sid-1* and *rde-10* mutants. The ratio of the viral siRNAs derived from RNA1 vs those from RNA2 in *rsd-2;sid-1* double mutant (1.03:1) was as low as in *rde-1* mutant, and lower than in *rsd-2* single mutant (2.28:1). However, such a difference was not observed between *rsd-3;sid-1* double mutant and *rsd-3* single mutant (Figure 3.5). There were hot spots of viral siRNAs to target specific regions of the viral genome (Figure 3.5A). Interestingly, one species of 22G siRNAs, 5'-GUACCG UAGACGAGAUUGAACUC-3' that is complementary to nucleotides 1847-1869 of Orsay virus RNA1 and represented 25% of the 22G siRNAs in N2 animals was found to be highly abundant in all of the sequenced worm strains (Figure 3.5C).

Figure 3.4 viRNA populations in mutants related to systemic RNAi

(A) Primary and secondary viRNA populations in strains N2, *rde-1, rde-10* and mutants related to systemic RNAi as indicated. 5′ independent small RNA sequencing captured both primary and secondary viRNAs. Data were grouped as sense or antisense and according to different lengths and the identity of the first nucleotide. (B) Percentage of antisense 22G viRNAs in the total population of viRNAs ranging from 20nt to 24nt long. While *rde-1* showed almost depleted 22G viRNA population, *rsd-2*, *rsd-3*, *rsd-6* and *rsd-2;sid-1*, *rsd-3;sid-1* were partially defective in the 22G secondary viRNA biogenesis. (C) Percentage of sense and antisense viRNAs in the total viRNA population.

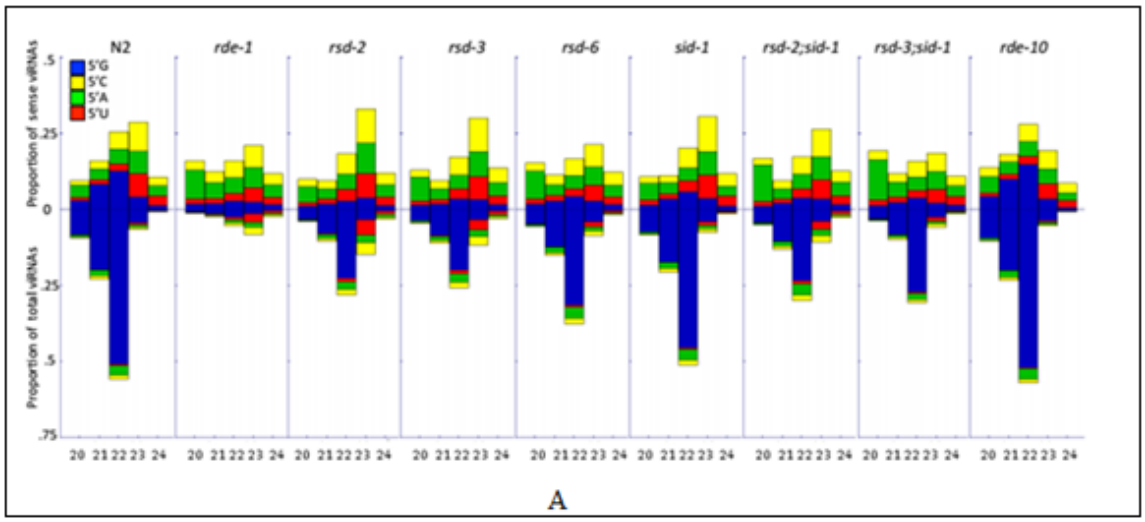

A

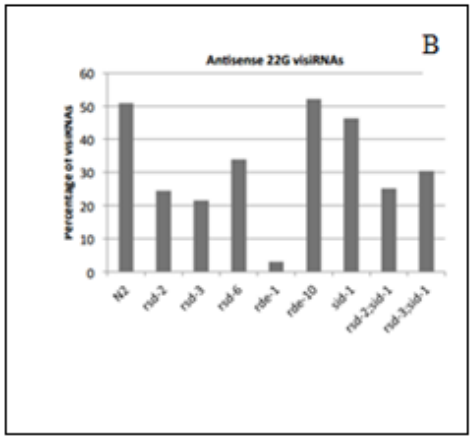

C

Strain	Sense	Antisense
N2	4.69%	95.31%
rde-1	80.53%	19.47%
rsd-2	39.34%	60.66%
rsd-3	43.90%	56.10%
rsd-6	31.36%	68.64%
sid-1	11.16%	88.84%
rsd-2;sid-1	38.20%	61.80%
rsd-3;sid-1	48.72%	51.28%
rde-1	3.59%	96.41%

Figure 3.5 Orsay virus genome coverage distribution of viRNA

(A) viRNA genome coverage distribution in the Orsay virus genome RNA1 and RNA2: Complete Orsay virus RNA1 and RNA2 sequences were downloaded from Genbank (HM030970.2 and HM030971.2). (B) Ratio of Orsay virus RNA1 derived viRNA to Orsay virus RNA2 derived viRNA (C) The most abundant 22G viRNA formed a stem-loop secondary structure, from mFold web server in the University of Albany. Arrows pointed to two end of the specific abundant 22G viRNA

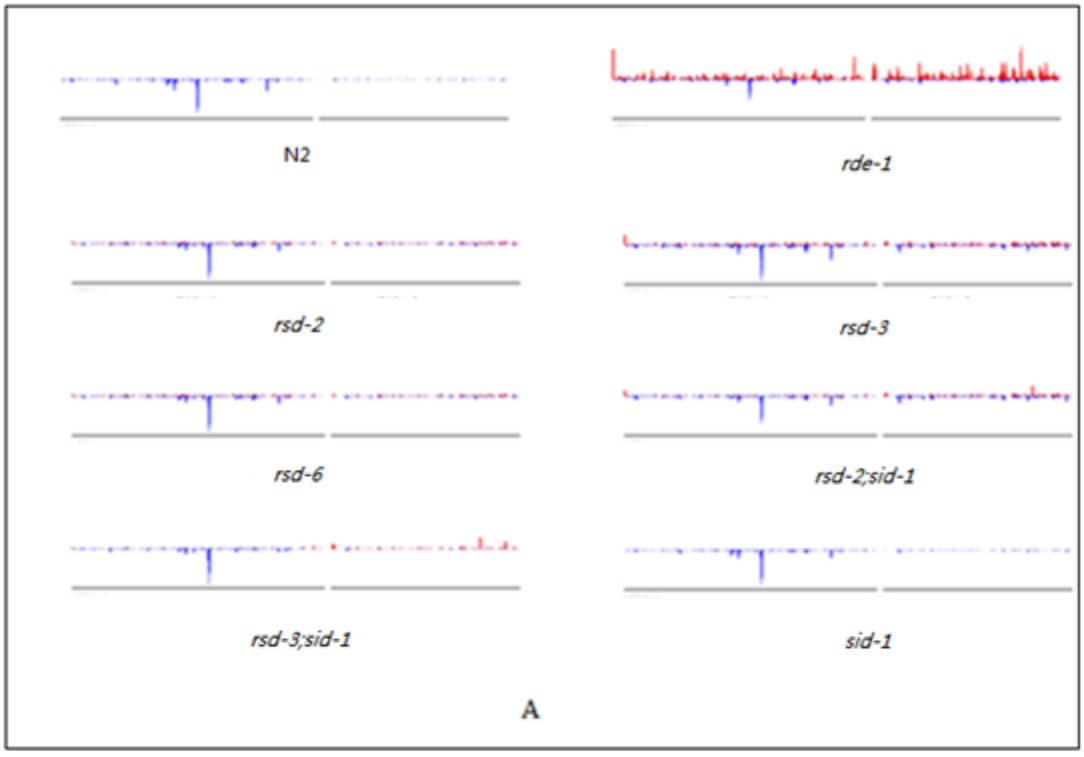
N2
rde-1
rsd-2
rsd-3
rsd-6
rsd-2;sid-1
rsd-3;sid-1
sid-1
A

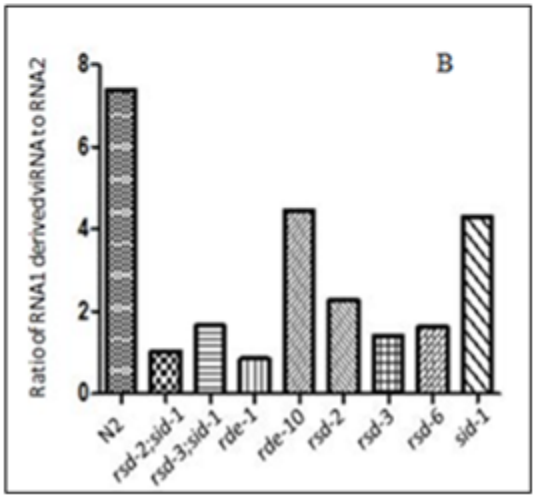
B
Ratio of RNA1 derived viRNA to RNA2
8
6
4
2
0
N2
rsd-2;sid-1
rsd-3;sid-1
rde-1
rde-10
rsd-2
rsd-3
rsd-6
sid-1

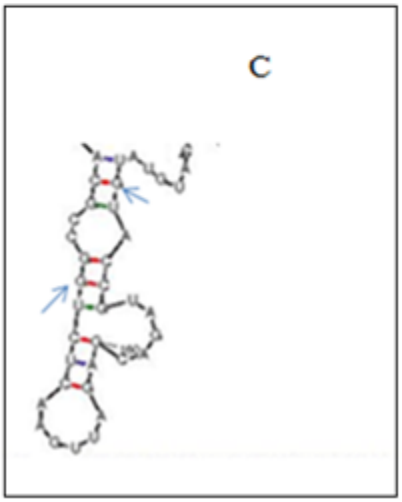
C

3.4 Discussion

Studies presented in this chapter characterized the infection and the antiviral RNAi response of *C. elegans* mutants defective in systemic RNAi to Orsay virus infection. The results showed that the genes responsible for systemic RNAi by controlling the transmission from somatic tissues to germline, including RSD-2, RSD-3 and RSD-6, played essential roles in antiviral RNAi against Orsay virus infection. My findings also indicated that the antiviral function of RSD-2 and RSD-6 did not require the formation of the complex among RSD-2, RSD-6, RDE-10 and RDE-11 involved in the dsRNA dosage sensitive response. In contrast, abolishing the function of the genes responsible for controlling the uptake or export of the RNAi spreading signals in systemic RNAi, including SID-1, RSD-4, SID-3 and SID-5, was insufficient to eliminate antiviral RNAi in *C. elegans*. Use of double mutant worms further revealed that the SID-1 pathway of systemic RNAi appeared to enhance antiviral RNAi against virus infection under conditions when Orsay virus efficiently replicated in *C. elegans*. Therefore, these findings, together with the results presented in the previous Chapter, for the first time provided evidence for an antiviral function of systemic RNAi in animals. This conclusion is consistent with an independent characterization of the antiviral activity of RSD-2 published recently by Guo and colleagues (Guo et al., 2013).

Comparison of the population of viral siRNAs by deep sequencing revealed that *rsd-2, rsd-3* and *rsd-6* mutant worms were all partially defective in the biogenesis of the viral secondary siRNAs. This finding indicated that robust production of the viral

secondary siRNAs was necessary for effective antiviral RNAi in animals. Recent studies have shown that siRNAs act as the spreading signals of RNAi in plants (Melnyk et al., 2011). Although it remains unclear if viral siRNAs spread to induce specific antiviral RNAi in naïve cells, the 2b protein of Cucumber mosaic virus inhibits systemic RNAi and blocks the synthesis of the viral secondary siRNAs (Guo and Ding, 2002; Diaz-Pendon et al., 2007; Wang et al., 2010). Thus, it could be possible that spread of the viral secondary siRNAs may also occur and potentiate antiviral RNAi in *C. elegans*. It is important to point out that the studies by Hunter and colleagues (Jose et al., 2011) ruled out a role for RDE-4, but not siRNAs, in systemic RNAi since processing of long dsRNA into siRNAs can be independent of RDE-4 (Habig et al., 2008; Guo et al., 2013).

Studies presented in this dissertation further showed that the genes from the systemic RNAi pathways exhibited similar antiviral activities against by either the infection of Orsay virus or the replication of the FHV replicon. Similar genetic requirements have also been presented previously for the core RNAi factors in the control of the FHV replicon and Orsay virus (Lu et al., 2005; Lu et al., 2009; Felix et al., 2011; Ashe et al., 2013; Guo and Lu, 2013; Guo et al., 2013). These observations support a model in which antiviral RNAi is induced in the cytoplasm following the production and immune recognition of the viral dsRNA replicative intermediates (Ding and Lu, 2011).

3.5 References

Ashe, A., T. Belicard, J. Le Pen, P. Sarkies, L. Frezal, N. J. Lehrbach, M. A. Felix and E. A. Miska (2013). A deletion polymorphism in the Caenorhabditis elegans RIG-I homolog disables viral RNA dicing and antiviral immunity. *Elife* **2**.

Diaz-Pendon, J. A., F. Li, W. X. Li and S. W. Ding (2007). Suppression of antiviral silencing by cucumber mosaic virus 2b protein in Arabidopsis is associated with drastically reduced accumulation of three classes of viral small interfering RNAs. *Plant Cell* **19**(6): 2053-63.

Ding, S. W. and R. Lu (2011). Virus-derived siRNAs and piRNAs in immunity and pathogenesis. *Curr Opin Virol* **1**(6): 533-44.

Felix, M. A., A. Ashe, J. Piffaretti, G. Wu, I. Nuez, T. Belicard, Y. F. Jiang, G. Y. Zhao, C. J. Franz, L. D. Goldstein, M. Sanroman, E. A. Miska and D. Wang (2011). Natural and Experimental Infection of Caenorhabditis Nematodes by Novel Viruses Related to Nodaviruses. *Plos Biology* **9**(1).

Franz, C. J., H. Renshaw, L. Frezal, Y. Jiang, M. A. Felix and D. Wang (2014). Orsay, Santeuil and Le Blanc viruses primarily infect intestinal cells in Caenorhabditis nematodes. *Virology* **448**: 255-64.

Guang, S., A. F. Bochner, D. M. Pavelec, K. B. Burkhart, S. Harding, J. Lachowiec and S. Kennedy (2008). An Argonaute transports siRNAs from the cytoplasm to the nucleus. *Science* **321**(5888): 537-41.

Guo, H. S. and S. W. Ding (2002). A viral protein inhibits the long range signaling activity of the gene silencing signal. *EMBO J.* **21**(3): 398-407.

Guo, X. Y. and R. Lu (2013). Characterization of Virus-Encoded RNA Interference Suppressors in Caenorhabditis elegans. *Journal of Virology* **87**(10): 5414-23.

Guo, X. Y., R. Zhang, J. Wang and R. Lu (2013). Antiviral RNA Silencing Initiated in the Absence of RDE-4, a Double-Stranded RNA Binding Protein, in Caenorhabditis elegans. *Journal of Virology* **87**(19): 10721-29.

Habig, J. W., P. J. Aruscavage and B. L. Bass (2008). In C. elegans, high levels of dsRNA allow RNAi in the absence of RDE-4. *PLoS ONE* **3**(12): e4052.

Jiang, H., C. J. Franz, G. Wu, H. Renshaw, G. Zhao, A. E. Firth and D. Wang (2014). Orsay virus utilizes ribosomal frameshifting to express a novel protein that is incorporated into virions. *Virology* **450-451**: 213-21.

Jose, A. M., G. A. Garcia and C. P. Hunter (2011). Two classes of silencing RNAs move between Caenorhabditis elegans tissues. *Nat Struct Mol Biol* **18**(11): 1184-8.

Jose, A. M., Y. A. Kim, S. Leal-Ekman and C. P. Hunter (2012). Conserved tyrosine kinase promotes the import of silencing RNA into Caenorhabditis elegans cells. *Proceedings of the National Academy of Sciences of the United States of America* **109**(36): 14520-25.

Lu, R., M. Maduro, F. Li, H. W. Li, G. Broitman-Maduro, W. X. Li and S. W. Ding (2005). Animal virus replication and RNAi-mediated antiviral silencing in Caenorhabditis elegans. *Nature* **436**(7053): 1040-3.

Lu, R., E. Yigit, W. X. Li and S. W. Ding (2009). An RIG-I-Like RNA Helicase Mediates Antiviral RNAi Downstream of Viral siRNA Biogenesis in Caenorhabditis elegans. *Plos Pathogens* **5**(2).

Melnyk, C. W., A. Molnar and D. C. Baulcombe (2011). Intercellular and systemic movement of RNA silencing signals. *Embo J* **30**(17): 3553-63.

Voinnet, O. (2005). Non-cell autonomous RNA silencing. *Febs Letters* **579**(26): 5858-71.

Wang, X. B., Q. Wu, T. Ito, F. Cillo, W. X. Li, X. Chen, J. L. Yu and S. W. Ding (2010). RNAi-mediated viral immunity requires amplification of virus-derived siRNAs in Arabidopsis thaliana. *Proc Natl Acad Sci U S A* **107**(1): 484-9.

Wu, Q., Y. Luo, R. Lu, N. Lau, E. C. Lai, W. X. Li and S. W. Ding (2010). Virus discovery by deep sequencing and assembly of virus-derived small silencing RNAs. *Proc Natl Acad Sci U S A* **107**(4): 1606-11.

Yang, H., Y. Zhang, J. Vallandingham, H. Li, L. Florens and H. Y. Mak (2012). The RDE-10/RDE-11 complex triggers RNAi-induced mRNA degradation by association with target mRNA in C. elegans (vol 26, pg 846, 2012). *Genes & Development* **26**(10): 1122-22.

Zhang, C., T. A. Montgomery, S. E. J. Fischer, S. M. D. A. Garcia, C. G. Riedel, N. Fahlgren, C. M. Sullivan, J. C. Carrington and G. Ruvkun (2012). The Caenorhabditis elegans RDE-10/RDE-11 Complex Regulates RNAi by Promoting Secondary siRNA Amplification. *Current Biology* **22**(10): 881-90.

Chapter 4: Conclusion and future directions

4.1 Conclusion

In summary, from the above chapters of this dissertation it can be concluded that the systemic RNAi genes RSD-2, RSD-6 and RSD-3 were also required in the antiviral defense against both Orsay virus infection and Flock house virus replicon. This conclusion is solid as multiple approaches including green fluorescence visual detection and statistical analysis, northern blot hybridization, western blot hybridization, qRT-PCR and fluorescence in-situ hybridization detections all provided consistent results. The major difference between the results from Orsay virus infection and the results from FHV FR1gfp replication lay in *rsd-3* mutant: while RSD-3 gene was as important as RSD-2 and RSD-6 in the antiviral immunity against FHV replication judged by the measurement of FR1gfp RNA1 accumulation levels, *rsd-3* was a weaker mutant for immunity against Orsay virus infection comparing to *rsd-2* or *rsd-6*. A possible reason for this variance is that RSD-3 is a homolog to the human enthoprotin, a component of the mammalian vesicle trafficking mechanism (Wasiak et al., 2002;Tijsterman et al., 2004). Vesicle trafficking system was taken advantage of by viruses for the intercellular transport. Though previous study indicated that the role of RSD-3 in systemic RNAi was not necessarily related to vesicle trafficking, it was still possible that RSD-3 contributed to the spreading of Orsay virus among the nematode cells through vesicle trafficking because virus trafficking may take different pathways from systemic RNAi spreading

(Han et al., 2008;Chambers and Takimoto, 2010;Meckes and Raab-Traub, 2011;Nour and Modis, 2014).

Though RSD-2 and RSD-6 were also involved in dosage sensitive RNAi response and 22G secondary siRNA biogenesis, other genes required for this mechanism like RDE-10 and RDE-11 were not indispensable in the *C. elegans* antiviral immunity. This finding indicated that the roles of RSD-2 and RSD-6 in antiviral immunity were not related to the formation of RSD-2/RSD-6/RDE-10/RDE-11 complex nor dosage RNAi response. Another indirect proof for the fact that the roles RSD-2 and RSD-6 played in antiviral immunity were not related to dosage sensitive RNAi response was that RSD-3, a gene not yet found to be present in the dosage RNAi complex, still played an important role in *C. elegans* antiviral immunity. Small RNA profiles indicated that secondary viRNA productions were partially abolished in *rsd-2, rsd-3* and *rsd-6* mutants. Another interesting finding of this research is that though *sid-1* single mutant as well as other single mutants in SID-1 related spreading RNAi pathways like *sid-3* or *sid-5* was not defective in antiviral immunity, double mutants of *sid-1;rsd-2* and *sid-1;rsd-3* did show additive effect on the accumulation levels of Orsay virus RNA1 comparing to the accumulation levels in *rsd-2* and *rsd-3* single mutants respectively. This was an unarguable proof of the importance of systemic RNAi in antiviral immunity. Moreover, the mechanism of RSD-2, RSD-3 and RSD-6's roles in antiviral immunity was different from their roles in core RNAi or dosage sensitive RNAi response, but very likely through their roles in spreading RNAi. And the spreading RNAi signals were possibly related to secondary viRNA biogenesis, as presented in small RNA profiling results.

A possible explanation to the finding that *sid-1* single mutant still has an intact antiviral immunity machinery but loss of SID-1 function in *rsd-2* or *rsd-3* mutants caused additive effects in antiviral immunity deficiency is that though the role of SID-1 was not significant alone, SID-1 might play a redundant role in the absence of the spreading RNAi related antiviral pathway participated by RSD-2 or RSD-3 genes. Therefore, RSD-2, RSD-3 and RSD-6 could act as the main and preferred components of the spreading mechanism of Orsay viral silencing signals independent of SID-1, SID-3, SID-5 or RSD-4, but SID-1 might also be a partially functional substitute for RSD-2 or RSD-3 in the absences of them.

Like many genes required for the antiviral immunity against HIV or other viruses, the expression level of RSD-2 was enhanced by more than two folds after Orsay virus infection in *rde-4* mutant- the mutant in which the replication level of Orsay virus reached the highest level comparing to other mutants like *rde-1* (Knapp et al., 2003;Elco et al., 2005;Nasr et al., 2012). This finding implied the importance of RSD-2 and other related genes in antiviral immunity- the abundant presences of Orsay viral RNA and particles would trigger the activation of RSD-2 related regulation mechanisms in *C. elegans*. However, this increase was not observable in N2 canonical strain and others, probably because only a large amount of Orsay virus presence could induce the expression of RSD-2 gene (Sarkies et al., 2013).

As was discovered in plants, spreading RNAi was proven to be important to antiviral immunity in *C. elegans* in this dissertation (Voinnet et al., 1998). Spreading

RNAi took its role as a crucial enhancer of the core RNAi machinery composed of RDE-1, RDE-4, DRH-1 and DCR-1. But the fact that *sid-1* single mutant- the mutant defective in uptake of dsRNA silencing signals was not at all deficient in antiviral immunity against Orsay virus infection indicated that unlike spreading of feeding, microinjection or transgenic RNAi signals in *C. elegans*, dsRNA was unlikely responsible for the systemic RNAi defense against Orsay virus infection or Flock house virus replicon among *C. elegans* cells. Therefore, similar to the results from plants, siRNA molecules were likely to be the spreading messengers of systemic RNAi responsible for the antiviral RNAi in *C. elegans*. RSD-2, RSD-3 and RSD-6 genes may facilitate the movement of these siRNA molecules derived from Orsay virus, either dependent on Dicer or independent of Dicer protein among the cells. In the absence of these proteins, SID-1 oriented systemic RNAi pathway could likely substitute the roles of RSD-2, RSD-3 and RSD-6 partially, this fact implied that dsRNA could work as spreading RNAi molecules for antiviral immunity under certain circumstances. The transmission of antiviral gene silencing spreading signals into naïve cell could initiate the innate immunity defense against virus infection in these cells. These systemic RNAi signals could be taken by the core RNAi machinery- for instance, siRNA molecules could be loaded into RISC complex or RdRp complexes to initiate downstream RNAi processes thus trigger antiviral RNAi in the absence of Orsay virus or other viruses in naïve cells. Thus the immunity triggered and further enhanced by *C. elegans* antiviral immunity was comparable to the innate immunity in mammals as a protection mechanism.

4.2 Future directions

4.2.1 Forward genetics screen

Unfortunately, the forward genetic mapping process aiming at searching for new genes or new components required for antiviral immunity in *C. elegans* did not meet with success. The details of these efforts and experiments using EMS mutagenesis and snip-SNPs mapping strategy would be further and clearly described in the appendix chapter. The failure in forward genetics mapping was caused by the following reasons: Firstly, the usage of green fluorescence signals as genetic marker for mapping could be misleading in most occasions even excluding the effect of autofluorescence by imposing specific sample selection criteria (Clokey and Jacobson, 1986; Chalfie et al., 1994). The occurrence of one or two misinterpretation of genetic markers would trigger a misleading direction for genetic positioning during Snip-SNPs mapping process. Moreover, during the numerous genetic mapping experiments, it was found that mapping processes based upon green fluorescence could very possibly mislead to mapping the mutation to chromosome V where the transgenic FR1gfp replicon located. Therefore, deficiency in exogenous RNAi, as shown by feeding RNAi results, seemed to be a more reliable indicator for genetic mapping. The reason for the existence of false positive signals is that the strain used in this dissertation contains multiple copies of the FR1gfp transgenic replicon which can be overexpressed in the nematode body thus produced a large amount of FR1gfp transcripts exceeding the capability of RNAi clearance effect. This shortcoming was overcome by using a single copy FR1gfp transgenic *C. elegans* strain which was quite unlikely to show false green fluorescence signals in the background of

wild type strains thus improves the easiness of genetic mapping (Mello et al., 1991; Frokjaer-Jensen et al., 2008).

Secondly, Snip-SNPs mapping method I used in this research was comparably time consuming and risky. Snip-SNPs mapping requires numerous rounds of genetic crosses to successfully position the mutation of interest to a small interval. New mapping strategy applied by our lab based on the *de novo* whole Gene Sequencing (WGS) strategy was a dramatically faster and more cost-effective way to precisely position a genetic lesion. However, as the mutant strain in most cases contained a large amount of mutation loads in its chromosome, a mutant retrieved from a genetic screen should be crossed with a polymorphic *C. elegans* strain. A cloud-based pipeline aimed at genetic research available on the Galaxy web platform called CloudMap was used by other group members to facilitate the data analysis process (Doitsidou et al., 2010;Minevich et al., 2012). This next generation forward genetics mapping method was also successfully utilized in other organisms like *Arabidopsis* to search for the gene of interest (Austin et al., 2011).

Thirdly, the failure in finding the location of mutation in *vde-10* was also a result from the vast introns and coding sequences contained in *rsd-2:* although mapping data seemingly positioned the mutation to an interval of 0.5cM and preliminary complementation data appeared to support the hypothesis that the mutation located within *vde-10* was in RSD-2 gene, no consistent sequencing result could prove that there was a mutation in RSD-2 exon regions. However, as RSD-2 could be transcribed into four

different mRNA isoforms, mutations in introns may also lead to a changed pattern of alternative splicing resulting in producing isoforms which might not participate in antiviral immunity in *C. elegans* (Venables, 2004; Han et al., 2008). As well there could be other intron-located mutations that could trigger the loss of competence in the antiviral immunity of *vde-10* mutant (Tijsterman et al., 2004).

Other than forward genetics screen, reverse genetics screen using the existed feeding RNAi bacteria library could also reveal more genes involved in the nematodes antiviral immunity (Fraser et al., 2000; Gonczy et al., 2000; Sun et al., 2011). This method has been utilized by the other lab members to search for the antiviral defense related genes that were not discovered yet. With these modifications, the project on searching for new components of the nematodes antiviral immunity now seems more promising and should progress more smoothly with much quicker outcomes.

4.2.2 Systemic RNAi and antiviral immunity

In spite of unexpected problems in forward genetics screening included in the following Appendix, this research was overall successful. It provided the first evidence for the function of systemic RNAi in animals' antiviral immunity, and the results were proven to be consistent both in FHV transgenic replicon model and authentic Orsay virus infection. It also proved that SID-1, a major systemic RNAi gene previously indicated to be not related to the *C. elegans* antiviral immunity did play roles in the defense against Orsay virus infection. This research also included efforts in forward genetics screen followed by map based cloning. But aside from the above achievements, more questions remained to be answered regarding the roles of systemic RNAi in antiviral immunity like: 1.What are

the spreading signals of antiviral immunity in *C. elegans* as main dsRNA importers and exporters SID-1/SID-3/SID-5/RSD-4 were not as important in exogenous RNAi? 2. What are the other components of the antiviral systemic RNAi pathway? Reverse or forward genetics screens current undergoing at our lab could help answer these questions. Y Two-Hybrid and Co-Immunoprecipitation (Co-IP) experiments can also help to identify known proteins from the systemic RNAi effector complex. The solution to the myth how systemic RNAi acts in antiviral immunity in animals may be key to the solution of RNAi delivery problems encountered both in the research and industry of RNAi therapy (Wang et al., 2010), and it will for sure make the health and welfare of humankind benefit in the near future.

4.2 References

Austin, R. S., D. Vidaurre, G. Stamatiou, R. Breit, N. J. Provart, D. Bonetta, J. Zhang, P. Fung, Y. Gong, P. W. Wang, P. McCourt and D. S. Guttman (2011). Next-generation mapping of Arabidopsis genes. *Plant J* **67**(4): 715-25.

Chalfie, M., Y. Tu, G. Euskirchen, W. W. Ward and D. C. Prasher (1994). Green fluorescent protein as a marker for gene expression. *Science* **263**(5148): 802-5.

Chambers, R. and T. Takimoto (2010). Trafficking of Sendai virus nucleocapsids is mediated by intracellular vesicles. *PLoS One* **5**(6): e10994.

Clokey, G. V. and L. A. Jacobson (1986). The autofluorescent "lipofuscin granules" in the intestinal cells of Caenorhabditis elegans are secondary lysosomes. *Mech Ageing Dev* **35**(1): 79-94.

Doitsidou, M., R. J. Poole, S. Sarin, H. Bigelow and O. Hobert (2010). C. elegans mutant identification with a one-step whole-genome-sequencing and SNP mapping strategy. *PLoS One* **5**(11): e15435.

Elco, C. P., J. M. Guenther, B. R. Williams and G. C. Sen (2005). Analysis of genes induced by Sendai virus infection of mutant cell lines reveals essential roles of interferon regulatory factor 3, NF-kappaB, and interferon but not toll-like receptor 3. *J Virol* **79**(7): 3920-9.

Fraser, A. G., R. S. Kamath, P. Zipperlen, M. Martinez-Campos, M. Sohrmann and J. Ahringer (2000). Functional genomic analysis of C-elegans chromosome I by systematic RNA interference. *Nature* **408**(6810): 325-30.

Frokjaer-Jensen, C., M. W. Davis, C. E. Hopkins, B. J. Newman, J. M. Thummel, S. P. Olesen, M. Grunnet and E. M. Jorgensen (2008). Single-copy insertion of transgenes in Caenorhabditis elegans. *Nat Genet* **40**(11): 1375-83.

Gonczy, P., C. Echeverri, K. Oegema, A. Coulson, S. J. M. Jones, R. R. Copley, J. Duperon, J. Oegema, M. Brehm, E. Cassin, E. Hannak, M. Kirkham, S. Pichler, K. Flohrs, A. Goessen, S. Leidel, A. M. Alleaume, C. Martin, N. Ozlu, P. Bork and A. A. Hyman (2000). Functional genomic analysis of cell division in C-elegans using RNAi of genes on chromosome III. *Nature* **408**(6810): 331-36.

Han, W., P. Sundaram, H. Kenjale, J. Grantham and L. Timmons (2008). The Caenorhabditis elegans rsd-2 and rsd-6 genes are required for chromosome functions during exposure to unfavorable environments. *Genetics* **178**(4): 1875-93.

Knapp, S., L. J. Yee, A. J. Frodsham, B. J. Hennig, S. Hellier, L. Zhang, M. Wright, M. Chiaramonte, M. Graves, H. C. Thomas, A. V. Hill and M. R. Thursz (2003). Polymorphisms in interferon-induced genes and the outcome of hepatitis C virus infection: roles of MxA, OAS-1 and PKR. *Genes Immun* **4**(6): 411-9.

Meckes, D. G., Jr. and N. Raab-Traub (2011). Microvesicles and viral infection. *J Virol* **85**(24): 12844-54.

Mello, C. C., J. M. Kramer, D. Stinchcomb and V. Ambros (1991). Efficient gene transfer in C.elegans: extrachromosomal maintenance and integration of transforming sequences. *EMBO J* **10**(12): 3959-70.

Minevich, G., D. S. Park, D. Blankenberg, R. J. Poole and O. Hobert (2012). CloudMap: a cloud-based pipeline for analysis of mutant genome sequences. *Genetics* **192**(4): 1249-69.

Nasr, N., S. Maddocks, S. G. Turville, A. N. Harman, N. Woolger, K. J. Helbig, J. Wilkinson, C. R. Bye, T. K. Wright, D. Rambukwelle, H. Donaghy, M. R. Beard and A. L. Cunningham (2012). HIV-1 infection of human macrophages directly induces viperin which inhibits viral production. *Blood* **120**(4): 778-88.

Nour, A. M. and Y. Modis (2014). Endosomal vesicles as vehicles for viral genomes. *Trends Cell Biol* **24**(8): 449-54.

Sarkies, P., A. Ashe, J. Le Pen, M. A. McKie and E. A. Miska (2013). Competition between virus-derived and endogenous small RNAs regulates gene expression in Caenorhabditis elegans. *Genome Res* **23**(8): 1258-70.

Sun, Y., P. Yang, Y. Zhang, X. Bao, J. Li, W. Hou, X. Yao, J. Han and H. Zhang (2011). A genome-wide RNAi screen identifies genes regulating the formation of P bodies in C. elegans and their functions in NMD and RNAi. *Protein Cell* **2**(11): 918-39.

Tijsterman, M., R. C. May, F. Simmer, K. L. Okihara and R. H. A. Plasterk (2004). Genes required for systemic RNA interference in Caenorhabditis elegans. *Current Biology* **14**(2): 111-16.

Venables, J. P. (2004). Aberrant and alternative splicing in cancer. *Cancer Res* **64**(21): 7647-54.

Voinnet, O., P. Vain, S. Angell and D. C. Baulcombe (1998). Systemic spread of sequence-specific transgene RNA degradation in plants is initiated by localized introduction of ectopic promoterless DNA. *Cell* **95**(2): 177-87.

Wang, J., Z. Lu, M. G. Wientjes and J. L. Au (2010). Delivery of siRNA therapeutics: barriers and carriers. *AAPS J* **12**(4): 492-503.

Wasiak, S., V. Legendre-Guillemin, R. Puertollano, F. Blondeau, M. Girard, E. de Heuvel, D. Boismenu, A. W. Bell, J. S. Bonifacino and P. S. McPherson (2002). Enthoprotin: a novel clathrin-associated protein identified through subcellular proteomics. *J Cell Biol* **158**(5): 855-62.

Appendix: Forward genetics screen and mapping

Abstract

In this appendix section, I described the efforts invested on forward genetics screen using EMS mutagenesis and snip-SNPs mapping strategy. Through EMS mutagenesis screens, 29 mutant strains were found to be consistently defective to antiviral immunity throughout different generations, as indicated by green fluorescence visual signals from FR1gfp reporter. Three mutants which showed most significant deficiencies in antiviral immunity- *vde-10, vde-54* and *vde-45* were selected for subsequent mapping oriented experiments. These three mutants were categorized into two classes based on their responses to *unc-22* and *pop-1* RNAi experiments: the RNAi machineries in *vde-45* and *vde-45* remained effective, whereas *vde-10* was a partial deficient mutant in RNAi. Due to the comparable easiness of mapping, *vde-10* was selected solely for genetic mapping. Using Snip-SNPs strategy, the mutation in *vde-10* was seemingly positioned in a small interval where RSD-2 gene located. However, no consistent results from mutant sequencing could confirm that there was mutation in the exons of RSD-2 gene.

5. 1 Introduction

As described in the introductory chapter, forward genetics research, especially EMS mutagenesis has been widely used as a powerful approach to search for genes which may have various function in a diverse variety of organisms including *C. elegans* (Brenner, 1974; Mullins et al., 1994; St Johnston, 2002; Kim et al., 2006). Due to the vast mutation loads in the genome caused by EMS treatment, mutant strains should undergo backcrosses to clean up the genetic background (Brown and Balling, 2001). Traditional two point mapping or three point mapping can be utilized to locate the mutation of interest to an interval containing a few cosmids, subsequently different cosmids could be used for the attempts to rescue the mutation phenotype. The cosmid which can rescue the mutation phenotype is confirmed to contain the gene of interest (Ling et al., 1999). However, in some genes required for the transgene process in *C. elegans* like RSD-2, cosmid rescue experiments could be less accessible (Han et al., 2008).

In this appendix, snip-SNPs mapping strategy based on SNP polymorphisms between reference strain Hawaiian CB4856 and canonical strain N2 was used in the mapping process (Wicks et al., 2001; Davis et al., 2005),and plenty influential researches used this strategy to map the genes of interest (Frokjaer-Jensen et al., 2008). This strategy includes two sequential steps- chromosomal mapping which aims at positioning the mutation on a specific chromosome, and interval mapping which narrows the genetic distance of the region that harbors the mutation to a few cosmids (Wicks et al., 2001).

Indicator selection is also an important factor towards a successful map-based cloning process (Vogel et al., 2012). Due to the existence of false green fluorescence signals, feeding RNAi response was utilized as an indicator of these mutants as it is more consistent and less misleading (Chalfie et al., 1994). As germline RNAi is abolished in the mapping reference strain CB4856 due to its deficiency in the Argonaute PPW-1 (Tijsterman et al., 2002), *unc-22* feeding RNAi was used as the sole indicator of mutant deficiency in antiviral immunity.

5. 2 Materials and methods

5.2.1 Forward genetics research strategy

I followed the following pipeline (Figure 5.1) to conduct research in this appendix. Parental hermaphrodites of *C. elegans* transgenic strain carrying FR1gfp replicon were treated with EMS reagent for 4 hours, after a one-hour recovery these animals were placed on numerous plates seeded with OP50. F2 progenies of these worms were carefully collected and screened for green fluorescence visual signals from FR1gfp reporters after heat treatment. The selected animals were scrutinized in two further generations in order to avoid the false-positive signals. The nematode strains passed two further generations of scrutiny were detected for green fluorescence signal intensity, three strongest mutants were selected for further RNAi response characterizing. Following chromosomal mapping and interval mapping based on CAPS and dCAPS analysis (Neff et al., 1998), the mutation was positioned in a small interval between two relatively close markers on the *C. elegans* genetic map.

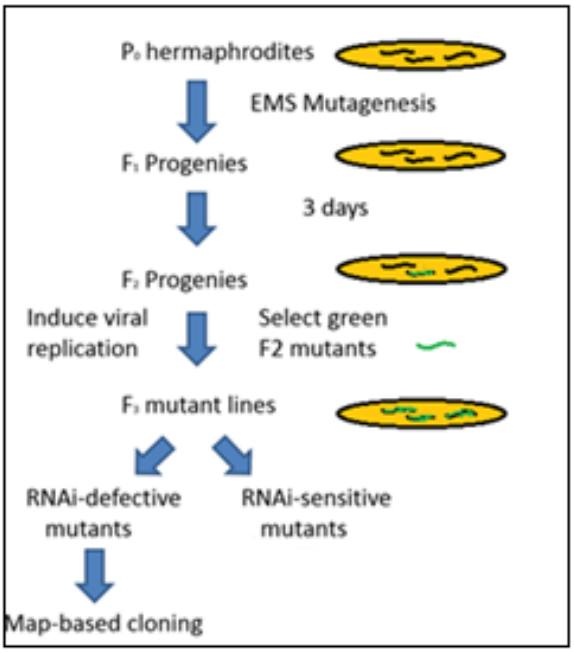

Figure 5.1 Screening for genes required by antiviral immunity

After mutagenesis, F2 progenies from EMS treated parents were selected for screen. These F2 progenies were detected for the presence of green fluorescence signals after heat induction. The phenotypes of these F2 animals as shown by green fluorescence signaling were further confirmed in F3 and F4 generation. These worms were then classified into two categories based on their responses to feeding and injection RNAi. The worm strain which showed deficiency in feeding RNAi was used for genetic mapping based on snip-SNPs strategy.

5.2.2 *C. elegans* strains:

The Bristol N2 strain was used as wild-type strain control. Alleles used in this appendix include *rde-1(ne300), rde-4(ne337), drh-1(tm1329), rsd-2(nl3307);* and the Flock house virus FR1gfp transgenic worm strain *irs91* was constructed and kind provided by Dr. Morris Maduro and Dr. Zhihuan Gao.

5.2.3 Maintenance of *C. elegans* strains

The animals were grown on Nematode Growth Media (NGM) plate seeded with OP50 *E. coli* strain as sole food source at 25°C room temperature. These plates were prepared using a peristaltic pump following sterilization protocols to dispense the NGM solution. The NGM filled plates were left at room temperature for 2 days before use to allow detection of possible contaminants especially to prevent mold growth and for water evaporation. Plates were stored in an air-tight container at room temperature for up to two weeks. The contaminated plates were washed with sterilized M9 buffer. Liquid was collected in a sterilized 5mL conical centrifuge tube with cap. 0.5mL 5N NaOH solution was mixed with 1ml bleach. This bleach- sodium hydroxide solution was added to the centrifuge tube with the nematode pellets.

5.2.4 EMS mutagenesis

The *C. elegans* population was synchronized for the EMS mutagenesis to keep most animals synchronized at late L4 larva stages: The eggs were aseptically transferred to 250ml of M9 Buffer [3g KH2PO4, 6g Na2HPO4, 5g NaCl, 1ml 1 M MgSO4, H2O to 1 liter] in a 1-2 liter flask and then allowed to incubate overnight at 20°C. The flask was

placed upon ice for 15 minutes to cool down and allow settle as pellets. The remaining liquid was transferred to a 50mL sterilized conical centrifuge tube and spin for approximately 5 minutes at 5000rpm to pellet the worms. Subsequently the worms were transferred to 250ml of S Basal solution [5.85 g NaCl, 1 g K2 HPO4, 6 g KH2PO4, 1ml 5M cholesterol and add H2O to 1 liter] inoculated with concentrated E. coli OP50 in sterilized flask. The nematodes growth was monitored by detection through a drop of the culture under the microscope. At 20°C it can be expected that mid-L1 larvae can be harvested after approximately 8 hours, mid-L2 larvae at approximately 18 hours, mid-L3 larvae at approximately 25 hours and mid-L4 larvae at approximately 37 hours respectively. After the synchronization process, the animals were washed off in 1ml M 9 buffer, 3 ml of the suspension is added 1 ml of freshly prepared 0.2 M EMS in M 9 buffer (final concentration 0.05 M). The standard treatment is 4 hours at room temperature kept in incubator at a rotation speed of 100rpm. After four hours of mutagenesis process the worms were washed twice carefully with M9 buffer, the rest of the worms were placed on 90mm diameter NGM plates seeded with OP50 *E. coli*. The animals were left on the plates for a one hour recovery. After the recovery the *C. elegans* growth and movement were under careful scrutiny, 10 individual healthy-looking worms were placed on one separate plate for reproduction of F1 progenies for future survey.

5.2.5 Verification of mutants defective in antiviral immunity

After more than one day growth and reproduction, P0 animals from EMS mutagenesis were removed after successfully laying 10 to 20 F1 eggs. These F1 progenies were left for a two to three days of growth at room temperature until they grew to adulthood and

able to produce F2 progenies. F2 animals were placed on the plates to grow for 48 hours till L4 stages. These F2 individuals underwent 34°C heat induction for 3.5 hours, and they were detected for green fluorescence after two days. The worms that showed strong and stable green fluorescence signals were selected and placed individually on 30mm diameter culture dishes. These phenotypes were confirmed within two further generations. Only those mutant strains which showed more than 50% of GFP expression in their F4 progenies were selected and confirmed as strong mutants of antiviral defense against FR1gfp replicon. As the autofluorescence signals generated from necrosis tissues and unhealthy worms were creating false positive signals, during both the selection and later verification process, only health-looking animals were picked to avoid this misleading direction.

5.2.6 Feeding assays for defects to RNAi response

The animals were allowed to feed for 2–3 days on plates seeded with *E. coli* carrying L4440 plasmids which can express dsRNA of *unc-22* and *pop-1*. The expression of dsRNA vectors was induced by IPTG at a 1mM concentration. Feeding L3/L4 worms was used if the assay will be carried out on the progeny. It was also possible to assay the progeny of RNAi treated L1s. *E. coli* designed for feeding experiments carried L4440 vectors which can express dsRNA targeting UNC-22 and POP-1 sequences. *unc-22* feeding experiment was applied to test the efficiency of somatic tissue RNA interference and *pop-1* feeding experiment was conducted aiming at testifying the efficiency of germline RNAi. The worms was fed with both *unc-22* and *pop-1* dsRNA in order to testify whether they were deficient in classical RNA interference.

5.2.7 Complementation tests

Complementation tests by genetic crosses were conducted aiming at verification if the genetic mutations responsible for mutant's deficiency in antiviral immunity were located in known genes. Males of *rde-1*, *rde-4*, *drh-1* and *rsd-2* mutants were crossed into the hermaphrodite mutants. More than 50 F1 progenies from successful genetic crosses as shown by the 1:1 ratio of males to hermaphrodites were collected for future research. F1 worms were treated with 3.5 hours heat induction in 34°C incubator, after two days green fluorescence signals were detected among this population for the verification of their resistance to antiviral immunity.

5.2.8 Single worm DNA extraction for genetic mapping

18ul of 1×PCR buffer and about 2ul of 10mg/ml proteinase K were placed in top of 50ul PCR tube. Single worms were picked into worm lysis buffer after they laid eggs. The animals were spin down to bottom of tube by centrifugation for 15 seconds at 13,000 rpm. The tube was snap frozen in liquid nitrogen twice. 2ul of mineral oil was added to the top of the worm lysis buffer in order to prevent vaporization. The tubes were incubated at 65°C for 180 minutes and subsequently inactivated by heating at 95°C for 15 min. The *C. elegans* DNA extract was stored at -80°C or -20°C freezer.

5.2.9 Chromosome mapping

After the F1 cross progenies between mutants and CB4856 strain were selected, they were placed individually on different plates to produce F2 progenies which showed recessive segregations in *unc-22* dsRNA feeding experiment. The worms that did not

show a strong twitching/paralyzed phenotype like wild type worms were selected as mutants. One marker per chromosome for each of the autosomes in *C. elegans* was chosen to identify the location of the mutant on the chromosome listed by M Wayne Davis in 2005 (Davis et al., 2005). The chromosome which showed a strong linkage to N2 marker was likely to be the chromosome where the mutation located, and others which were shown to be heterozygote were considered to be not the chromosome the mutation located on. The thermo cycle condition for PCR was: 95°C denaturing for 5 minutes, followed by 95°C denaturing 30 sec, 60°C annealing for 30 sec and 72°C extension for 30 sec- repeated for 29 cycles, 72°C elongation for final 5 min. NEB buffer 1 was used in the digestion experiments, though *Dra*I activity does not reach the peak in NEB buffer 1, it was found that six hours digestion at 37°C was enough to differentiate mutant phenotypes. The digestion products were analyzed on 4% agarose EB (ethidium bromide) gel thereafter.

5.2.10 Interval mapping

After the mutation was located on chromosome IV, interval mapping was utilized to accurately locate the mutation of interest. CB4856 males were crossed into the mutant strain, F1 progenies of successful crosses were selected and placed on NG, and plates seeded with OP50 *E. coli* strain and allowed to lay self-fertilized embryos of F2 and F3 progenies. F2 worms were collected for genomic DNA extraction. The responses to RNAi of F2 progenies were tested in the same way as chromosomal mapping. DNA extract was used for more than 10 PCR reactions and subsequent CAPS/dCAPS

experiment (methods selected based on whether a favorable mutation which can differentiate N2 and CB4856 existed) was used to identify the location of mutations. Similar PCR and restriction enzyme digestion conditions as chromosomal mapping were applied here.

5.3 Results

5.3.1 Antiviral RNAi deficient mutants discovered from EMS mutagenesis

Visible mutation phenotypes among the EMS mutagenesis progenies were used to verify the efficiency of EMS mutagenesis experiment. In each of the three EMS mutagenesis experiments, about 60% of each sort of phenotypes of mutants were found compared to Sydney Brenner's experiment, proving the efficiency of EMS mutagenesis experiment (Table 5.1). Three independent EMS mutagenesis experiments were conducted to search for genes which antiviral immunity in *C. elegans* required. From the green fluorescence expression detection experiments, GFP expression patterns and signal intensities were applied to measure the deficiencies of antiviral immunity in these worm strains. The worms which originated from the same plates and showed a similar pattern of GFP expression inside their bodies were likely the same allele of one gene derived identical gametes (Figure 5.2). These mutants with deficiencies in antiviral immunity were named "*vde"* (viral silencing defective) mutants; they were picked out specifically and carefully placed on individual plates for reproduction and following RNAi responses testing and other phenotypes verification.

Set Phenotype	Total
Dumpy	38
Long	1
Blistered	2
Uncoordinated	84
Abnormal	3

Table 5.1 Numbers of EMS mutants with visible physiological phenotypes

Phenotypes were detected in adult F2 progenies of EMS mutagenesis at 25°C. “Dumpy” mutants worms showed a physiological defect; “Long” mutants are much longer and thinner comparing to wild type; “Roller” mutants are strains of uncoordinated movement worm mutants moving by consistently rolling by one side; “Abnormal” worms showed various defects and abnormality in their physiology, most commonly notched heads’ presences; “Him” mutants showed extraordinarily higher incidences of male progenies; and “blistered” mutants had a blister formed within the cuticle.

During the green fluorescence signal detection of F2 generation mutant strains, GFP expression patterns and signal intensities were measured respectively. Further confirmations were conducted through the visual fluorescence signals detection and statistics calculation of the percentages of F3 and F4 animals which showed the presences of green fluorescence after heat induction. 29 confirmed mutants were selected from three respective EMS mutagenesis experiment (Table 5.2), they were proven to be consistently deficient in antiviral immunity in different generations and repeated experiments. This result further indicated that GFP expression sometimes could be misleading especially in individual worm. Moreover, it was also found that the statistic data of the percentage of worms which showed green fluorescence signals could be a more reliable measurement to demonstrate the defects in antiviral immunity. Various green fluorescence expression patterns of *vde-2*, *vde-5* and *vde-8* were shown in Figure 5.2.

Among the 29 *C. elegans* mutant strains defective in antiviral immunity, three mutants appeared to be the strongest by the criteria of GFP reporter signaling. These three mutants were *vde-10*, *vde-45*, and *vde-54* as presented by Figure 5.3A. Moreover, a larger proportion of these worms showed green fluorescence signals in most parts of their bodies (Figure 5.3B). And all these mutants appeared to be healthy and reproductive, based upon the number of embryos they produced, their growth rate and their movements.

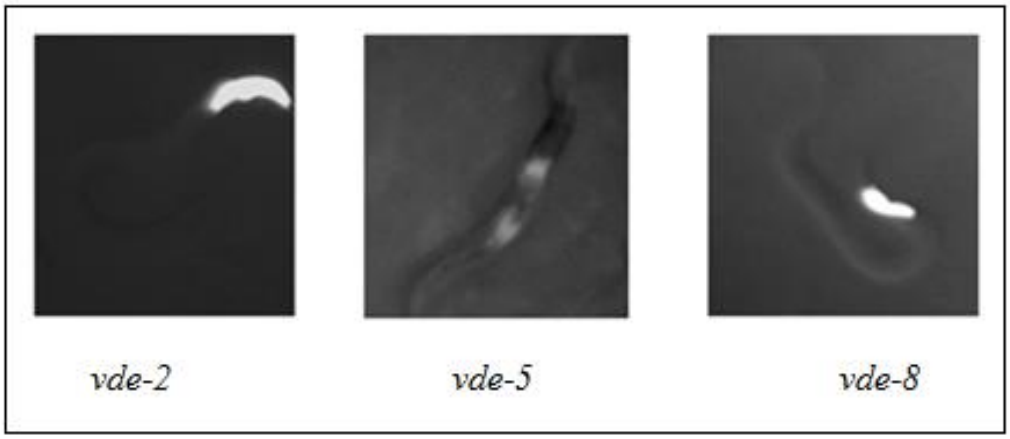

Figure 5.2 Examples of mutants defective in antiviral immunity

29 mutants with consistent and strong green fluorescence signals were identified based upon green fluorescence signals. Though the signaling patterns might vary, all of them had more than 50% of individuals showed the presence of green fluorescence after heat treatment 3.5 hours induction at 34°C. Images were taken two days post heat induction using fluorescence microscopy.

	PlateI	PlateII	PlateIII	PlateIV	PlateV	PlateVI	PlateVII	PlateVIII	PlateIX	PlateX
mutant No.	No.1-5	No.6-9	No.10-14	No.15-22	NO.23-25	NO.26-28	NO.29-31	NO. 32-36	NO. 37-40	NO.41-43
	PlateXI	PlateXII	PlateXIII	PlateXIV	PlateXV	PlateXVI	PlateXVII	PlateXVIII	PlateXIX	PlateXX
mutant No.	NO.44-46	NO.47-51	NO.52-54	NO.55-57	NO.58-60		NO.61-63	NO.64-66	NO. 67-71	NO.72-75

Mutant	vde-1	vde-2	vde-3	vde-4	vde-5	vde-6	vde-7	vde-8	vde-9	vde-10	vde-11	vde-12	vde-13	vde-14	vde-15
GFP signal	NO	YES	NO	NO	YES	NO	NO	YES	NO	YES	YES	NO	NO	NO	YES
Mutant	vde-16	vde-17	vde-18	vde-19	vde-20	vde-21	vde-22	vde-23	vde-24	vde-25	vde-26	vde-27	vde-28	vde-29	vde-30
GFP signal	NO	YES	YES	NO	NO	YES	NO	YES	YES	YES	NO	YES	NO	NO	NO
Mutant	vde-31	vde-32	vde-33	vde-34	vde-35	vde-36	vde-37	vde-38	vde-39	vde-40	vde-41	vde-42	vde-43	vde-44	vde-45
GFP signal	YES	YES	YES	NO	NO	NO	NO	NO	NO	YES	NO	NO	NO	YES	YES
Mutant	vde-46	vde-47	vde-48	vde-49	vde-50	vde-51	vde-52	vde-53	vde-54	vde-55	vde-56	vde-57	vde-58	vde-59	vde-60
GFP signal	YES	NO	NO	YES	NO	NO	NO	YES	YES	NO	NO	YES	NO	YES	NO
Mutant	vde-61	vde-62	vde-63	vde-64	vde-65	vde-66	vde-67	vde-68	vde-69	vde-70	vde-71	vde-72	vde-73	vde-74	vde-75
GFP signal	NO	YES	NO	YES	NO	YES	NO	NO	YES	NO	NO	NO	NO	NO	NO

Table 5.2 Antiviral deficient mutants from EMS screen

The following mutants: *vde-2*, *vde-5*, *vde-8*, *vde-10*, *vde-11*, *vde-15*, *vde-17*, *vde-18*, *vde-21*, *vde-23*, *vde-24*, *vde-25*, *vde-27*, *vde-31*, *vde-32*, *vde-33*, *vde-40*, *vde-44*, *vde-45*, *vde-46*, *vde-49*, *vde-53*, *vde-54*, *vde-57*, *vde-59*, *vde-62*, *vde-64*, *vde-66* and *vde-69* were proven to be consistently defective in antiviral immunity as indicated by the presence of green fluorescence signals after 3.5 hours heat induction at 34 °C in two separate generations.

Figure 5.3 Green fluorescence signals expression in *vde-10, vde-45* and *vde-54*

(A) Visual detection of green fluorescence signals in three mutants after heat induction. Heat induction was conducted at 34 °C for 3.5 hours. Images were taken two days post heat induction. (B) Percentages of animals which showed GFP expression after heat induction. Heat induction was conducted at 34°C for 3.5 hours. 100 adult animals were selected randomly for GFP reporter scoring. Y axis represented the percentage of worms that showed green fluorescence signals. Error bars represented Standard Error of the Mean (SEM) from three biological repeats.

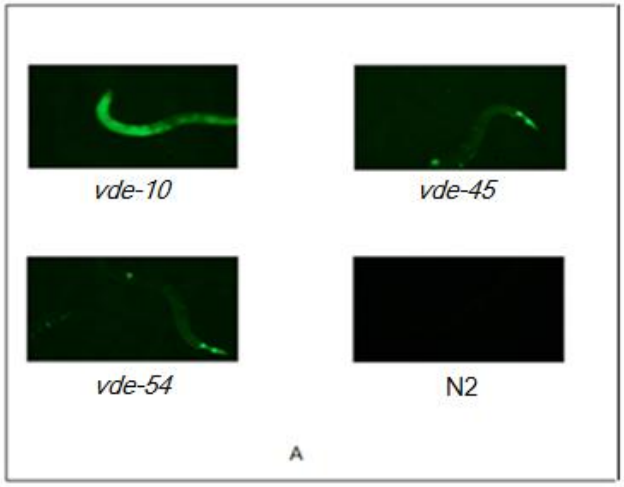
vde-10
vde-45
vde-54
N2
A

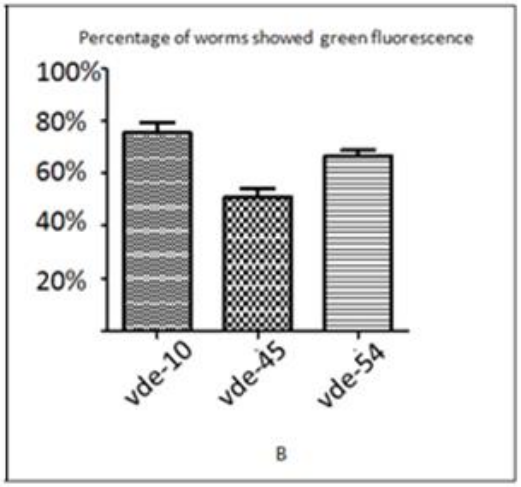
Percentage of worms showed green fluorescence
100%
80%
60%
40%
20%
vde-10
vde-45
vde-54
B

5.3.2 RNAi responses of the mutants

As previous research demonstrated that RNAi responses can be used as an indicator for mapping and RNA interference genes were required in the *C. elegans* antiviral immunity, these mutants were categorized into different groups based on their responses to RNAi. The exogenous RNA interference in these worms were confirmed by *unc-22* and *pop-1* feeding RNAi experiments and *unc-22* dsRNA injection RNAi experiments. The results combined indicated that *vde-45* and *vde-54* were both deficient in antiviral immunity but not deficient in exogenous RNA interference like *drh-1,* whereas *vde-10* was deficient in classic RNAi response as shown by *pop-1* feeding RNAi. However, for *vde-10*, *unc-22* feeding test result appeared to be more complicated: Its *unc-22* feeding RNAi resulted in a partial decrease in the movement ability, as the percentage of twitching/paralyzed *vde-10* nematodes was smaller than that of N2 but significantly higher than that of *rde-1*. These results appeared to be contradictory: *vde-10* was resistant to *pop-1* feeding, as the *pop-1* feeding experiment which proved that the *vde-10* mutants had no significant dead embryos phenotype (Figure 5.4A, Figure 5.4B). Therefore, in order to rule out the possibility *that unc-22* feeding RNAi experiment was not efficient, I conducted microinjection of unc-22 dsRNAs into *vde-10* the bodies to initiate *unc-22* RNAi. And the injection RNAi results (Figure 5.4C) were consistent with the results from feeding RNAi.

Figure 5.4 RNAi responses of mutants: *vde-10, vde-45* and *vde-54*

(A) *unc-22* feeding showed that *vde-10* was deficient in feeding dsRNA experiment. dsRNA of *unc-22* was used to feed N2 and mutant worms at room temperature. 100 adult worms were randomly selected and counted respectively for their RNA interference phenotypes. Twitching and paralyzed phenotypes were added together to indicate the exogenous RNA interference responses in mutants. Error bars represented the SEM of three biological repeats. (B) *pop-1* feeding results of mutant worms indicated *vde-10* was resistant to *pop-1* feeding while *vde-45* and *vde-54* were not. Images were taken 4 days post growth on the bacteria that can express *pop-1* dsRNA. Effective silencing of POP-1 gene can be shown by the numbers of dead embryos which did not hatch. Wild type strain N2 served as negative control of deficiency in RNA interference while *rde-4* served as positive control. (C) *unc-22* injection results showed that *vde-10* was still partially resistant to *unc-22* RNAi after injecting dsRNA into the nematode bodies. Error bars represented the SEM of three biological repeats.

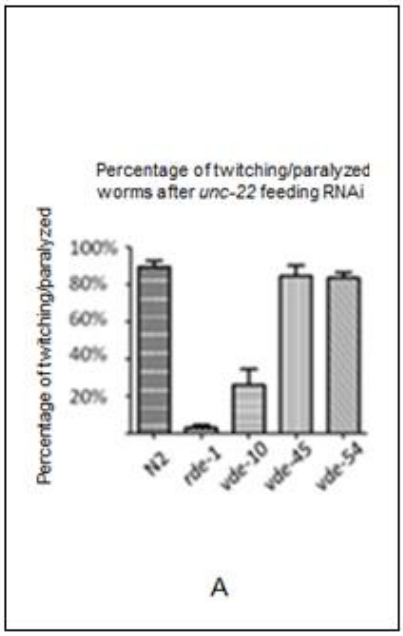
Percentage of twitching/paralyzed worms after *unc*-22 feeding RNAi
Percentage of twitching/paralyzed
100%
80%
60%
40%
20%
N2
rde-1
vde-10
vde-45
vde-54
A

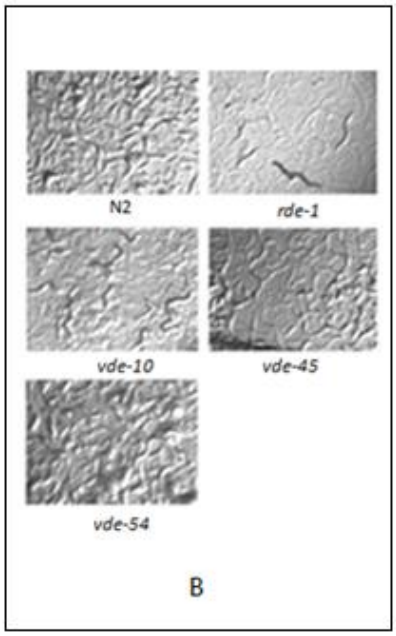
N2
rde-1
vde-10
vde-45
vde-54
B

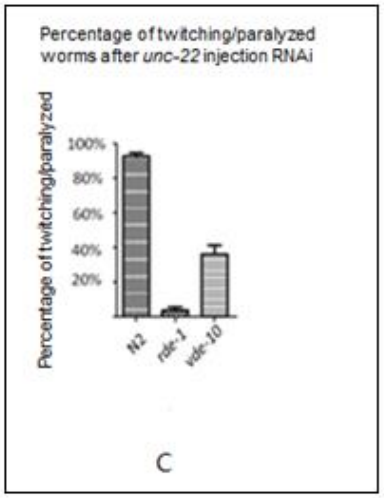
Percentage of twitching/paralyzed worms after *unc*-22 injection RNAi
Percentage of twitching/paralyzed
100%
80%
60%
40%
20%
N2
rde-1
vde-10
C

vde-10 but not *vde-45* or *vde-54* was selected for genetic mapping because of the following reasons: Firstly, *vde-10* had a stronger deficiency to antiviral immunity compared to *vde-45* and *vde-54*, as *vde-10* showed a brighter GFP signal and higher proportion of worms that could show GFP reporter signals after heat induction. Secondly, the green fluorescence signals in individual worms were insufficient to confirm that the worm strain was deficient in antiviral immunity, since certain individuals even in wild type N2 worm strain would show GFP expression after heat induction, and sometimes in mutants of *rde-4* and *rde-1*, the strongest mutants in worms antiviral silencing some individuals did not show green fluorescence after heat induction. However, RNAi responses could be a more accurate indicator of the mutants as numerous forward genetics researches have been conducted based on RNAi response phenotypes. As CB4856 strain was resistant to *pop-1* feeding caused by the *C. elegans* Argonaute protein PRG-1 mutation but still sensitive to *unc-22* feeding, it was possible to map the location of mutation using response to *unc-22* feeding RNAi as an indicator. This phenotype was applied by Craig Mello and Ronald Plasterk to search for genes required for RNAi and spreading of RNAi signals and thus it could be more feasible.

The finding that the mutation was a component in the RNAi machinery led to the question if this mutation was caused by the known genes: especially RDE-1, RDE-4, DRH-1. Therefore these three genetic mutants were crossed with *vde-10* to conduct complementation tests. *vde-45* and *vde-54* were also crossed with *drh-1* mutant in order to verify if they were alleles of *drh-1* since DRH-1 was proven to be not essential in *C. elegans* classic RNA interference machinery; Complementation experiment of *vde-45*,

vde-54 with *rde-1*, *rde-4* would be unnecessary, since *vde-45*, *vde-54* were still responsive to exogenous RNA interference while *rde-1* and *rde-4* were not.

None of the complementation test results from F1 cross progenies of ♂*rde-1*×♀*vde-10*, ♂*rde-4*×♀*vde-10* or ♂*drh-1*×♀*vde-10* genetic crosses showed significantly stronger GFP expressions after heat induction and two days growth in 25°C compared to the F1 progenies from negative control from ♂*drh-1*×♀*rde-1*. This result suggested that *rde-1*, *rde-4*, *drh-1* and *dcr-1* can complement the deficiency in antiviral immunity of *vde-10*. As a result, none of RDE-1, RDE-4, nor DRH-1 genes were responsible for the deficiency in the antiviral immunity of *vde-10* mutant strain. In addition, it proved that the mutation in *vde-10* was recessive. The possibility that mutation located on sex chromosome was also excluded because very few of male F1 progenies which contained only one X chromosome from *vde-10* showed green fluorescence after heat induction.

Moreover, neither of the complementation test results from ♂*drh-1*×♀*vde-45* nor ♂*drh-1*×♀*vde-54* showed significantly stronger expression of GFP reporter signal. Therefore, the antiviral immunity deficiencies of *vde-45* and *vde-54* were not caused by DRH-1 gene mutation. However, *vde-45* and *vde-54* were not used for the following sequencing due to lack of reliable genetic marker.

5.3.3 Chromosomal mapping

Aiming at position the mutation of interest on a specific chromosome, hermaphrodites of the mutant nematodes were crossed with males of Hawaiian CB4856 mapping reference strain to produce F1 progenies; these F1 progenies were further placed on different plates

individually to reproduce F2 progeny of worms which showed phenotype segregations- roughly 1/4 of these progenies showed deficiencies in exogenous RNAi after *unc-22* feeding RNAi. 9 F2 progenies that showed resistances to *unc-22* feeding were selected respectively for chromosomal mapping. One SNP marker per chromosome was used to position the mutation to one specific autosome according to chromosomal linkage, as the possibility of sex chromosome was already ruled out previously from the results of F1 cross progenies which merely carried one X chromosome from the mutant. CAPS analysis was utilized to genotype the progenies with mutant phenotypes.

The result of CAPS analysis (Figure 5.5) using different sets of primers on each chromosome indicated that only the SNP marker from chromosome IV showed close linkage to the mutation of *vde-10*, whereas chromosomes I, II, III, V markers related CAPS analysis all showed to be heterozygote products of both strands from wild type Bristol N2 and Hawaiian CB4856 strain. Therefore it became clear that the mutation responsible for *vde-10* deficiency in antiviral immunity- as shown by the resistance to feeding dsRNA of *unc-22* was located on chromosome IV and no recombinant of the chromosomal IV marker region was observed.

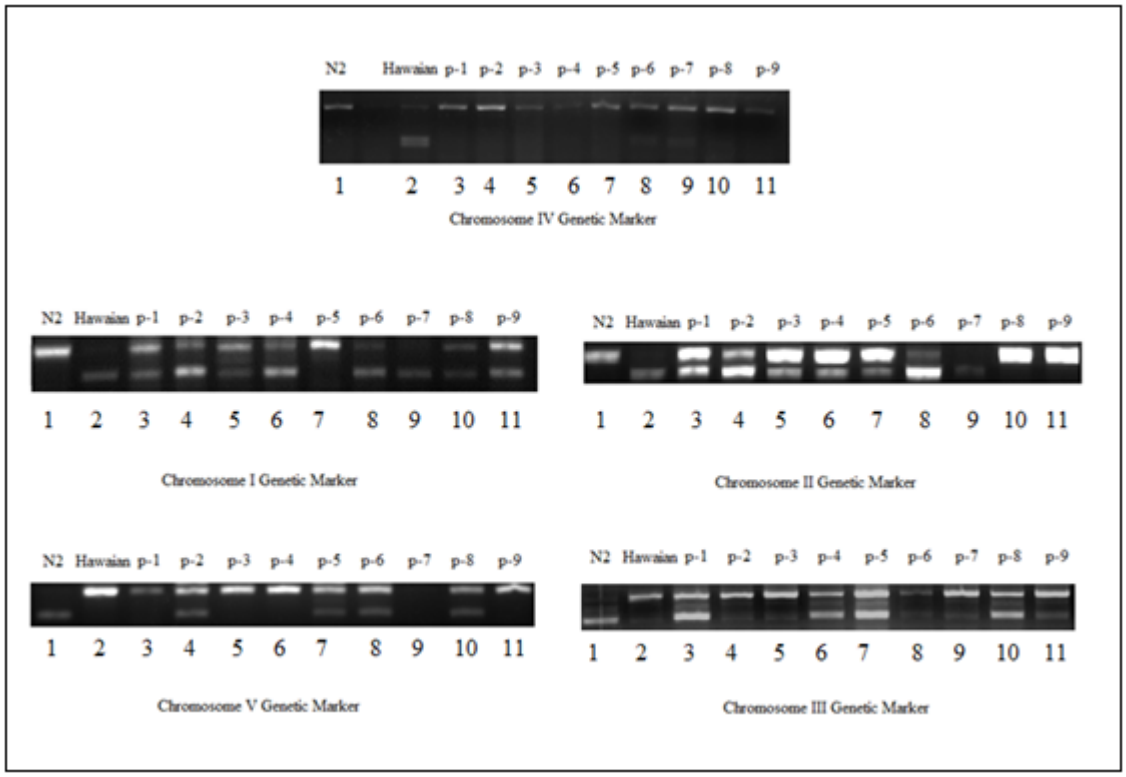

Figure 5.5 Chromosomal mapping positioned the mutation to chromosome IV.

N2 and Hawaiian CB4856 strain and 9 F2 progenies were selected respectively; DNA samples were extracted from these worms. Chromosomal snip-SNPs markers from Wicks et al., 2001 were used to detect SNP polymorphism of each marker. Samples named p-1, p-2, p-3, p-4, p-5, p-6, p-7, p-8 and p-9 were the nine F2 progenies which showed mutant-like RNAi defective phenotypes.

5.3.4 Interval mapping

Interval mapping was conducted based on Snip-SNPs strategy and traditional Three-Point Mapping using the genetic markers on chromosome IV to narrow down the gap between two genetic markers after chromosomal mapping positioned the mutation of desire on one chromosome IV. Numerous cross progenies of the mutant hermaphrodites and males of CB4856 worms and their RNAi phenotypes were measured by *unc-22* feeding RNAi responses. After detection of more than 100 mutants the mutation region was narrowed down between two genetic markers: Chromosome IV +9.38cM and Chromosome IV +9.8cM in an interval of 0.42cM. Hence this mutation was likely to be residing between Chromosome IV +9.38 and Chromosome IV +9.8. Furthermore, chromosome IV +9.5 marker appeared to be close to the mutation site as no recombinants were found from more than one hundred mutants phenotype F2 progenies. Genes which located in this interval included RSD-2- (location IV: 9.50 +/- 0.080 cM), RSD-2 appeared to be a strong candidate. Its exogenous RNAi phenotypes appeared to match with *vde-10*: While *rsd-2* mutant was deficient in RNA interference by *pos-1* feeding RNAi targeted germline expressed gene just as *pop-1* feeding results of *vde-10*, it remained partially functional in *unc-22* feeding RNAi like *vde-10* (Han et al., 2008). The following Table 5.3 was a list containing some of the dCAPS analysis results of the individual mutants which were crucial during the interval mapping process to position the mutation of interest to the small interval.

	1	2	3	4	5	6	7	8	9
Chr IV 8	N2	N2	N2/Ha	N2/Ha	N2	N2	N2	N2	N2/Ha
Chr IV 9.38	N2	N2	Ha	N2	N2	N2	N2	N2	N2/Ha
Chr IV 9.5	N2	-	-	N2	N2	N2	-	-	N2/Ha
Chr IV 9.8	N2	N2	N2/Ha	N2	N2	N2	N2	N2	N2/Ha
Chr IV 10.49	N2	N2	Ha	N2/Ha	N2	N2	N2	N2	N2/Ha
Chr IV 12	N2	N2	Ha	N2/Ha	N2	N2	N2/Ha	N2/Ha	N2/Ha

	10	11	12	13	14	15	16	17	18
Chr IV 8	N2/Ha	N2	N2	N2	N2	N2	N2	N2	N2
Chr IV 9.38	N2/Ha	N2	N2	N2	N2	N2	N2	N2	N2
Chr IV 9.5	-	-	-	N2	N2	N2	N2	N2	-
Chr IV 9.8	N2	N2	N2	N2	N2	N2	N2	N2	N2
Chr IV 10.49	-	N2	N2/Ha	N2	N2	N2	N2	N2	N2
Chr IV 12	-	N2	N2/Ha	N2	N2	N2	N2	N2	N2

	19	20	21	22	23	24	25	26	27
Chr IV 8	N2	N2	N2	N2	N2	N2	N2	N2	N2/Ha
Chr IV 9.38	N2/Ha	N2	N2	N2	N2	N2	N2	N2	N2
Chr IV 9.5	N2	N2	N2	N2	N2	N2	N2	N2	N2
Chr IV 9.8	N2	N2	N2	N2	N2	N2	N2	N2	N2
Chr IV 10.49	-	N2	N2/Ha	N2	N2	N2	N2	N2	N2
Chr IV 12	-	N2	N2/Ha	N2	N2	N2	N2	N2/Ha	N2

	28	29	30	31	32	33	34	35	36
Chr IV 8	N2	N2/Ha	N2	N2	N2	N2	N2	N2	N2
Chr IV 9.38	N2	N2/Ha	N2	N2	N2	N2	N2	N2	N2
Chr IV 9.5	N2	N2/Ha	N2	N2	N2	N2	N2	N2	N2
Chr IV 9.8	N2	N2/Ha	N2	N2	N2	N2	N2	N2	N2
Chr IV 10.49	N2	N2/Ha	N2	N2	N2	N2	N2	N2	N2
Chr IV 12	N2	N2/Ha	N2	N2	N2	N2	N2	N2	N2

Table 5.3 Genetic positioning in interval mapping

DNA samples for the interval mapping experiments were extracted from F2 cross progenies. Chromosomal markers used from up to down: Chromosome IV+8 cM, Chromosome IV+9.38 cM, Chromosome IV+9.5 cM, Chromosome IV+9.5 cM, ChromosomeIV+10.49 cM, ChromosomeIV+12 cM.

5.3.5 Verification of the mutant *vde-10* as RSD-2 allele did not succeed

I continued to testify the hypothesis that RSD-2 was responsible for the *vde-10* antiviral immunity deficiency. *rsd-2(pk3307)* mutant hermaphrodites were crossed with males of FHV FR1GFP transgenic *C.elegans*. After heat induction, strong and clearly enhanced green fluorescence signals were detected in *rsd-2(pk3307)* mutant with FHV FR1GFP replicon transgene. The result in Figure 5.6 indicated that RSD-2 was required for the *C. elegans* antiviral immunity defense system.

Although *rsd-2* allele was also deficient in antiviral immunity, later sequencing of RT PCR product was conducted to further confirm that RSD-2 was the gene responsible for antiviral immunity deficiency in *vde-10*. The first preliminary sequencing result indicated that mutant *vde-10* harbored a 9281 G/A transition in its 11^{th} exon which would cause an amino acid switch. However, this result was not repeatable in following generations of the mutant strain as there was no other mutation detected in the exons of RSD-2 in *vde-10* mutant strain which can result in the premature stop codon or alteration of critical amino acid site.

Figure 5.6 *rsd-2(pk3327)* mutant was defective in antiviral immunity against FR1gfp

rsd-2 strain (pk3327) was crossed with FHV FR1gfp strain. Worms were heat treated in 34°C incubators for 3.5 hours. Images were taken two days post heat induction. Most of *rsd-2* mutants carrying FR1GFP transgenic replicon showed strong green fluorescence signals after two days.

5.4. Discussion

In this appendix, EMS based forward genetics screenings were conducted to search for genes required for antiviral RNAi using FR1gfp transgenic *C.elegans* strain. After each EMS mutagenesis screen, a large number of individual animals which did show green fluorescence signaling after heat induction were found in F2 progenies population. However, in these experiments it was proven that more than 60% (46 out of 75) worms accidentally showed false positive signals during the first screening. This result indicated that the presence of green fluorescence in individual animals could be misleading whereas statistics analysis of the percentage of nematodes which showed green fluorescence expression from a large amount of animals was more accurate.

As the GFP expression could be misleading sometimes especially as an indicator for genetic mapping, RNAi response phenotype was applied as an indicator for genetic mapping. Therefore, *vde-10,* a strong defective mutant in antiviral immunity and also deficient in feeding RNAi was chosen for the subsequent genetic mapping target. Snip-SNPs strategy was used to map *vde-10.* After chromosomal and interval mapping, *vde-10* was positioned on a small interval between the markers of chromosome IV +9.38 and chromosome IV +9.8 which contains gene RSD-2. RSD-2 was found to be required in *C. elegans* antiviral immunity by Rui Lu through reverse genetics screen (Lu et al., 2009). Therefore it became a clear candidate responsible for the deficiency in antiviral immunity in *vde-10* mutant strain. However, though genetic mutant of RSD-2: *rsd-2(nl3307)* showed strong deficiency in antiviral immunity and preliminary complementation result seemingly suggested that *rsd-2* and *vde-10* did not have complementation effect in

antiviral defense, no exon mutations which can cause alteration of RSD-2 functions in *vde-10* could be found.

A possible cause of this may be that *vde-10* harbored a mutation in its vast length of introns (exceeding 14,000bp) which caused its antiviral immunity deficiency: For example, RSD-2 contains four isoforms and alternative slicing pattern may be disrupted as a result from intron mutations. Furthermore, it might also be a false result from mapping resulted from inaccurate mutant phenotype or response detection which disrupted the positioning of chromosomal and interval genetic markers. With new mapping strategy based on high throughput deep sequencing, our lab currently faced much fewer problems with genetic mapping of mutagenesis progeny.

5.5. References

Brenner, S. (1974). Genetics of Caenorhabditis-Elegans. *Genetics* **77**(1): 71-94.

Brown, S. D. and R. Balling (2001). Systematic approaches to mouse mutagenesis. *Curr Opin Genet Dev* **11**(3): 268-73.

Chalfie, M., Y. Tu, G. Euskirchen, W. W. Ward and D. C. Prasher (1994). Green fluorescent protein as a marker for gene expression. *Science* **263**(5148): 802-5.

Davis, M. W., M. Hammarlund, T. Harrach, P. Hullett, S. Olsen and E. M. Jorgensen (2005). Rapid single nucleotide polymorphism mapping in C-elegans. *Bmc Genomics* **6**.

Frokjaer-Jensen, C., M. W. Davis, C. E. Hopkins, B. J. Newman, J. M. Thummel, S. P. Olesen, M. Grunnet and E. M. Jorgensen (2008). Single-copy insertion of transgenes in Caenorhabditis elegans. *Nat Genet* **40**(11): 1375-83.

Han, W., P. Sundaram, H. Kenjale, J. Grantham and L. Timmons (2008). The Caenorhabditis elegans rsd-2 and rsd-6 genes are required for chromosome functions during exposure to unfavorable environments. *Genetics* **178**(4): 1875-93.

Kim, Y., K. S. Schumaker and J. K. Zhu (2006). EMS mutagenesis of Arabidopsis. *Methods Mol Biol* **323**: 101-3.

Ling, H. Q., G. Koch, H. Baumlein and M. W. Ganal (1999). Map-based cloning of chloronerva, a gene involved in iron uptake of higher plants encoding nicotianamine synthase. *Proc Natl Acad Sci U S A* **96**(12): 7098-103.

Lu, R., E. Yigit, W. X. Li and S. W. Ding (2009). An RIG-I-Like RNA Helicase Mediates Antiviral RNAi Downstream of Viral siRNA Biogenesis in Caenorhabditis elegans. *Plos Pathogens* **5**(2).

Mullins, M. C., M. Hammerschmidt, P. Haffter and C. Nusslein-Volhard (1994). Large-scale mutagenesis in the zebrafish: in search of genes controlling development in a vertebrate. *Curr Biol* **4**(3): 189-202.

Neff, M. M., J. D. Neff, J. Chory and A. E. Pepper (1998). dCAPS, a simple technique for the genetic analysis of single nucleotide polymorphisms: experimental applications in Arabidopsis thaliana genetics. *Plant J* **14**(3): 387-92.

St Johnston, D. (2002). The art and design of genetic screens: Drosophila melanogaster. *Nat Rev Genet* **3**(3): 176-88.

Tijsterman, M., K. L. Okihara, K. Thijssen and R. H. Plasterk (2002). PPW-1, a PAZ/PIWI protein required for efficient germline RNAi, is defective in a natural isolate of C. elegans. *Curr Biol* **12**(17): 1535-40.

Vogel, C., G. Innerebner, J. Zingg, J. Guder and J. A. Vorholt (2012). Forward genetic in planta screen for identification of plant-protective traits of Sphingomonas sp. strain Fr1 against Pseudomonas syringae DC3000. *Appl Environ Microbiol* **78**(16): 5529-35.

Wicks, S. R., R. T. Yeh, W. R. Gish, R. H. Waterston and R. H. A. Plasterk (2001). Rapid gene mapping in Caenorhabditis elegans using a high density polymorphism map. *Nature Genetics* **28**(2): 160-64.